Functional analysis of the anion exchanger 1 by knock in mouse models

DISSERTATION

zur Erlangung des akademischen Grades

doctor rerum naturalium (Dr. rer. nat.)

vorgelegt dem Rat der Medizinischen Fakultät

der Friedrich-Schiller-Universität Jena

von Rizwan Mumtaz (M.sc.)

geboren am 01.12.1979 in Lahore (Pakistan)

im Oktober 2011

Gutachter

1. Prof. Dr. Christian Hübner
Institute of Human Genetics, University Hospital Jena, Germany

2. Prof. Dr. Carsten A. Wagner
Institute of Physiology, University of Zurich, Switzerland

3. Prof. Dr. Dominique Eladari
Faculty of Medicine, University of Paris Descartes, France

Tag der öffentlichen Verteidigung: 5th June 2012

To my Abbu, Ammi and Phophoo

List of abbreviations

°C	Degree celsius
AD	Autosomal dominant
AE 1	Human Anion exchanger 1
Ae 1	Mouse Anion exchanger 1
AR	Autosomal recessive
ATP	Adenosine triphosphate
bp	Base pair
CA II	Carbonic anhydrase 2
CCD	Cortical collecting duct
cDNA	Complementary deoxyribonucleic acid
Cl^-	Chloride
CO_2	Carbon dioxide
C-terminal	Carboxyl terminal
DAPI	4',6-Diamidino-2-phenylindole
dATP	Deoxyadenosine-5'-triphosphate
dCTP	Deoxycytidine-5'-triphosphate
dGTP	Deoxyguanosine-5'-triphosphate
DIDS	4,4'-Diisothiocyanatostilbene-2,2'-disulfonate
DNA	Deoxyribonucleic acid
dRTA	Distal renal tubular acidosis
DTA	Diphtheria toxin A
dTTP	Deoxythymidine-5'-triphosphate
eAE1	Erythrocyte AE1 isoform
EDTA	Ethylene diamide tetra acetic acid
ER	Endoplasmic reticulum
h	Hour (s)
H^+	Proton
H^+-ATPase	Hydrogen adenosine triphosphatase
HCO_3^-	Bicarbonate
HEK-293 cells	Human embryonic kidney 293 cells
HEPES	4-(2-hydroxyethyl)-1-Piperazineethanesulfonic acid
HS	Hereditary spherocytosis
IMCD cells	Inner medullary collecting duct cells
K^+	Potassium
kAE1	Kidney AE1 isoform
kDa	kilo Dalton
KI	Knock In
KO	Knockout
LB medium	Luria Bertani medium
MCD	Medullary collecting ducts
MDCK cells	Madin Darby canine kidney cells
mg	Milligram (s)

min	Minute (s)
ml	Milliliter (s)
mM	Millimolar
mmol	Millimole
MOPS	3-(N-morpholino) propanesulphonic acid
mRNA	Messenger ribonucleic acid
Na^+	Sodium
NaCl	Sodium chloride
NBC	Sodium/bicarbonate co-transporter
neo	Neomycine Casette
ng	Nanogram (s)
NH_4Cl	Ammonium chloride
NHE	Sodium/proton exchanger
nM	Nanomolar
nmol	Nanomole
nt	Nucleotide (s)
N-terminal	Amino terminal
PBS	Phosphate-buffered solution
pCO_2	Partial pressure of carbon dioxide
PCR	Polymerase chain reaction
pmol	Picomole
pO_2	Partial pressure of oxygen
RNA	Ribonucleic acid
RNase	Ribonuclease
rpm	Revolutions per minute
RT	Room temperature
SAO	Southeast Asian ovalocytosis
SDS	Sodium dodecyl sulfate
sec	Second (s)
SEM	Standard error of the mean
SLC	Solute carrier
SOC medium	Super optimal broth
TAE	Tris-acetate-EDTA
Taq	Thermus aquaticus
TBST	Tris-buffered saline added with Tween 20
TM	Transmembrane
UV	Ultraviolet
v H^+ATPase	Vacuolar Hydrogen adenosine triphosphatase
WT	Wild-type
α-IC cells	α-Intercalated cells
β-IC cells	β-Intercalated cells
µg	Microgram (s)
µl	Microliter (s)
µM	Micromolar

Contents

Summary

The kidney is one of the homeostatic regulators in the human body to maintain electrolyte and acid-base balance. An imbalance in acid-base regulation can lead to serious pathophysiological conditions. Possible reasons for a disturbed pH homeostasis are defects in genes encoding the transport proteins of the kidney. Mutations in the gene encoding the anion exchanger 1 (SLC4A1, AE1) is one of the genes that has been shown to cause distal renal tubular acidosis.

During this study I have generated the first knock-in (KI) mouse models for autosomal dominant distal renal tubular acidosis (dRTA). These two independent knock-in (KI) mouse models, R607H and L919X, correspond to the human mutations R589H and R901X, respectively. No morphological and anatomical differences were observed in KI mice compared to WT littermates. In contrast, the established KI mouse models exhibit a renal acid secretion defect in steady state conditions which was also observed during a classical acid loading test. These observations were made on consecutive days while mice were housed in metabolic cages over a period of one week to measure urine pH and electrolytes. The blood gas analysis showed no significant differences in both KI mice compared to WT littermates. Human Patients with these mutations also show dRTA with lower blood pH and bicarbonate levels.

A significant reduction of Ae1 expression levels was observed in cortical collecting ducts (CCD) of KI mouse kidneys by immunohistochemical analysis. The reduction in the protein expression is possibly due to the dominant negative effect of the mutations. The decrease in protein expression levels in KI kidney was validated by western blotting. Quantification of the transcript levels in the KI kidney tissues did not support a decrease in mRNA levels due to nonsense medicated mRNA decay. Thus, post-transcriptional effects are responsible for the decrease in Ae1 protein levels and account for dRTA.

In summary, both KI mouse models provide valuable tools to further elucidate the pathomechanisms of AE1-related dRTA.

Zusammenfassung

Die Niere ist ein wichtiger Regulator der Homöostase des Elektrolyt-und Säure-Base-Haushalts. Störungen dieser Homöostase sind mit schwerwiegenden klinischen Folgen für die betroffenen Patienten verbunden. Eine der Ursachen einer gestörten pH-Regulation sind Defekte in verschiedenen Ionentransportern, die eine wichtige Rolle in der Regulation des Säure-Base-Haushalts spielen. Ein prominentes Beispiel für einen solchen Defekt sind Mutationen im SLC4A1-Gen, das für den Anionenaustauscher AE1 kodiert. Veränderungen im SLC4A1-Gen führen zum klinischen Bild der distalen renal-tubulären Azidose (dRTA).

Im Rahmen meiner Dissertation habe ich die ersten Knockin-Mauslinien (KI) für das Slc4a1-Gen zum Studium des Pathomechanismus der autosomal-dominanten dRTA hergestellt. Es wurden durch homologe Rekombination zwei unabhängige Mauslinien generiert, bei denen die Missense-Mutation R607H in das Slc4a1-Gen eingefügt wurde (diese entspricht der humanen Mutation R589H), sowie im zweiten Fall die Nonsense-Mutation L919X (diese entspricht der humanen Mutation R901X bei Patienten mit dRTA). Die jeweiligen heterozygoten KI-Mäuse wiesen keine offensichtlichen morphologischen Unterschiede im Vergleich zu ihren Wildtyp-Geschwistertieren auf. Daraufhin erfolgte eine Analyse des Säure-Base- sowie Elektrolythaushalts der Mäuse im Rahmen einer Versuchsreihe im metabolischen Käfig. Interessanterweise zeigte sich bei heterozygoten KI-Tieren beider Linien ein massiver Säuresekretionsdefekt, der sowohl unter Ruhebedingungen als auch nach Säurebelastung der Tiere nachweisbar war. Die Blutgasanalyse zeigte demgegenüber keine signifikanten Unterschiede zwischen KI- und Vergleichstieren. Diese Ergebnisse decken sich mit den laborchemischen Befunden von Patienten mit dRTA.

Auf zellulärer Ebene konnte in beiden Linien eine signifikante Reduktion des Expressionsniveaus von Ae1 im kortikalen Sammelrohr heterozygoter KI-Tiere durch immunhistochemische Analysen nachgewiesen werden. Die Abnahme der Expression konnte durch Western-Blot Analysen bestätigt werden. Im Gegensatz dazu ergab die Quantifizierung der Ae1-Transkriptmenge in der Niere keine Abnahme der mRNA-Menge von Slc4a1. Somit scheinen posttranskriptionale Effekte für die Abnahme der Ae1-Proteinmenge und somit der dRTA verantwortlich zu sein.

Zusammenfassend ist es im Rahmen der Dissertation gelungen, zwei Tiermodelle herzustellen und zu charakterisieren, die zum Verständnis des Pathomechanismus der AE1-assoziierten distal renal-tubulären Azidose beitragen.

1. Introduction

1.1. Body homeostasis and acid-base balance

The term homeostasis, originated from the Greek: ὅμοιος, *hómoios*, "similar" and στάσις, *stásis*, "standing still", is an important prerequisite for our body to maintain a constant internal milieu. Systemic acid-base homeostasis is maintained via complex interactions among metabolism, regulated exhalation of CO_2 by the lungs and acid or base excretion/reclamation by the kidneys (Wagner, Kovacikova et al. 2006).

Optimal activity of the physiological processes requires the control of intracellular and extracellular pH. pH is defined as the negative decadic logarithm of the proton (H^+) concentration:

$$\mathrm{pH} = -\log_{10}[H^+]$$

The pH of blood and extracellular fluids must be kept within a narrow physiological range around pH 7.4. Systemic pH homeostasis is achieved through integrated functions of intracellular and membrane bound acid-base transporters of the kidneys, lungs, and gut, coordinated and regulated by the endocrine and nervous system (Alper 2002).

A controlled regulation of acid-base balance is necessary to maintain biochemical and metabolic functions of cells and organs. Therefore, a number of physiological buffering systems exist to control the pH of the body (Giebisch and Windhager 2009). A buffer is a substance that helps to keep a constant pH by reversibly consuming or releasing protons (Boron, Boulpaep et al. 2009). Proteins, organic and inorganic phosphates, hemoglobin, creatinine, urate salts, and ammonia are relevent intra- and extracellular buffers. However, in biological systems the most important buffering system is the weak base HCO_3^- in the CO_2-HCO_3^- steady state (Tresguerres, Buck et al. 2010).

$$CO_2 + H_2O \leftrightarrows H_2CO_3 \leftrightarrows H^+ + HCO_3^-$$

Cellular enzymes and chemical reactions are sensitive to pH, and cells actively transport H^+ and HCO_3^- across their cell membrane to maintain intracellular pH (Casey, Grinstein et al. 2010). Extracellular pH and systemic acid-base balance are very important for normal organ and cellular function (Wagner, Devuyst et al. 2009). A disturbance in normal body acid-base status is associated with higher morbidity and mortality in patients with chronic kidney disease (Bailey 2005). Imbalances in the extracellular pH affect the stability and density of the

bone and can result or contribute to osteopenia and osteoporosis (Jehle, Zanetti et al. 2006; Arnett 2008).

A standard western diet leads to the generation of approximately 1 mmol of nonvolatile mineral acid per kilogram of body weight (Cohen, Feldman et al. 1997). Maintenance of systemic acid-base balance requires renal excretion of an equivalent amount of acid. The kidney meets this requirement using two principal mechanisms: reabsorption of filtered HCO_3^- by the proximal tubule and net acid excretion as titratable acids and NH_4^+ by the distal nephron (Kurschat and Alper 2008).

1.2. Role of membrane proteins in acid-base balance

Membrane proteins are approximately one third of all proteins encoded by eukaryotic genomes (Muller, Wu et al. 2008). These proteins perform their functions as enzymes, receptors, channels, structural proteins and transporters and are involved in essential biological processes such as electron transport, transmembrane signalling, nerve conduction and nutrient uptake. The phospholipid bilayer, the basic structural unit of the cell membrane, is mostly impermeable to water soluble molecules, ions and water. Transport across membranes is necessary to maintain ion concentration gradients which are essential prerequisites for the function of most mammalian cells, e.g. epithelial cells in the kidney. The transport of H^+ and HCO_3^- across the cell membrane regulates the intra and extracellular pH homeostasis. The transport across cellular membranes can be categorised into passive and active transport processes.

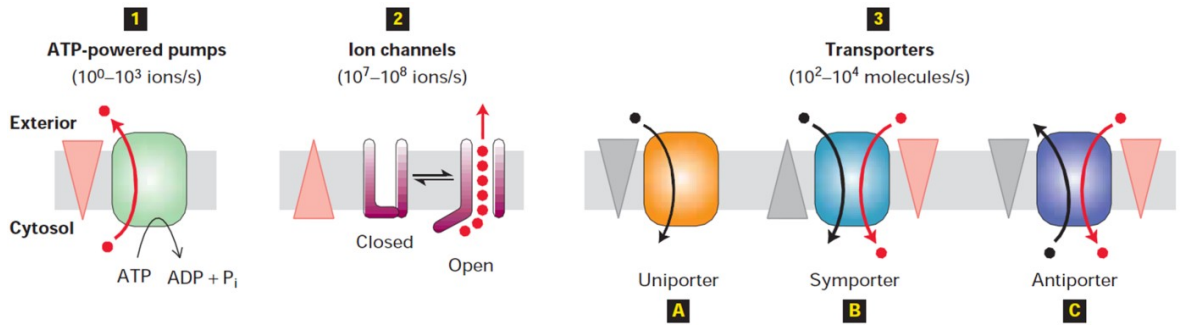

Figure 1.1 Overview of membrane transport proteins. (**1**) ATP-powered pumps utilize the energy released by ATP to move ions or small molecules against the concentration gradient. (**2**) Channels allow the movement of specific ions or water along with their concentration gradient. Transporters further divided into three groups. (**3A**) Uniporters transport a single type of molecule down its concentration gradient. The co-transporters can be (**3B**) symporters, also known as cotransporters or (**3C**) antiporters, commonly called as exchangers, catalyse the movement of one molecule against its concentration gradient (black circles), driven by movement of one or more ions down an electrochemical gradient (red circles) (Lodish 2003).

1.2.1. Passive and active transport across membranes

Gases and small uncharged polar molecules can readily move across membranes by passive transport. Their transfer rate is depending upon the concentration gradient across membranes. When integral membrane proteins are involved in passive transport this is known as facilitated transport (Lodish 2003). Transport proteins can be classified in four groups, namely pores, channels, carriers (also referred to as transporters and exchangers) and pumps. The expression of some transport proteins can be specific for tissues, cell types, and sometimes membrane domains. Others are expressed in most, if not all cell membranes (Reuss 2008).

Ion channels and the porins are example of proteins, which have a polar pore through which ions and other hydrophilic compounds can pass. Transporters bind molecules to be transported and help them to pass through the membrane by a conformational change.

Active transport works (always) opposite to the concentration gradient and therefore requires an input of energy, which is usually supplied by the hydrolysis of ATP. Transport systems in the membranes are essential for the cells to regulate volume, nutrient uptake, waste removal internal pH value, and to establish ion gradients, which are required for oxidative phosphorylation and stimulation of muscle and nerve cells (Koolman and Röhm 2005).

1.3. Solute carriers and anion exchanger proteins

To maintain a physiological cellular environment, molecules must be delivered into and removed from cells and organelles. This important role is performed by transport proteins that reside in plasma and intracellular membranes. The solute carrier (SLC) families includes more than 300 genes that encode passive transporters, ion-coupled transporters, and exchangers (Landowski, Suzuki et al. 2008).

Anion exchangers are key regulators of intracellular homeostasis by maintaining physiological balance from cells to whole organs by transporting different anions such as Cl^-, HCO_3^-, SO_4^{2-} and oxalate across cell membranes. Their pivotal role in the regulation of intracellular pH, cell volume, CO_2 metabolism, cell shape, contractility and contribution to cell growth, as well as ion gradients has been previously known. Two important anion exchanger families support to maintain the physiological functions of eukaryotic systems, the classical anion exchanger (AE) gene family, known as solute carrier 4 (SLC4) and a multifunctional anion exchanger family solute carrier 26 (SLC26). Differences in the tissue distribution and regulation of the specific anion exchanger proteins allow the precise regulation of bicarbonate transport throughout the human body (Pushkin and Kurtz 2006; Bonar and Casey 2008).

1.3.1. Solute carrier family 4 (SLC4) and anion exchanger 1 (AE1)

The SLC4 gene family includes 10 members. This solute carrier family can be subdivided into two major subfamilies based on the function: anion exchangers (AEs) and sodium coupled bicarbonate co-transporters (NBCs) (Romero 2005; Landowski, Suzuki et al. 2008).

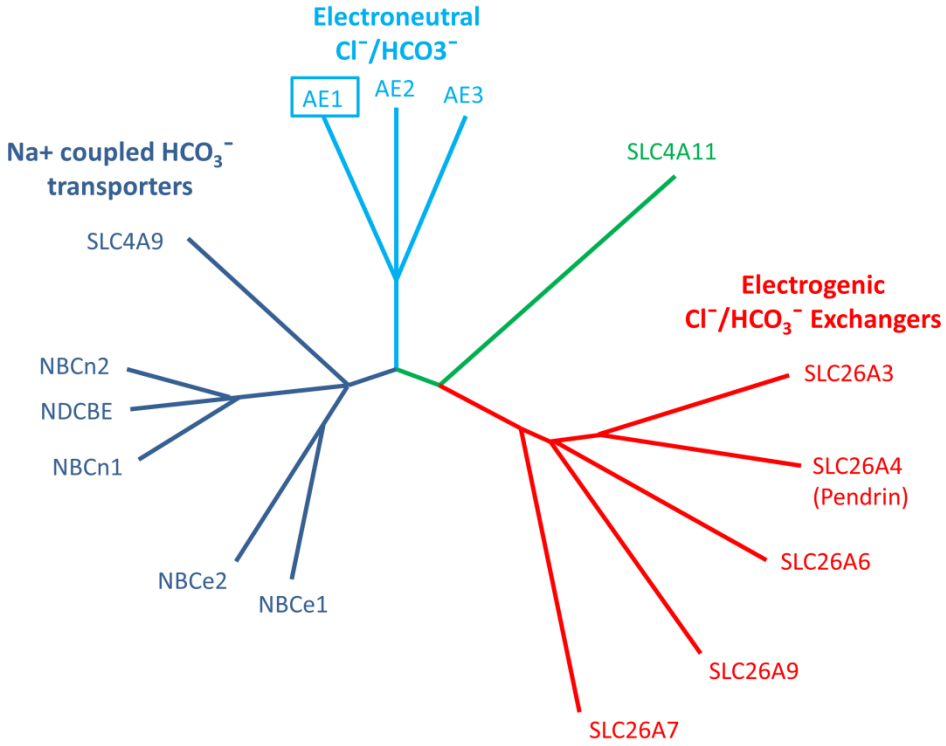

Figure 1.2 Phylogenetic dendrogram of human bicarbonate transporters. The length of the line represents the relative evolutionary distance. Bicarbonate transporters clearly cluster into three families, each of which is coloured and labelled. SLC4A11, which may or may not be a bicarbonate transporter, is placed midway between the electrogenic and electroneutral Cl^-/HCO_3^- exchangers (Cordat and Casey 2009).

The first three human AEs (AE1-3) have been characterized as electroneutral exchangers, which carry one monovalent anion in exchange for a second monovalent anion. These anion exchangers transport HCO_3^- and Cl^- and this electroneutral transport process is inhibited by stilbene disulfonate derivatives such as DIDS (Landowski, Suzuki et al. 2008). All SLC4 polypeptides are structurally very similar, consist of an N-terminal hydrophilic, cytoplasmic domain followed by a hydrophobic, polytopic transmembrane domain, and completed by a C-terminal cytoplasmic domain. Many SLC4 genes express 5′-variant transcripts from different promoters to generate one or more isoforms with distinct N-terminal amino acid sequences (Alper 2006). The AE1 gene encodes the longer erythroid AE1 (eAE1, band 3) and the shorter kidney AE1 (kAE1) which initiates at Met66 in human and at Met80 in mice (Kopito, Andersson et al. 1987; Kudrycki and Shull 1993) (see figure 1.3). The mouse AE2 gene encodes five N-terminal variant polypeptides (the human gene encodes only four), while the

AE3 gene encodes two variant N-terminal and two variant C-terminal polypeptide sequences (Alper 2009).

1.4. Anion exchanger 1 (AE1, SLC4A1)

AE1, the Cl^-/HCO_3^- exchanger of erythrocytes, was one of the first transporters to be physiologically identified. Among the members of the SLC4 family, AE1 was also the first to be cloned (Kopito and Lodish 1985). AE1 is also known as the Band 3 protein for its position in the SDS-polyacrylamide gel electrophoresis of the erythrocyte membrane proteins. AE1 (SLC4A1) represents 25% of the total membrane proteins of red blood cells and is the most abundant membrane glycoprotein in erythrocytes (Kopito and Lodish 1985). AE1 is an important structural component of red blood cell membranes and also involved in the movement of CO_2 from organs to the lungs.

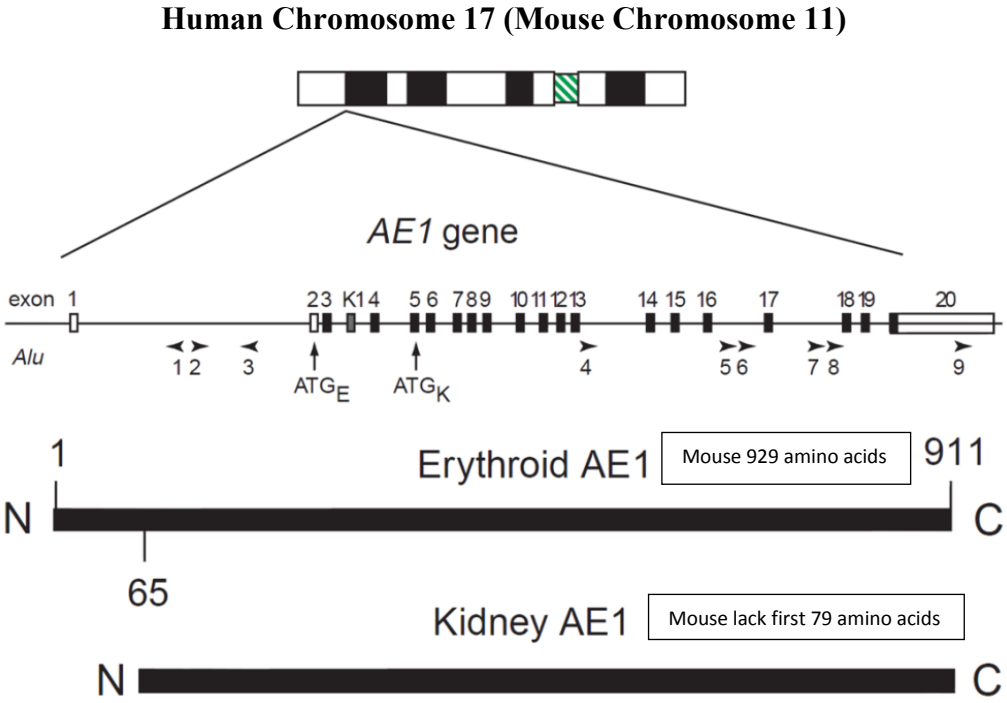

Figure 1.3 The human anion exchanger 1 (AE1) gene. The human AE1 gene is located on chromosome 17 (Mouse chromosome 11), spans 20 kb and consists of 20 exons and 19 introns. Exons are indicated by vertical filled and unfilled bars while introns by lines between the bars. The same gene encodes both the erythroid (eAE1) and the kidney (kAE1) protein isoforms using different promoters and start codons, resulting in different lengths of the respective polypeptides. The eAE1 contains 911 (mouse 929) amino acids whereas kAE1 lacks 65 (mouse 79) amino acids at the N-terminus (Yenchitsomanus 2003).

In the kidney, a shorter N-terminal variant of AE1 (kAE1) is the major isoform. This variant is derived from an alternative promoter site that results in a unique transcript that lacks the

first 65 amino acids (Human) of erythroid hAE1 (Brosius, Alper et al. 1989). AE1 (SLC4A1) is localized to the basolateral membrane of α-intercalated cells of the collecting duct (Alper, Kopito et al. 1988; van Adelsberg, Edwards et al. 1993; Huber, Asan et al. 1999; Alper, Darman et al. 2002) where it is essential for normal distal urinary acidification (Stehberger, Shmukler et al. 2007). AE1 is also expressed at lower levels in the heart with a cardiac specific isoform (Richards, Jaconi et al. 1999).

Ae1 knock out (KO) mice exhibit dRTA characterized by spontaneous hyperchloremic metabolic acidosis with low net acid excretion and inappropriate, alkaline urine without bicarbonaturia. The basolateral Cl^-/HCO_3^- exchange activity in acid secretory intercalated cells of isolated superfused Ae1 KO medullary collecting duct was reduced, but alternative bicarbonate transport pathways were upregulated. Ae1 KO mice also manifest nephrocalcinosis associated with hypercalciuria, hyperphosphaturia, and hypocitraturia. A severe urinary concentration defect in Ae1 KO mice was accompanied by dysregulated expression and localization of the aquaporin-2 water channel (Stehberger, Shmukler et al. 2007).

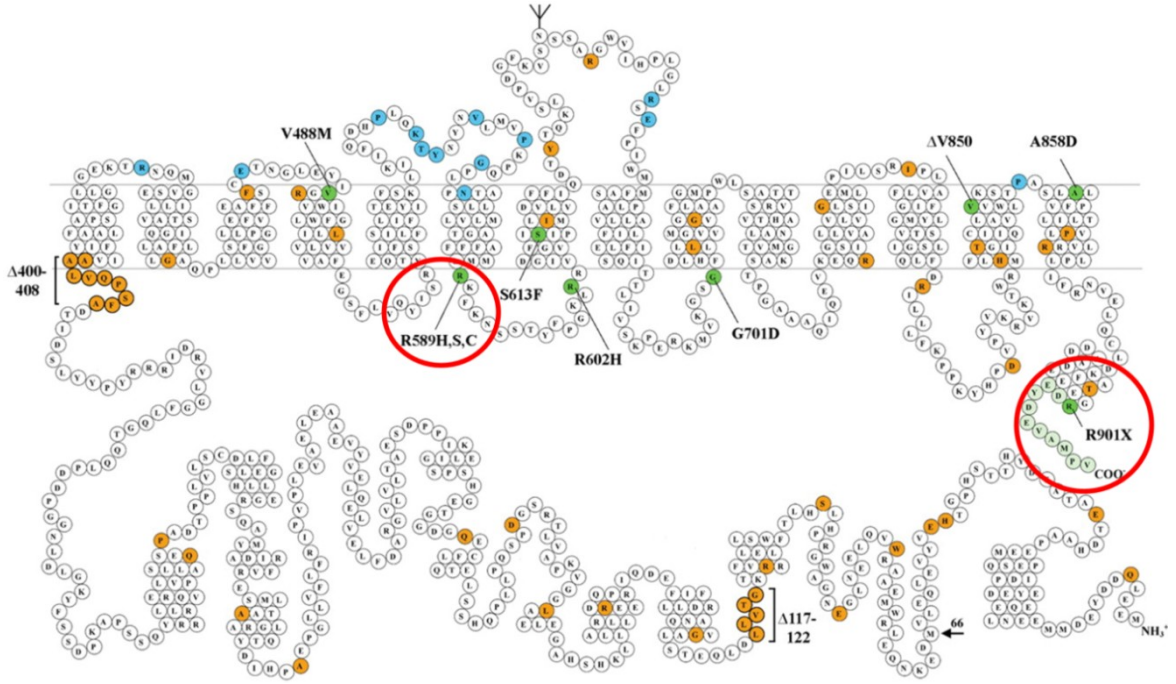

Figure 1.4 Topological model of the human AE1 secondary structure. Highlighted sites of missense or in-frame deletion mutations associated with dRTA (green); frameshift, nonsense, in-frame deletion, and missense mutations associated with hereditary spherocytosis (HS) and other erythroid phenotypes (orange); and sites of blood group polymorphisms (blue). Consecutive green residues at the C terminus represent the dRTA mutation R901X. Consecutive orange residues at Δ117–22 and Δ400–408 represent in-frame deletions. Red circles indicate the mutation selected to generate KI mice (Alper 2002; Zhu, Lee et al. 2003).

1.4.1. Topological organization of AE1

The model of the AE1 monomer can be seen in figure 1.4. AE1 is present as a dimer or tetramer in the red blood cell membrane (Alper 2009). The N-terminal domain of human AE1 is located in the cytoplasm, where cytoskeletal components, haemoglobin, or glycolytic enzymes can attach (Chu and Low 2006; Campanella, Chu et al. 2008; Chu, Breite et al. 2008). The N-terminal domain provides the binding sites for the erythroid cytoskeletal proteins ankyrin-1 (Chang and Low 2003; Stefanovic, Markham et al. 2007), protein 4.2 (Toye, Ghosh et al. 2005), the ERM protein 4.1R (Salomao, Zhang et al. 2008) and integrin-linked kinase (Keskanokwong, Shandro et al. 2007).

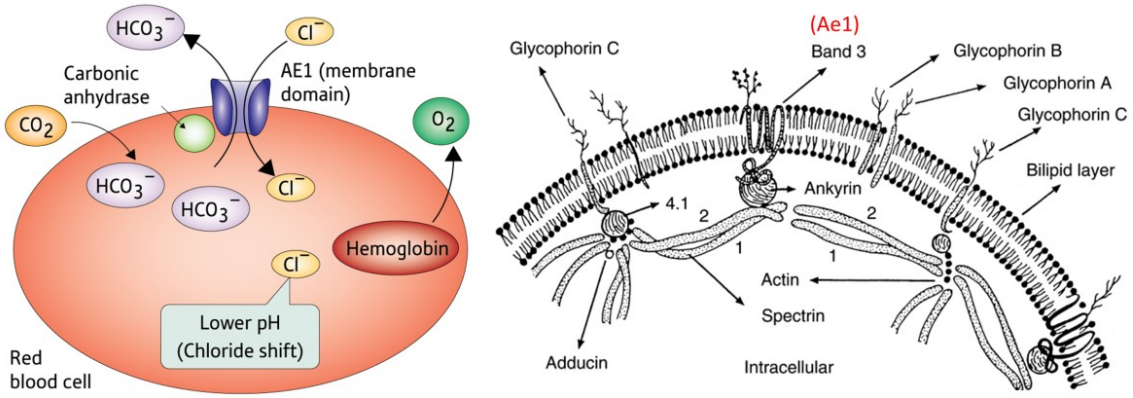

Figure 1.5 Structural and functional organization of human erythroid AE1 Adapted from (Wrong, Bruce et al. 2002) Schematic representation of exchange of bicarbonate (HCO_3^-) and chloride (Cl^-) ions via AE1, which promotes the release of oxygen from haemoglobin by lowering the pH within the red blood cell. (Riken research Japan)

Analysis of the AE1 amino acid sequence suggests a transmembrane domain model with 14 α-helical transmembrane spans, including two re-entrant loops in the C-terminal portion of the transmembrane domain as predicted by cysteine scanning mutagenesis studies of AE1 (Zhu, Lee et al. 2003; Zhu and Casey 2004). The chemical modification of AE1 in intact red blood cells has suggested that in addition to glutamate residues histidine, arginine and lysine residues each contribute to anion transport and selectivity (Stewart, Kurschat et al. 2008).

The binding site for the stilbene inhibitors is believed to be the lysine residues that react covalently (Salhany, Cordes et al. 2005). The central transmembrane domain of AE1 carries out the anion exchange function as well as carries the interaction sites for glycophorin A, which acts like a `β-subunit' for AE1 trafficking and optimal function in red blood cells (Young, Beckmann et al. 2000; Williamson and Toye 2008). The C-terminal tail of AE1 and

other SLC4 polypeptides contains one or more acidic motifs that may serve as a binding site for cytoplasmic carbonic anhydrase II (CAII) (Vince and Reithmeier 1998; Reithmeier 2001; Sterling, Reithmeier et al. 2001).

1.5. The Kidney as an organ for acid-base balance

1.5.1. Basic anatomy

The Kidneys are paired retroperitoneal organs in the posterior part of the abdomen on each side of the vertebral column (Madsen, Nielsen et al. 2008). Two major regions can be seen in the longitudinal dissection of the kidney in figure 1.6, the cortex and the medulla. The medulla can be further divided into the outer and the inner medulla and the outer medulla sub-divided into an inner and an outer stripe (figure 1.7).

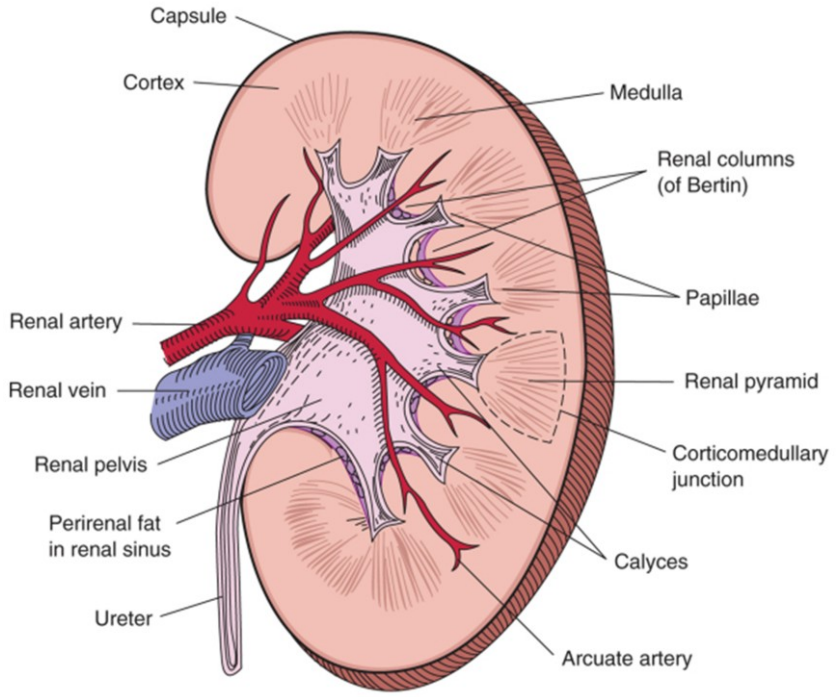

Figure 1.6 The bisected kidney depicting important anatomic structures. (Madsen KM, Nielsen S, Tisher CC: Anatomy of the Kidney. In: Brenner and Rector's the Kidney, 8th ed., WB Saunders, 2008)

1.5.2. Physiology of acid secretion by the kidney

The nephron is the basic functional unit of the kidney. The primary urine is filtered in the glomerulus, and then the filtrate passed the tubular system of the kidney. The post glomerular tubules of the nephron are lined by highly polarized cells; one surface is in contact with the urine and the other with interstitial fluid (Devonald 2004). Therefore, transport proteins reside very strictly either to the apical or the basolateral side of the plasma membrane. Moreover, a

highly specialized machinery is required to bring these transport proteins to their appropriate site of action (Devonald 2004).

The kidneys control the acid-base homeostasis by the following two ways: (1) reabsorption of bicarbonate (HCO_3^-) filtered at the glomerulus and (2) the excretion of acid (H^+) and ammonium (NH_4^+) to accomplish production of "new" bicarbonate to replace that consumed by dietary or endogenous metabolic acids (Hamm and Nakhoul 2008).

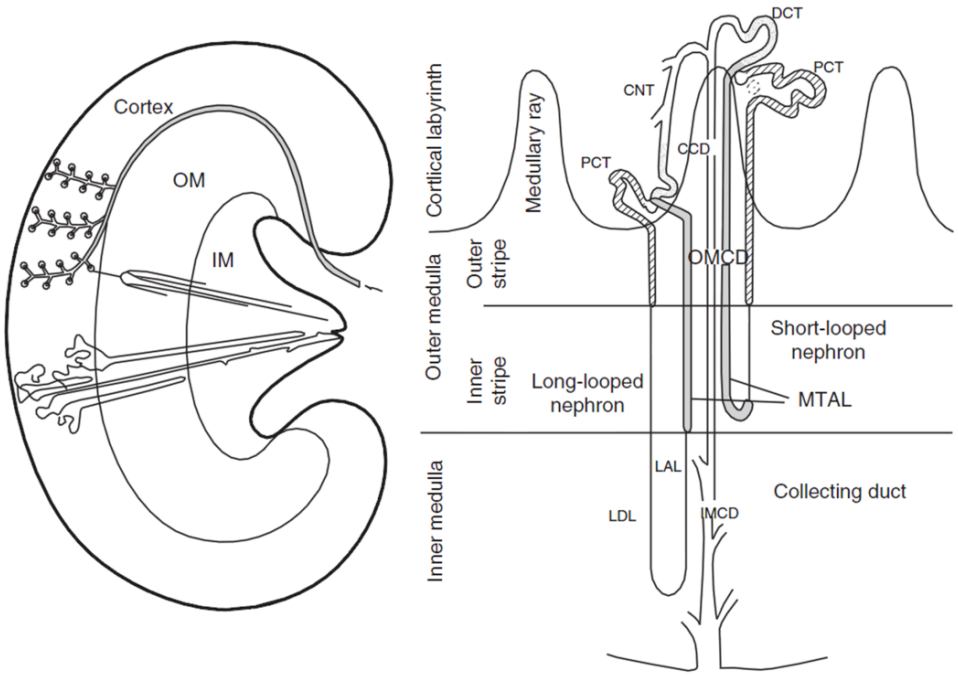

Figure 1.7 Basic anatomy of the kidney and nephron. The tip of the conical inner medulla (IM) known as papilla; PCT, proximal convoluted tubule; LDL, long descending thin limb of Henle; LAL, long-ascending thin limb of Henle (inner medulla only); MTAL, medullary thick limb of Henle (outer medulla only); DCT, distal convoluted tubule; CNT, connecting tubule; CCD, cortical collecting duct; OMCD, outer medullary collecting duct; IMCD, inner medullary collecting duct. (Thomas 2009)

Reabsorption of the filtered HCO_3^- in the proximal tubule accounts for the ≈75% to 80% of the total HCO_3^- in glomerulus filtrate. In proximal renal tubular acidosis non-absorbed HCO_3^- spills into the urine, ultimately lowering plasma HCO_3^-. However, normally almost all of the filtered HCO_3^- is reabsorbed (Shayakul and Alper 2000; Hamm and Nakhoul 2008). The mechanism is based on the reabsorption of H^+ and HCO_3^- ions are generated in tubular cells with the help of CAII. The H^+ ions are then secreted into the lumen via a Na^+/H^+ exchanger in the apical membrane and the HCO_3^- ions transferred via a basolateral Na^+–HCO_3^- co-transporter (Unwin, Shirley et al. 2002). The H^+-ATPase actively secrete H^+, and these ions react with filtered HCO_3^- to form H_2CO_3, which is rapidly converted to CO_2 and H_2O by another form of CA(IV) present in the luminal membrane of the proximal tubule. The CO_2

and H_2O then diffuse into the cell (Laing, Toye et al. 2005). Generation of "new" HCO_3^- is the second important role of kidney; "new" HCO_3^- refers to HCO_3^- that is produced by the kidneys, but that was not filtered at the glomerulus. Production of new HCO_3^- is accomplished by excretion of titratable acid (TA) and excretion of NH_4^+. The titratable acid equals the amount of acid (H^+) that is added to tubular fluid along the nephron, thus titrating urinary buffers. Titratable acid is a function of both urine pH and buffering capacity (Hamm and Simon 1987).

HCO_3^- that is not reabsorbed by the proximal tubule can be reabsorbed by the epithelial cells of the thick ascending limb. The major apical mechanism for HCO_3^- entry into the cell is NHE3, with basolateral membrane Cl^-/HCO_3^- exchanger AE2/SLC4A2 probably mediating base efflux across the basolateral membrane into the interstitium (Watts and Good 2004).

The distal nephron includes distal convoluted tubule, the connecting tubule, the cortical collecting duct, the outer medullary collecting duct, and the initial portion of the inner medullary collecting duct. The connecting segment and collecting ducts consists of two major cell types; principal cells account for approximately 60% of tubular epithelial cells and intercalated cells for the remaining 40%. Two main types of intercalated cells are present in the connecting segment and cortical collecting duct the type A or α-intercalated cells which secrete H^+ and type B or β-intercalated cells which secrete HCO_3^- (Batlle, Ghanekar et al. 2001; Wagner and Geibel 2002).

Acid secreting α-intercalated cells express the vacuolar H^+-ATPase at the apical membrane and the Cl^-/HCO_3^- exchanger (AE1) at the basolateral membrane. Conversely, the HCO_3^- secreting β-intercalated cells express the H^+-ATPase at the basolateral membrane and the Cl^-/HCO_3^- exchanger (Pendrin) at the apical membrane. All intercalated cell types express the cytoplasmic carbonic anhydrases CA II (Kurschat and Alper 2008).

The complex heteromeric H^+-ATPase is encoded by 14 genes and comprise of two major domains, a transmembrane V0 segment and an intracellular catalytic V1 segment. The B1 and a4 subunit is encoded by the ATP6V1B1 and ATP6V0A4 genes respectively, are expressed at high levels in the collecting duct intercalated cells, as well as in narrow and clear cells of the epididymis, in the ciliary body of the eye, in the inner ear, and in the placenta (van Hille, Richener et al. 1994; Smith, Skaug et al. 2000; Stehberger, Schulz et al. 2003; Wagner, Finberg et al. 2004).

The acid secreting α-intercalated cells transport HCO_3^- across the basolateral membrane by the SLC4A1 electroneutral Cl^-/HCO_3^- exchanger, kidney AE1 (kAE1) and the β-intercalated cells secrete HCO_3^- through an apical Cl^-/HCO_3^- exchanger (Pendrin)(see Figure 1.8) (Alper,

Natale et al. 1989; van Adelsberg, Edwards et al. 1993; Royaux, Wall et al. 2001). Expression of pendrin is reduced in rat kidney by acid loading and modestly increased in response to alkali loading (Wagner, Finberg et al. 2002; Frische, Kwon et al. 2003; Petrovic, Wang et al. 2003).

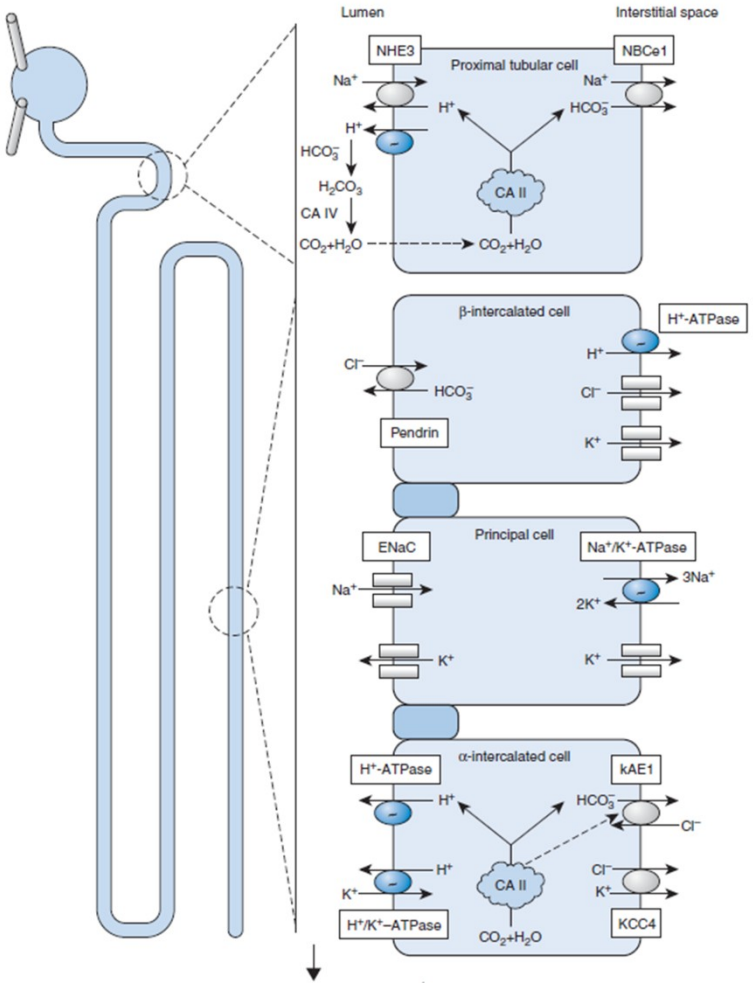

Figure 1.8 Schematic model of renal acidifying mechanisms: HCO_3^- reabsorption in proximal tubular cells and H^+ secretion in α-intercalated cells of the collecting duct.
Protons are secreted at the apical membrane by the NHE3 Na^+/H^+ exchanger and by the vacuolar H^+-ATPase in the proximal tubule. Carbonic anhydrase (CA) IV catalyzes the formation of CO_2 from H_2CO_3 and the CO_2 can enter intracellularly by diffusion. H_2CO_3 is formed in the presence of cytosolic CA II, and HCO_3^- is transported out of the cell at the basolateral surface by Na^+/HCO_3^- co-transporter NBCe1.
In α-intercalated cells of the cortical collecting duct, protons are transported out of the cell into the lumen by the vacuolar H^+-ATPase. HCO_3^- generated inside the cells leaves via the anion exchanger 1 (kAE1) in exchange for Cl^- entry across the basolateral membrane. The β-intercalated cells secrete HCO_3^- in exchange for Cl^- via their apical anion exchanger pendrin. In contrast to α-intercalated cells, they can express a basolateral vacuolar H^+-ATPase. (Kurschat and Alper 2008).

The anion exchanger pendrin (PDS, SLC26A4) was initially identified as being mutated in patients suffering from Pendred syndrome (Everett, Glaser et al. 1997; Scott, Wang et al. 1999). In the kidney, pendrin is specifically expressed on the luminal membrane of β-intercalated cells (Royaux, Wall et al. 2001; Kim, Kwon et al. 2002). It mediates Cl^-/HCO_3^- exchange releasing bicarbonate into the urine and reabsorbing chloride. Pendrin is critical for bicarbonate secretion during metabolic alkalosis (Royaux, Wall et al. 2001).

1.6. Familial renal tubular acidosis

The importance of renal acid-base transport has been revealed by mutations found in several genes involved in this task in patients with inborn forms of renal tubular acidosis. Loss of function in AE1, ATP6V1B1 and ATP6V0A4 genes due to different mutations are possible

causes of hereditary renal tubular acidosis (RTA). The underlying mechanisms have been also studied in genetically altered mouse models and cell culture systems (Finberg, Wagner et al. 2005; Wagner, Kovacikova et al. 2006).

The term renal tubular acidosis (RTA) is applied to a group of transport defects in the reabsorption of bicarbonate (HCO_3^-), the excretion of protons (H^+), or both. This condition was first described in the 1930's (Lightwood 1935; Karet, Gainza et al. 1998; Rodriguez Soriano 2002). Distal RTA arises when the collecting duct fails to remove the excess acid load of a normal diet into the urine and it is often associated with mutations in the AE1 protein (Quilty, Li et al. 2002; Karet 2008).

In the distal type of RTA (dRTA), the secretion of hydrogen ions (H^+) in the distal tubule of the nephron is impaired, whereas the proximal reabsorption of bicarbonate and other solutes is intact (Batlle, Ghanekar et al. 2001). The classic type of RTA (type I or dRTA) is characterized by a reduced net acid excretion and inability to lower urinary pH below 5.5 before or after acid loading (Batlle and Kurtzman 1982; Caruana and Buckalew 1988). Hereditary dRTA comes in three variants: autosomal dominant and autosomal recessive with or without deafness (Fry and Karet 2007; Alper 2010). Genetic defects in AE1 and the a4 or B1 subunit isoforms of vH^+-ATPase lead to defective acid secretion by intercalated cells in the distal tubule and collecting duct, which results in renal tubular acidosis (Karet, Finberg et al. 1999; Alper 2002).
Primary dRTA results in metabolic acidosis of variable severity, usually with hypokalemia, hypercalciuria, and hypocitraturia. Rickets and osteomalacia can develop in both dominant and recessive forms, although dominant disease typically presents more mildly in adolescence or adulthood, and recessive in infancy/early childhood where growth retardation is common (Karet 2002). Chronic metabolic acidosis decreases renal excretion of citrate while increasing calcium excretion, which favors the formation of kidney stones and nephrocalcinosis (Batlle, Ghanekar et al. 2001). Hereditary autosomal dominant dRTA in general (but not always) presents at later age, sometimes not until adulthood, and with milder phenotype than the recessive form of dRTA (Karet 2002; Fry and Karet 2007).

The diagnosis of classic dRTA is based on the finding of a high urine pH in the setting of a systemic metabolic acidosis. The systemic pH may be fully compensated (so called "incomplete" dRTA), in which case a failure of urinary acidification should be addressed pharmacologically by an oral ammonium loading test or the recently proposed combination of

furosemide/fludrocortisone as an alternative (Batlle and Kurtzman 1982; Unwin, Shirley et al. 2002). Distal renal tubular acidosis can be treated with appropriate doses of oral alkali supplementation (5–15 mEq · kg^{-1} · day^{-1} of bicarbonate) to reverse the metabolic acidosis and normalize bone growth in children (Kurtzman 2000).

1.7. Mutations associated with the human AE1 gene

AE1 is the most abundant protein in erythrocytes and highly expressed in the acid-secreting α-intercalated cells of the renal collecting duct. In erythrocyte, eAE1 stabilizes the underlying cytoskeleton and increases the CO_2 carrying capacity of blood. In the kidney, intercalated cell absorbs HCO_3^- via kAE1 upon apical H^+ excretion into the urine. Therefore, mutations in AE1 gene are thus, not surprisingly, characterized by erythroid and renal phenotypes (Kurschat and Alper 2008; Stewart, Kurschat et al. 2008).

1.7.1. Mutations in AE1 causing erythrocyte phenotypes

Hereditary spherocytosis (HS) is a common congenital haemolytic anaemia which is associated with osmotically fragile red cells with varying degrees of abnormal spheroidal shape. This disease can result from defects in any of the red cell skeletal components which are involved in stabilizing the lipid bilayer (Hassoun and Palek 1996). Mutations in the erythroid isoform of AE1 (eAE1) causes hereditary spherocytic (HS) anemia. Many of these mutant alleles generate instable transcripts, therefore resulting erythrocytes express reduced total levels of the wild type eAE1 polypeptide, but often in the setting of dosage compensation by the wild type allele (Alper 2009). The autosomal dominant HS patients almost always have apparently normal renal acidification. Alterations in the conserved arginines in the membrane domain result in hereditary spherocytosis (Jarolim, Rubin et al. 1995). The Southeast Asian Ovalocytosis (SAO) is caused by an autosomal dominant, heterozygous in-frame deletion of AE1 amino acids 400–408 (see figure 1.4). The deletion of these amino acids in AE1 alters the shape of erythrocytes (Southeast Asian ovalocytosis, SAO) but exhibits no clinical pathology. It is also suggested that the prevalence of SAO in areas prone to cerebral malaria epidemics provides a natural protection because of increased rigidity of the erythrocyte membrane (Tanner 1997; Allen, O'Donnell et al. 1999).

1.7.2. Distal renal tubular acidosis (dRTA) due to AE1 mutations

Distal renal tubular acidosis (dRTA) is characterized by impaired urinary acid excretion in the distal part of kidney tubules. In most cases hereditary dRTA caused by the defect in acid

secreting intercalated cells (α-IC) of the collecting ducts is due to mutations in AE1. Missense mutations in kidney AE1 (SLC4A1) are associated with autosomal dominant distal tubular acidosis, which is characterized by malfunctioning urinary acidification (Jarolim, Shayakul et al. 1998).

Several mutations in the membrane spanning domain of AE1 at R589 in TM 6 (Bruce, Cope et al. 1997; Jarolim, Shayakul et al. 1998; Karet, Gainza et al. 1998), S613F in TM 7 (Bruce, Cope et al. 1997), DV850 (Bruce, Wrong et al. 2000), and an 11-amino acid deletion in the cytoplasmic C terminus (Karet, Gainza et al. 1998) can produce an autosomal dominant distal renal tubular acidosis (dRTA) that has no associated erythrocyte pathology. Most of these mutations (R589H, R589C, R589S, G609R, R901X) caused aberrant targeting of kAE1 in polarized kidney cells of the transporter (Devonald, Smith et al. 2003; Toye, Banting et al. 2004), but few others (G701D and S773S) resulted in AE1 misfolding (Kittanakom, Cordat et al. 2004). The AE1 mutants associated with dominant dRTA expressed in *Xenopus* oocytes usually exhibit normal or modestly reduced Cl^- and HCO_3^- transport function which cannot explain the renal phenotype. The defective urinary acidification is thought to arise from the trafficking defects of these mutant polypeptides in the polarized epithelial cells.

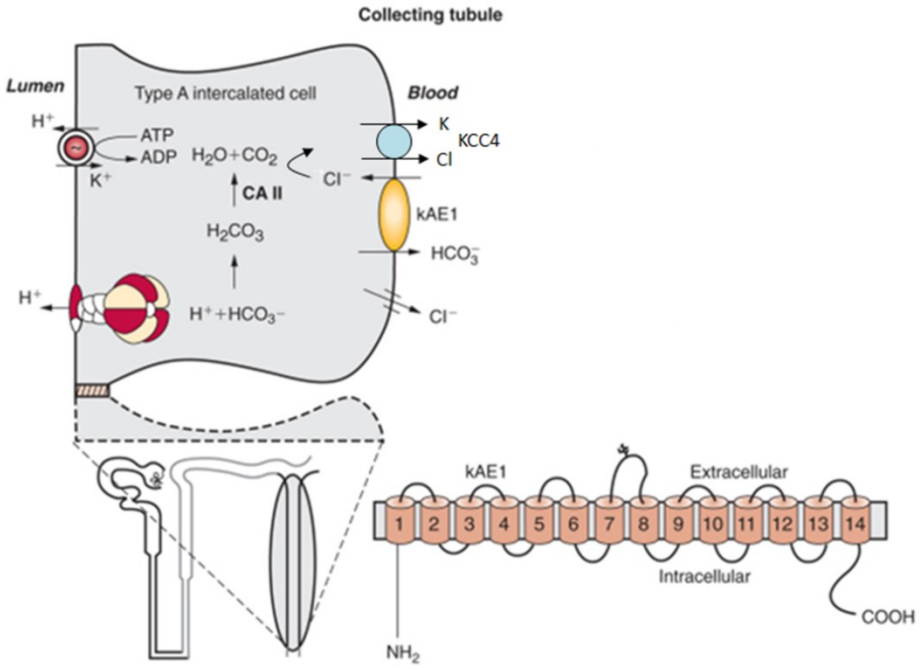

Figure 1.9 The α-intercalated cell in the collecting tubule of the distal part of the nephron
Type A-intercalated cells (α-IC) in the collecting tubule secrete H^+ into the lumen via H^+ -ATPase. The generation of H^+ is catalysed by carbonic anhydrase II the resulting HCO_3^- is transported across the basolateral membrane through the AE1 HCO_3^-/Cl^- exchanger. Mutations in AE1 and the B1 unit of H^+-ATPase cause autosomal dominant and autosomal recessive distal renal tubular acidosis (Bonnardeaux and Bichet 2008).

Some of the dominant dRTA mutant proteins such as AE1 R589H (Jarolim, Shayakul et al. 1998) and S613F are retained in the endoplasmic reticulum, and exert a dominant negative trafficking phenotype within heterodimers with the wild type AE1 polypeptide (Alper 2009).
A second group carries only one truncating mutation, AE1 R901X causes the deletion of 11 amino acids in the C-terminal in a dominant dRTA manner. It has been shown that this mutant accumulates either uniquely in the apical membrane or in both apical and basolateral membranes of polarized MDCK cells, possibly due to the loss of a sorting or retrieval signal related to residues 904–907 (Devonald, Smith et al. 2003; Toye, Banting et al. 2004; Cordat, Kittanakom et al. 2006). It is proposed that the presence of functional, mistargeted kAE1 in the apical membrane of the α-IC cells likely short-circuits acid secretion through a co-dominant mechanism. However, substantial intracellular retention of this mutant has been observed (Cordat 2006) and more extensive, engineered truncation of the C-terminal tail further increased intracellular retention of the mutant protein (Dahl, Jiang et al. 2003; Cordat 2006). Mistargeting of kAE1 to the apical membrane can be due to the mutation of sequence elements in both the N-terminal cytoplasmic domain and in the C-terminal cytoplasmic tail. Basolateral localization of human kAE1 possibly depends upon two phosphorylatable tyrosines, Y359 in the N-terminal cytoplasmic domain and Y904 in the C-terminal tail (Toye, Banting et al. 2004).

The homozygous AE1 mutants causing recessive dRTA are geographically localized to Southeast Asia (Tanphaichitr, Sumboonnanonda et al. 1998; Bruce, Wrong et al. 2000).
The AE1 G701D is a common example of a recessive dRTA mutation. In this case the mutant protein is retained inside the cell, but the trafficking to the cell surface can be rescued by coexpression of glycophorin A. This rescue by an erythroid protein which is not expressed in renal intercalated cells can explain the normal erythroid AE1 expression in these patients (Tanphaichitr, Sumboonnanonda et al. 1998). The recessive dRTA caused by compound heterozygous mutations of AE1 is sometimes accompanied by the south asian ovalocytosis or the hereditary spherocytosis. The functionally inactive SAO allele fails to complement a recessive loss-of-function in the α-intercalated cell (Bruce, Wrong et al. 2000). The knock out animal models of AE1 exhibit disease phenotypes, severe hemolytic anemia (Peters, Shivdasani et al. 1996) and a hypercoagulable state (Hassoun, Wang et al. 1998), accompanied by complete dRTA (Stehberger, Shmukler et al. 2007).

1.8. Aim of this study

Renal tubular acidosis (RTA) is a failure of renal regulatory mechanisms to maintain systemic pH homeostasis. Hereditary distal renal tubular acidosis (dRTA) is associated with mutations in genes that result in a defect of H^+ secretion by intercalated cells in the distal nephron. The anion exchanger 1 (AE1) is expressed in the basolateral membrane of α-intercelated cells of the kidney tubules and is thought to support urinary acid secretion by retrieving back HCO_3^- into the blood. Mutations in the human AE1 gene are supposed to result in mistargeting or loss of functional protein.

The main focus of this study was to generate mouse models for dRTA to study the pathophysiology of the disease by introducing the respective mutation into the mouse Ae1 gene. The underlying cellular mechanisms of dRTA are poorly understood. So, Ae1-knock in mice were generated to address **1.** the underlying cellular pathology, **2.** to study the potential compensatory mechanisms and **3.** to access the long term effects of dRTA on the formation of kidney stones and other secondary effects associated with dRTA.

These mouse models can also be used to study the effect of the impaired protein expression in homozygous condition that has so far not been detected in human patients.

2. Materials and methods

2.1. Materials

2.1.1. Chemicals

The chemicals used during this work were of analytical grade and purchased from sigma, merck, or carl roth. Enzymes were obtained from Roche, Invitrogen, New England Biolabs and Fermentas. Oligonucleotides were synthesized at MWG-Biotech. Radioactive nucleotides were obtained from Hartmann analytic.

2.1.2. Microbial strains and laboratory animals

The list of bacterial strains and experimental organisms were described in table 2.1.

Table 2.1 Organisms and bacterial strains used in this study

Bacterial Strain	Escherichia coli TOP' 10	Stratagene
Bacterial Strain	Escherichia coli XL1 blue	Stratagene
Laboratory Animals	*Mus musculus* (C57BL/6J)	Animal facility at the University Hospital Jena (Research centre Jena)

2.1.3. Bacterial vectors

The following bacterial vectors were used in order to clone the targeting construct to produce KI mouse lines.

Table 2.2 Vectors used for cloning of the targeting vectors

Vectors	Notes
pBluescript SK (+/–)	Stratagene
pKO Scrambler 901	Stratagene

2.1.4. Antibodies

Following antibodies and their respective working concentrations for Western blotting and/or immunohistochemistry experiments were used.

Table 2.3 Antibodies used for Western Blotting and Immunohistochemistry

	Working concentration		
Antibodies	Western Blot	Immunohistochemistry	Source
anti Pendrin guinea pig	1:20000	1:1000	Prof. Wagner Lab Zurich
anti Pendrin rabbit	1:20000	1:1000	Prof. Wagner Lab Zurich
anti AE 1 guinea pig	1:20000	1:1000	Prof. Wagner Lab Zurich
anti AE 1 rabbit	1:20000	1:1000	Prof. Wagner Lab Zurich
v-ATPase B1/2(H-180)	1:1000	1:500	Santa Cruz Biotechnologies
anti β-actin	1:1000		Santa Cruz Biotechnologies
ECL mouse IgG, HRP-Linked (from sheep)	1:4000		Amersham(GE healthcare)
ECL rabbit IgG, HRP-Linked (from donkey)	1:4000		Amersham(GE healthcare)
anti-guinea pig IgG Alexa Fluor 488		1:1000	Molecular probes Invitrogen
anti-rabbit IgG Alexa Fluor 488		1:1000	Molecular probes Invitrogen

2.2. Methods

2.2.1. Microbiology methods

2.2.1.1. Preparation of chemocompetent bacteria

The preparation of chemo competent bacteria was started with a preculture of E. coli XL1 Blue in 2 ml ψ broth medium (LB-broth medium, 4 mM $MgSO_4$, 10 mM KCl, 3 µg / ml tetracycline adjusted to pH 7.0 and autoclaved), grown overnight at 37 ° C while shaking. The next morning, 500 ml ψ broth medium was inoculated with 1 ml of the preculture and grown at 37 ° C with shaking until an optical density of 600 nm (OD600) of 0.3-0.6 was achieved. After removal of the culture from the incubator, the bacteria were cooled on ice and pelleted in a centrifuge (Beckman) at 3000 rpm for 5 minutes at 4 ° C. The supernatant was discarded and the pellet was resuspended in 150 ml icecold TFB1 buffer (15% glycerol, 10 mM $CaCl_2$, 30 mM potassium acetate, 100 mM RbCl, 50 mM $MnCl_2$, pH 5.8 adjusted with CH_3COOH) and incubated on ice for 60 minutes. After incubation on ice the bacterial suspension was centrifuged again at 3000 rpm for 5 minutes at 4 ° C.

The supernatant was discarded and the pellet was resuspended in filtered sterile, ice-cold TFB2 buffer (15% glycerol, 10 mM MOPS, 75 mM $CaCl_2$, 10 mM RbCl), by pipetting. The competent cells were divided into aliquots on ice (300 µl). The aliquots were immediately snapfrozen in liquid nitrogen and stored at -80 °C until use.

2.2.1.2. Transformation of competent bacteria

An aliquot of chemocompetent bacteria was thawed on ice, and the plasmid DNA to be transformed was mixed with 50µl of competent bacteria and incubated on ice for 20 minutes. To induce the uptake of the plasmid the bacteria was given a heat shock at 37°C for 2 minutes. After a brief cooling on ice, 300µl of SOC medium (0.5% yeast extract, 2% tryptone, 10 mM NaCl, 2.5 mM KCl, 10 mM $MgCl_2$, 10 mM $MgSO_4$, 20 mM glucose, pH 7.0) was added and incubated at 37°C on shaker for 45 minutes. The bacteria were then pelleted by centrifugation at 4000rpm for 5 minutes. 300 µl of supernatant was removed and the pellet was resuspended in the remaining SOC medium. The suspension was plated out on LB-Agar plates containing the appropriate antibiotic. The inverted plates were incubated at 37 °C overnight.

2.2.1.3. Screening of lambda phage library

To prepare the targeting vectors for generation of transgenic mice by homologous recombination DNA fragments of 15-25 kb containing the desired gene are necessary. To obtain such a genomic DNA fragment a phage library (Lambda FIX II, Stratagene) was used. The phage library carries the bacteriophages with incorporated mouse genomic DNA fragments flanked by the phage genome. Isolation of the mouse genomic fragment carrying the desired gene was done with the help of a radiolabelled probe binding to the exons of interest of the particular gene.

The screening of phage library is based on transduction principle in which, mixture of phages and bacteria were grown on agar plates. The DNA is subsequently transformed to a positively charged nylon membranes with a high binding capacity for nucleic acids. These membranes were hybridized with radiolabelled probe generated against part of specific genomic fragments and analysed to obtain genomic fragments of gene of interest to use for further cloning in bacteria.

E. coli XL-1 Blue MRA bacteria were grown at 37 °C in 100 ml LB medium containing 0.2% maltose and 10 mM $MgSO_4$ until the optical density of OD600 = 1 was achieved. Maltose is an essential part of the medium as it helps to transduce bacteria via the Maltose receptor of λ phage. The MRA bacteria were pelleted by centrifugation at 3000 rpm for 15 minutes at 4 °C. The bacterial pellet was washed with 10 mM $MgSO_4$ and resuspended again in 20 ml of 10 mM $MgSO_4$ and stored at 4°C for up to 2 weeks.

The screening of the λ phage library was carried out in two different steps and by using two different sizes of agar plates. 150 mm plates were used for the entire library at first step as well as at the end for preparative isolation of a bacterial clone carrying the DNA fragment of interest and 90 mm plates were used for the further enrichment of clones with the desired fragment of genomic DNA. 450 µl and 150µl of MRA bacterial suspension were used for 150 and 90 mm plates respectively. 150 µl or 450µl of MRA bacterial suspension was incubated with (a predetermined titrated amount of) λ phages at 37 °C on shaker for 20 minutes.

This bacterial-phage mixture was added to 9 ml (150 mm plate) or 3 ml (90 mm plate) pre-melted (at 47 ° C in water bath) 1% agar LB medium, mixed well and the top agar was spread evenly on pre-warmed agar plates of the respective size. The resulting plates were dried for about 15 minutes at room temperature and incubated at 37 °C overnight.

After overnight incubation, plates grown with plaques were cooled to 4 °C, so that nylon membrane (Biodyne A0.45 microns, 82 and 132 mm, Pall Life Sciences) can easily be used to transfer the plaque DNA on top agar. Membranes were incubated with cooled plates for 1-2 minutes, during this time a sharp scalpel was used to cut the membrane together with agar at 3 different positions to give an orientation to incubating membranes for later analysis.

After this short incubation DNA side of membranes lying upside down were treated with denaturing buffer (1.5 M NaCl, 0.5 M NaOH) and with neutralization buffer (1.5 M NaCl, 0.5 M Tris, pH 8.0) for 2 minutes and 5 minutes respectively. The membranes were then incubated for 1 minute in wash buffer (0.2 M Tris, 2X SSC) and air-dried. The DNA was fixed on membranes by baking at 80 °C for 2 hours.

To find out positive clones carrying the desired gene fragment from the λ phage library the membranes were hybridized with respective radioactively labelled probe (see Section molecular biology). After hybridization and subsequent washing, membranes were exposed to X-ray films to visualize the signal indicating the presence of positive clones. Agar plates were place on the X-ray films with the correct orientation and pieces of agar were removed as single clones according to the location of signal. Agar pieces with positive clones were suspended in 1 ml SM buffer (5.8 g NaCl, 2 g $MgSO_4.7H_2O$, 50 ml Tris-HCl pH 7.5, 5 ml 2% gelatine in 1L H_2O) with 20 µL of chloroform and incubated overnight at 4 °C after vortexing.

After overnight incubation the mixture containing agar pieces was diluted 1:1000 times to ultimately isolate a single clone in another round of selection, 1µl of this dilution were incubated with 10, 100 and 150µl of MRA bacteria for 20 minutes at 37 °C with shaking. Mixture of phage clones with MRA bacteria was added to 3 ml (90 mm plate) pre-warmed 1% agarose in LB medium at 47 °C and evenly spread on a LB plate. The resulting plates were dried for 15 minutes at room temperature and then incubated at 37 °C overnight. Membranes were incubated again with plates as mentioned above by following the same procedure to ultimately isolate a single phage clone with the DNA fragment of desired gene. Once the single phage clones were obtained, the titer of the phage suspension was determined and 150 mm plates were used to prepare the DNA (see DNA preparation of λ phage).

2.2.2. Molecular biology methods

2.2.2.1. Cloning of targeting vector

2.2.2.1.1. Restriction digest

In order to clone existing DNA or newly synthesized PCR products, restriction digest of plasmid or genomic DNA was performed by using restriction enzymes with the respective buffers from Fermentas and New England Biolabs. For the cloning of DNA fragments into appropriate vector, 1-2 µg of insert and 5 µg of vector were digested with 10 units of the respective restriction enzymes and incubated overnight at 37 °C in order to achieve a complete digestion.

Special conditions were applied to digest DNA for Southern blots. 5-10 micrograms of genomic DNA with 20-30 units of restriction enzyme was incubated at the respective temperature overnight. The next morning 10 units of enzyme was added and incubated for at least 1 hour to further enhance the restriction digest efficiency.

2.2.2.1.2. Blunting of sticky ends and dephosphorylation

To fill the DNA overhanging ends (blunting of sticky ends) T4 DNA polymerase was used. Before starting the filling of overhanging ends, restrictions enzymes were deactivated by heating at 65 or 80 °C for 20 minutes and after cooling on ice, 1 µl of 10 mM dNTPs and 1 µl T4 DNA polymerase (Fermentas) was added and incubated at 12 °C for 20 minutes. Finally, the T4 DNA polymerase was inactivated at 75 °C for 20 minutes. Dephosphorylation of restricted vectors was done by alkaline phosphatase (Roche). For this purpose the restriction enzymes were inactivated by heating and then incubated with 1µl of Calf Intestine Alkaline Phosphatase for 60 minutes at 37 °C. Vector DNA was purified by gel electrophoresis after heat inactivation at 75 °C.

2.2.2.1.3. Agarose gel electrophoresis

Separation of DNA fragments from PCR reactions or restriction digests was achieved by horizontal gel electrophoresis carried out in agarose gel chambers (Amersham Biosciences).

Agarose concentrations between 1 and 2% were used depending on the respective DNA fragment size. Agarose was boiled in 1X TAE buffer (40 mM Tris-acetate, 1 mM EDTA), and prior to pouring the gel, 0.5 µg / ml ethidium bromide was added.

For gel loading the DNA samples were mixed with 6X DNA loading buffer (10 mM Tris-HCl, 30% glycerol, 0.25% bromophenol blue, 0.25% xylene cyanol). The DNA fragments

were separated in 1X TAE by applying a constant voltage between 30 - 150 V depending on the desired separation time. After separation the DNA fragments were visualized under UV light.

2.2.2.1.4. DNA ligation

In order to create the desired plasmid constructs, insert and vector fragments with compatible ends were ligated to each other. Ligation efficiency depends on various factors, such as complete digestion of the respective restriction fragments as well as the ratio between insert to vector. This ratio was determined by molecular weights of respective DNA fragments and their concentration in the ligation mixture. Such ratios were adjusted accordingly to insert a 20-30 bp linker or a few kb fragments into a vector.

For a typical ligation mixture, 1µl of vector, 2µl of 10X ligation buffer, 1µl of T4 DNA Ligase (New England Biolabs) and respective amount of a DNA fragment to be ligated was added and the final volume of 20 µl was adjusted with H2O. Ligation mixture was incubated overnight at 4°C and 2-5 µl of this ligation mix was used to transform chemocompetent bacteria.

2.2.2.1.5. DNA sequencing

In order to verify that the reading frame and the nucleotide sequence of cloned constructs as well as for the analysis of the point mutation created in targeting vector or knock in mice, DNA sequencing was performed. For sequencing reactions 1µl of plasmid or 1µl of mouse genomic DNA was added in a 0.2 ml tube, along with 10 pmol of the sequencing primers, 2µl of sequencing buffer, 1 µl of Big Dye (ABI) and H_2O up to 10µl. In a thermocycler the 10 µl reaction was subjected to the following sequencing program cycle.

Table 2.4 Cycling temperatures and duration of Sequencing PCR

Step	Temperature	Time
Initial denaturation	96°C	60 sec
Denaturation	96°C	10 sec
Annealing	55°C	8 Sec
Elongation	60°C	4 min
	4°C	∞

These steps were repeated for 28 times.

After completion of the reaction, the DNA was precipitated by adding 1/10th vol. of 3 M Na Acetate (pH 5.5) and 2.5 vol. of ethanol, and centrifuging for 10 min at 14000 rpm. After a

70% (v/v) ethanol wash, the pellet was dried and solved in 10µl of Hi-Di™ Formamide (ABI) for further analysis.

2.2.3. Isolation and purification of nucleic acids

2.2.3.1. Isolation of DNA from λ-phage

Mouse genomic DNA was purified from λ-phage grown on three fully lysed plates with large plaques. After cooling the plates to room temperature, 10 ml of SM buffer was added to each plate and incubated overnight at 4 °C with gentle shaking. The supernatant from all three plates was collected in a 50 ml falcon and 1 ml of chloroform was added in the tube. After vigorous vortexing bacterial cell debris were pelleted by centrifuging at 4000 g, for 15 minutes at 4 °C.

Beckman Ultra-Clear centrifuge tubes (25x89 mm) were used for CsCl density gradient purification of phage DNA. 25 ml of the supernatant was taken into the tube containing 3 ml of 3 M CsCl (prepared in SM buffer) forming the bottom layer and 5 ml of 5 M CsCl (prepared in SM buffer) making the upper layer. Special attention needs to be taken for layering the different concentration of CsCl over the phage suspension to prevent the mixing.

The centrifuge tubes were centrifuged at 25,000 rpm for 2 hours at 20 ° C with a SW28 rotor in a Beckman ultracentrifuge, after careful balancing the weight. The lower band carrying the λ-phage was collected with a syringe by puncturing the Beckman Ultra-Clear centrifuge tube and filled up to 5ml by adding 5M CsCl.

This final 5 ml mixture was transferred to a smaller Beckman Ultra-Clear centrifuge tube (14x89 mm,) and overlaid with 3.5 ml of 5 M CsCl in SM buffer followed by 4.5 ml of 3 M CsCl in SM buffer. The sample tubes were centrifuged in Beckman centrifuge at 35,000 rpm for 90 minutes at 20 °C in a SW40T1 rotor. The lower band with the λ-phage was taken in a volume of 600-900 µl by puncturing the tube in a syringe and divided into aliquots of 150 µl. 15 µl of 2 M Tris-HCl, 0.2 M EDTA, pH 8.5, and 150 µl of formamide was added into 150 µl of phage suspension and after mixing well incubated at room temperature for 30 minutes. Phage DNA was precipitated by adding 150 µl of H_2O followed by 900µl of 100% ethanol. Precipitated DNA was washed in 70% ethanol and dissolved in 150µl of TE buffer overnight at 4 °C.

The desired fragment of the mouse genomic DNA was isolated from phage DNA by restriction digestion and gel electrophoresis. To separate the mouse genomic DNA fragment

from phage DNA, NotI or SalI were used as restriction enzymes and a long 0.8% agarose gel with bigger loading pockets was run overnight at 40V, due to bigger molecular weight and size of these genomic DNA fragments. At the end, the mouse genomic DNA fragment was purified from agarose gel and subsequently cloned into a bacterial vector.

2.2.3.2. Mini preparation of plasmid DNA bacterial clones

A single bacterial colony was inoculated in 3-5 ml of LB containing 50 mg/ml of Ampicillin in a sterile culture tube. The culture was grown overnight at 37 °C with shaking (180 rpm), after which 1.5 ml of the culture was transferred to an Eppendorf tube. The bacteria were collected by centrifugation and the pellet was resuspended in 100 µl of P1 buffer (50 mM glucose, 25 mM Tris-HCl pH 8.0, 10 mM EDTA, 100 µg/ml RNase A). Alkaline lysis of the bacteria was performed by adding 200 µl of P2 buffer (200 mM NaOH, 1 % SDS w/v) and gently mixing the tubes by inversion. After a short incubation on ice, 150 µl of P3 Buffer (5.0 M, Potassium Acetate pH 4.8) was added and the tubes were gently inverted several times to mix. Removal of the precipitated proteins from the lysate was achieved by a 5 min centrifugation at 14000 rpm. The supernatants were transferred to new 1.5 ml tubes and 900 µl of 100% ethanol were added. The plasmid DNA was precipitated by centrifugation at 14000 rpm for 5 min. DNA pellets were washed once with 70 % (v/v) ethanol, allowed to dry, and dissolved in TE or water.

2.2.3.3. Midi preparation of plasmid DNA

Applications like electroporation of targeting construct into embryonic stem cells with plasmids require highly pure and intensely supercoiled DNA. To achieve this quality of plasmid DNA, it was prepared using the Midi Kit from Qiagen according to manufacturer's instructions.

2.2.3.4. Slot lysis

Slot lysis was performed to analyse the insertion of DNA fragments ≥ 500bp to a vector after ligation. This offers a quick and inexpensive way to check a large number of clones to make a preliminary selection of clones with insert. The principle of slot lysis is based on the lowered running speed of DNA clones carrying the insert during the gel electrophoresis. If a clone is identified with the successful insertion of a respective DNA fragment the remaining volume of bacterial culture was used for a mini-DNA extraction and clone was further analysed by restriction digests and DNA sequencing. Slot lysis was performed in a 96-well plate, 100 µl of

bacterial culture was added to the plate and bacteria were pelleted by centrifugation at 4000 rpm for 10 minutes.

The bacterial pellets were resuspended in 20 µl of protoplast buffer (30 mM Tris-HCl, 5 mM EDTA, 50 mM NaCl, 20% sucrose, 50 g/ml RNase, 50 mg / ml lysozyme). Gel pockets were loaded with the 14 µl lysis buffer (89 mM Tris-HCl, 89 mM boric acid, 2.5 mM EDTA, 2% SDS, 5% sucrose, 0.04% Bromophenol Blue) and bacterial mixture (20µl) was added. Bacteria were lysed and the plasmid DNA was separated in an electric field according to size.

2.2.3.5. Purification of DNA from an agarose gel

Under UV light, the DNA bands were excised from the agarose gel using a sharp scalpel and placed in to a 1.5 ml tube. The DNA was purified by using the DNA recovery kit (Zymoclean, USA) according to the manufacturer's instructions.

2.2.3.6. Purification of DNA for ES cell culture

For electroporation of the targeting construct into embryonic stem cells for homologous recombination, linearized DNA with the highest quality was needed. For this purpose 80-100µg of purified DNA was digested with 80-100 units of NotI restriction enzyme in final volume of 250 µl overnight at 37 °C. 10-20 units of the same enzyme was used next morning to incubate further for 2 hours at 37°C to increase the efficiency of DNA digestion. 2µl of an aliquot was used to check the complete linearization of the targeting construct by gel electrophoresis.

After successful digestion of the DNA the remaining digestion mixture was added up to volume of 500µl with H2O. Then, 1 volume of TE-buffered phenol-chloroform-isoamyl alcohol mixture (25:24:1, Roth, Karlsruhe) was added and mixed briefly by gently inverting the tube several times. The DNA sample was centrifuged at 13,000 rpm for 10 minutes at 4 °C and upper aqueous phase was taken into new tube. After two times washing with chloroform-isoamyl alcohol (24:1) to remove the remains of phenol, DNA was precipitated by adding 1 volume of isopropanol and 1/10 vol. of 3 M sodium acetate pH 5.2. The precipitated DNA was washed with 70% ethanol, air dried and dissolved overnight in ES cell culture grade pure H_2O. DNA concentration was measured by Nano-drop and adjusted to the concentration of 1µg/µl.

2.2.3.7. Phenol-chloroform extraction of mouse genomic DNA from tail biopsy

Phenol-chloroform extraction was performed for the purification of mouse genomic DNA from the mouse tail biopsy. A tail biopsy of 0.2 to 0.3 cm was taken and incubated overnight in 500 µl lysis buffer (50 mM Tris, 100 mM EDTA, 100 mM NaCl, 1% SDS, pH 8.0) supplemented with 10 µl of proteinase K (14mg/ml) at 55 °C.

After cooling the lysate one volume of TE-buffered phenol-chloroform-isoamyl alcohol mixture (25:24:1, Roth, Karlsruhe) was added and mixed by rotating the sample for 5 minutes at room temperature. The DNA sample was centrifuged at 13,000 rpm for 10 minutes at 4 °C and upper the aqueous phase was transferred into new tube. After two times washing with chloroform-isoamyl alcohol (24:1) to remove the remains of phenol, DNA was precipitated by adding 1 volume isopropanol and 1/10 vol. 3 M sodium acetate pH 5.2. The precipitated DNA was washed with 70% ethanol, air dried and dissolved in 150µl of TE buffer overnight at 4 °C and stored until use at 4 °C. This DNA was further used for genotyping PCR and Southern blot.

2.2.3.8. DNA extraction from mouse tail biopsies by hot-shot method

Genomic DNA extraction was also performed from tail biopsies of mouse by a faster method called Hot-Shot to analyse mouse genotypes by polymerase chain reaction. A tail biopsy of 0.2 to 0.3 cm was taken and incubated in 75 µl of alkaline lysis buffer (25 mM NaOH, 0.2 mM EDTA, pH 12.0 without setting) for 60 minutes at 95 ° C. After briefly cooling down the sample on ice, 75 µl of the neutralization buffer (40 mM Tris-HCl, pH 5.0 without adjustment) was added and stored at 4 °C for further PCR analysis of mouse genotype.

2.2.3.9. Purification of RNA from mouse tissues

Trizol (Invitrogen) was used for isolation of RNA from mouse tissues. Tissues were removed from anesthetized mouse after perfusion with 1X PBS (137 mM NaCl, 2.7 mM KCl, 10 mM Na_2HPO_4, 2 mM KH_2PO_4). Removed tissues were ground in liquid nitrogen with a mortar and pestle and transferred into a 50 ml falcon with little bit of liquid nitrogen, 1 ml Trizol per 100 mg tissue was added after liquid nitrogen had evaporated.

Samples were vortexed briefly and incubated for 5 minutes at room temperature. To pellet the cellular debris tissue samples were centrifuged for 5 minutes at 4000g at 20 °C and the supernatant was transferred to a new tube. 200µl of chloroform per 1 ml Trizol was added and shaken vigorously by hand for 15 seconds.

Afterwards samples were incubated for 2 minutes at room temperature and then centrifuged at 13,000 rpm at 4 °C for 15 minutes. The aqueous (upper) phase was transferred into a new tube and RNA was precipitated by adding 1 volume of isopropanol. This mixture was incubated for 10 minutes at RT and centrifuged at 13000 rpm at 4 °C for 10 minutes. The resulting RNA pellet was washed with 75% ethanol, air dried, and carefully dissolved in RNase free water and stored at -80 °C until further use.

2.2.4. Polymerase chain reaction (PCR)

Polymerase chain reaction (PCR) was performed for the amplification of DNA fragments of interest, for cloning of southern and northern blot probes as well as for the genotyping of transgenic mice. The Taq DNA polymerase (Invitrogen, USA) was used to amplify smaller DNA fragments (up to 1Kb). For longer DNA fragments (> 1000bp) Expand polymerase (Roche) was used. A typical reaction was performed in a volume of 25 µl with 0.1 -1 µg of template, 1x of reaction buffer (Invitrogen), 10 pmol of each primer, 0.5 mM of each dNTP's (Invitrogen) and 0.1µl of Taq DNA polymerase.

The reactions were performed either in the T-Gradient PCR machine or the T3000 thermo cycler from Biometra. A standard PCR reaction protocol given in the following table, however, annealing temperatures and elongation times were calculated specifically for each primer pair. If the PCR product generated was subsequently used for cloning, the entire reaction was loaded on a gel for electrophoresis. The PCR product was excised from the gel and purified prior to restriction enzyme digest.

Table 2.5 Typical PCR cycling temperatures and duration

Step	Temperature	Time
Initial denaturation	95°C	5 min
Denaturation	95°C	30 sec
Annealing	55-60°C	30 Sec
Elongation	72°C	1 min/1000bp
	4°C	∞

These steps were repeated for 35 times.

2.2.4.1. Genotyping PCR

Genotyping PCR was performed on DNA isolated from mice tail biopsies. Genotyping of both KI mice (R607H & L919X) was done in a reaction mixture containing 3 primers that allows controlling the removal of neo selection cassette after cre-recombination. A typical reaction was performed in a volume of 25 µl with 0.1 -1 µg of template, 1x of reaction buffer (Invitrogen), 10 pmol of each primer, 0.5 mM of each dNTP (Invitrogen) and 0.1µl of Taq DNA polymerase (Invitrogen). The reactions were performed either in the T-Gradient PCR machine or the T3000 thermo cycler from Biometra.

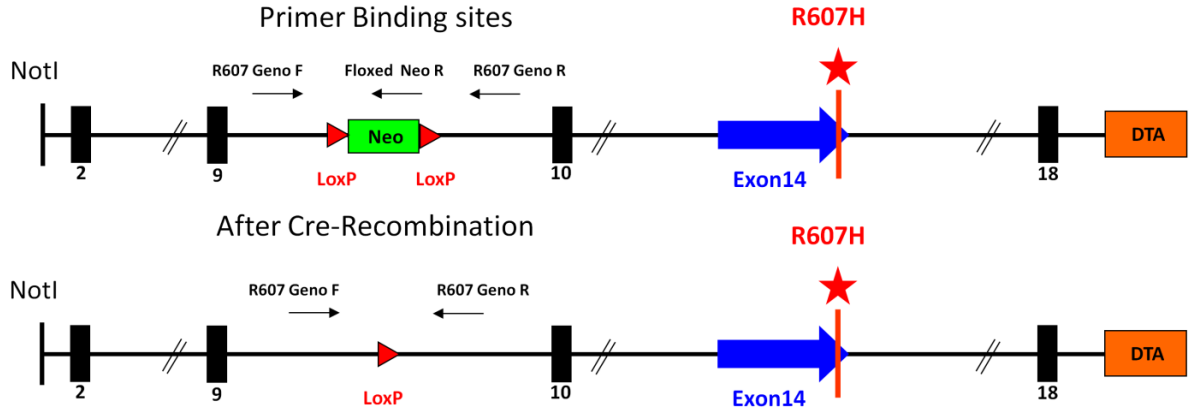

Figure 2.1 Genotyping scheme of R607H Knock In mice

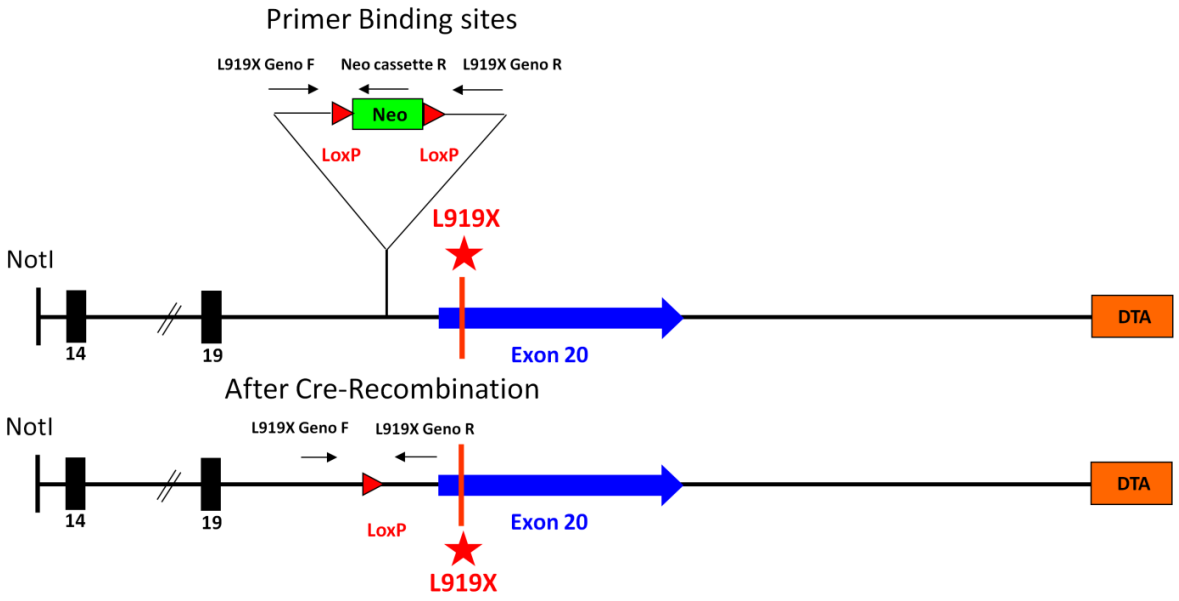

Figure 2.2 Genotyping scheme of L919X Knock In mice

Table 2.6 List of Primers used for genotyping, mutagenesis and real-time PCR

Genotyping primers L919X	Sequence (5'-3')
L919X Geno F	GTC TCC GTC TTG GTC TGC TGT G
L919X Geno R	TGG ACA AGC CCT GCT GTC CCT A
Neo Cassette R	GGG GCC ACC AAA GAA CGG AGC CGG
Genotyping primers R607H	
R607H Geno F	TAG CTC CTT CTA CCC CAC CCA
R607H Geno R	CCA GAG GTA CAT GGT AAA ACA TTG TC
Floxed Neo R	GGA AGA CAA TAG CAG GCA TGC
Mutagenesis Primers R607H	
R607H Mut F	CTTGCCATGACGCTACATAAGTTCAAGAACAGC
R607H Mut R	GCTGTTCTTGAACTTATGTAGCGTCATGGCAAG
Mutagenesis Primers L919X	
L919X Mut F	CCTTTGACGAGGAGAATGGCTAGGATGAATATGACGAAGTGC
L919X Mut R	GCACTTCGTCATATTCATCCTAGCCATTCTCCTCGTCAAAGG
Real Time Q-PCR Primers	
Ae1-RT PCR1F	GGC ACC TAC ACA CAG AAA C
Ae1-RT PCR1R	GGA GGC AAA CAT CAT CCA C
Ae1-RT PCR2F	AGG ACC TGG TGT TGC CAG AG
Ae1-RT PCR2R	CGG TTA TGC GCC ATG GA

2.2.4.2. Reverse transcription

RNA concentration was determined by absorption of the sample at 260 nm with Nano-drop device (Thermo Scientific, USA). 500 ng of RNA was used for reverse transcription. At first stranderd complementary DNA (cDNA) synthesis was performed using random hexanucleotide primers and Superscript III kit according to the manufacturer's instructions (Invitrogen, USA). Final cDNA was diluted to 50 ng/µl and stored at -20°C.

2.2.4.3. Real time Q-PCR

Complementary DNA (cDNA) of kidney cortex and medulla, primers (see table 2.6) and the SsoFast EvaGreen Supermix (Bio-Rad Laboratories GmbH) were used for quantitative real time PCR with the CFX96 real time system (Bio-Rad Laboratories GmbH). Actin was used as a housekeeping gene. All PCR reactions were coupled to melting-curve analysis to confirm the amplification specificity. The relative quantification was calculated with the analysis software that was provided by the Bio-Rad laboratories. Transcript abundance in the mouse kidney tissue was analysed.

2.2.5. Cell biology methods

2.2.5.1. Mouse embryonic stem cell culture and blastocyst injection

Mouse embryonic stem cell culture and blastocyst injection was done by core unit of transgenic mice production in the university hospital Jena.

2.2.6. Southern blot

For southern blot analysis, DNA prepared from embryonic stem cells or genomic DNA of the mouse was taken (10 to 50 µg) and digested overnight with 20-30 units of a restriction enzyme (Fermentas) at the appropriate temperature. The resulting fragments were separated by a 0.8% agarose gel electrophoresis and ethidium bromide was used to visualize under UV light and documented. To facilitate the transfer of large DNA fragments to a nylon membrane (Hybond XL, GE Healthcare) the gel was washed several times with distilled water and incubated with 0.25 M HCl for 15 minutes. After repeated washing with distilled water, the gel was equilibrated in 0.4 M NaOH for 15 minutes and a capillary blot was built with 0.4 M NaOH for overnight. After blotting overnight the nylon membrane was baked for 2 hours at 80 °C to immobilize the DNA on the membrane. Membrane was briefly washed in 2X SSC before hybridizing with the radiolabelled probe.

2.2.7. Radio-labelling of probes with ^{32}P

^{32}Phosphorous dCTP was used to label the probes. Prior to labelling the DNA fragment (300-700 bp) used as probe was cut out from a plasmid with the help of a suitable restriction enzyme. 25-50 ng of this gel purified DNA fragment was dissolved in 45µl of TE buffer and denatured at 95 °C for 5 minutes.

After cooling on ice the sample was briefly centrifuged and the contents of the denatured probe was transferred into a Rediprime II (GE Healthcare, USA) tube containing lyophilized

dATP, dTTP, dGTP and DNA polymerase. At the end 5µl of ^{32}P-dCTP was added and mixed well by pipetting. The reaction mixture was incubated for 30 minutes at 37 °C.

For purification of unbound radiolabelled nucleotides, probe mix was added on the top of a G50 column (GE Healthcare, USA) and purified according to the manufacturer's instructions. Radiolabelling efficiency of the probe was measured with a Beckman scintillation counter by taking 1µl aliquot of labelled probe. The final activity in the hybridization mix (7% SDS, 10% PEG, 1.5 x SSPE, 0.1 mg/ml fish sperm DNA (Roche)) was set to 500000 cpm/ml.

Prehybridization of the respective membrane was done for 2 hours at 68 °C in pre-hybridization mix (7% SDS, 10% PEG, 1.5 X SSPE, 0.1 mg / ml fish sperm DNA (Roche)) to reduce the nonspecific binding of the probe to the membrane. The membrane was hybridized with the radio-labelled probe overnight at 68 °C. The membrane was washed twice with preheated washing buffer (2X SSC, 0.1% SDS) at 68 °C for 20 minutes. Membrane was wrapped in thin plastic film and placed in a cassette for overnight exposure to a phosphorimager plate (Fuji Films, Japan). The PhosphoImage Analyzer (FLA-3000 Series, Fujifilm) was used for analysis.

2.2.8. Biochemical techniques

2.2.8.1. Preparation of proteins

2.2.8.1.1. Cytosolic membrane preparation

Cytosolic proteins were prepared by grinding mouse tissues in a mortar with a pestle with liquid nitrogen and by adding 10-fold volume of lysis buffer (3% SDS, 30 mM Tris, 5 mM EDTA, 30 mM NaF, 10% glycerol, pH 7.4, complete protease inhibitor cocktail (Roche)).

This mixture was further homogenised in glass potter (Potter S, Sartorius) and pelleted by centrifugation at 13,000 rpm, 4 °C for 10 minutes. The supernatant containing cytosolic proteins was transferred to a new tube, the protein concentration was determined by the BCA method (Pierce kit) and aliquots were frozen (2µg/µl) in 1 X Laemmli buffer at -80 °C.

2.2.8.1.2. Membrane protein preparation

Frozen tissues taken from PBS perfused mice were taken and grinded with mortar and pestle in liquid nitrogen and transferred to a 50 ml Falcon. 1 ml of Homogenization buffer (0.25% sucrose, 10 mM Hepes, 1 mM EDTA, pH 7.4 complete with protease inhibitor cocktail (Roche)) for 200mg tissue was added and the tissue was homogenized in a glass potter (Potter S, Sartorius). Cell debris was separated by centrifugation at 800 g, 4 ° C for 5 minutes

and the supernatant was transferred to a new tube. The supernatant obtained was centrifuged to pellet the cellular organelles and mitochondria at 10,000 g, 4 ° C for 15 minutes.

Membrane proteins were pelleted by centrifugation of the supernatant in polycarbonate centrifuge tubes (Beckman) at 110000 g, 4 ° C for 1 hour and incubated overnight at 4 °C in sample buffer (50 mM NaCl, 1 mM EDTA, 0.75% Triton, 1% Chaps, 10% glycerol, pH 7.5 complete protease inhibitor cocktail (Roche)). The protein concentration was determined by the BCA method (Pierce kit) and aliquots were frozen (2µg/µl) in 1 X Laemmli buffer at -80 °C.

2.2.8.2. Western blot

A semi quantitative analysis of protein expression was performed by Western blotting. For this purpose proteins were separated based on their molecular weights on a SDS polyacrylamide gel, made up of an upper 5% stacking gel and lower 8-10 % polyacrylamide running gel. The Bio-Rad Mini-PROTEAN 3 system was used for casting and running of the gel. Before loading the gel, 20-30µg of protein was denatured in 1x Laemmli buffer at 60 ° C for 10 minutes and cooled on ice. Denatured proteins were loaded to the SDS polyacrylamide gel and separated according to their size by electrophoresis in a running buffer (25 mM Tris, 250 mM glycine, 0.1% SDS).

Proteins were transferred to a nitrocellulose membrane (PROTRAN, Whatman) by wet electro blotting system in a transfer buffer (Glycine 39 mM, 48 mM Tris, 0.037% SDS, pH 8.3) on ice at 400 mA over 70 minutes. Membranes were analysed for transfer of the proteins with Ponceau-S staining and subsequent washing with distilled water.

Detection of protein expression was done by using specific antibodies. For this purpose membranes were briefly washed with 1X TBST (150 mM NaCl, 50 mM Tris, 0.02 % (v/v) Tween 20; pH 7.9) and incubated with blocking buffer (5% skimmed milk powder in TBST) for 1-2 hours at room temperature followed by incubation with the primary antibody in blocking buffer at 4 °C overnight. The membrane was washed 3 times in 1X TBST for 10 minutes each. Then membranes were incubated with the secondary antibody coupled with horseradish peroxidase (HRP) in TBST for 1-2 hours at room temperature. Membranes were washed again 3 times in TBST and the HRP-coupled secondary antibody was detected by enhanced chemiluminescence on an X-ray film (ECL, Millipore).

2.2.8.3. Immunohistochemistry

In order to visualize the localization of the proteins of interest, immunohistochemial analysis of mouse kidneys were performed. Mice were anaesthetised by intraperitoneal injection of (2ml ketamine (50mg/ml), 0.7 ml Rompin (2%) in 5.6 ml 0.9 % NaCl) according to body weight (20g ≈ 100µl) before perfusion. Transcardial perfusion was performed in anaesthetized adult mice (WT or KO, 6-8 weeks of age) with 4% PFA in 1X PBS.

Kidneys were removed and post fixed in 4 % PFA in 1X PBS for 2 hours at room temperature followed by 3 times washing with 1X PBS. Kidneys were dissected in 2 halves in transverse manner and incubated in 30% w/v sucrose solution in 1X PBS for 2-3 days at 4 °C for cryoprotection. Kidneys were frozen in OCT compound (Tissue-Tek, USA) and 7 µm cryosections were cut in a cryotome (- 24 °C, Leica, Germany).

Rehydration was performed by washing the sections with 1X PBS for 15 minutes at room temperature and antigen retrieval was done by treating the sections with 1% SDS in PBS for 5 minutes. Slices were washed 3 times in 1X PBS for 5 minutes each and were subsequently blocked in blocking buffer (1%BSA in 0.02 % sodium azide PBS) for 30 minutes at room temperature. The primary antibody was applied in the specific working dilution in 0.02 % sodium azide PBS solution for overnight at 4 °C. Hypertonic PBS (1X PBS + 18g NaCl per litter) was used to wash sections 2 times each for 5 minutes followed by 1X PBS. Slices were stained with fluorescently labelled secondary antibodies (Alexa Fluor 488- and 555-coupled goat anti-rabbit, goat anti-guinea pig, Invitrogen) diluted 1:1000 in 0.02 % sodium azide PBS at room temperature for 1 hour. Sections were washed with Hypertonic PBS for 2 times each for 5 minutes followed by 1X PBS wash. Cell nuclei were stained by 4',6-diamidino-2-phenylindole (DAPI; 1µg/mL) and sections were analysed by confocal microscopy (Leica TCS SP5, Germany).

2.2.9. Animal experimentation

2.2.9.1. Metabolic cage studies

All metabolic cage studies of both KI mice lines were performed in the animal facility of the University hospital Jena according to the permission from local laboratory animal welfare institute. Mice were housed at a constant room temperature (24±1 °C) with 12-h light/dark cycle. For convenience, the 12:12 light/dark cycle was inverted. Mice were given deionised water ad libitum and pair-fed with standard laboratory chow.

All experiments were performed on male mice (R607H KI and L919X KI) of 2 to 3 months of age. Animals were housed in metabolic cages (Techniplast, Italy) and the intake of food and water as well as body weight were monitored throughout the experiment.

Urine collection was performed daily under mineral oil in the urine collector for urine pH measurements as well as the urine electrolytes concentration. After one week on deionised water mice were give a pulse of 0.28 M NH4Cl solution for 24 hours to study the acid secretion efficiency of both KI mice verses WT control.

The urine pH and creatinine concentration was determined in the department of clinical chemistry University hospital of Jena.

Blood was taken in heparin-treated capillary tubes retro-orbitaly and immediately analysed for pH, pCO2 and pO2 on independent mice cohort with ABL 77 blood gas analyser (Radiometer, Denmark).

3. Results

Mutations of the anion exchanger 1 (AE1) are the major cause of hereditary distal renal tubular acidosis. The point mutation R589H and the c-terminal 11-amino acid truncation R901X are two familiar mutations in the human AE1 gene. These mutations were chosen to generate two independent knock in (KI) mouse models. The R607H mice correspond to the human R589H and L919X mice to the human R901X mutations.

The first part of this work includes the generation of R607H and L919X KI mice by site specific mutagenesis and homologous recombination. The second part of this study comprises the analysis of the disease phenotypic effects of the missense R607H and the nonsense L919X mutations in mice.

3.1. Generation of Ae 1 knock in mice

The directed mutations of the Ae 1 gene in the mouse were performed by homologous recombination in pluripotent embryonic stem cells. Transfection of murine embryonic stem cells (ES cells) with a target vector, which contains segments of genomic sequence of the target gene results in the recombination of the genomic sequences with homologous regions in target gene.

The desired recombination events were identified as positive ES cell clones. These ES cell clones were expanded *in vitro* and injected in early mouse embryos (blastocysts). As results of successful blastocyst injection chimeric mice were born, these mice were partially made of cells from the original blastocysts and parts of the injected recombinant ES cells. These animals were used as progenitors for generation of KI mouse lines, although germ cell-forming stem cells are derived from the injected recombinant ES cells.

3.1.1. Construction of the targeting vectors

The pKO scrambler vector was used as a backbone to clone the targeting constructs for the R607H and L919X KI mice. The vector includes a multiple cloning site and a diphtheria toxin alpha (DTA) cassette at the 3' end as a negative selection marker. Upon homologous recombination the DTA cassette does not integrate into the genome. A random integration of the construct with the DTA cassette into the genome leads to the subsequent expression of the diphtheria toxin resulting in the cell death. The neomycin resistance cassette (neo) was used as a positive selection marker to screen the successful recombination events. NotI linearized targeting vector was used for ES cell electroporation

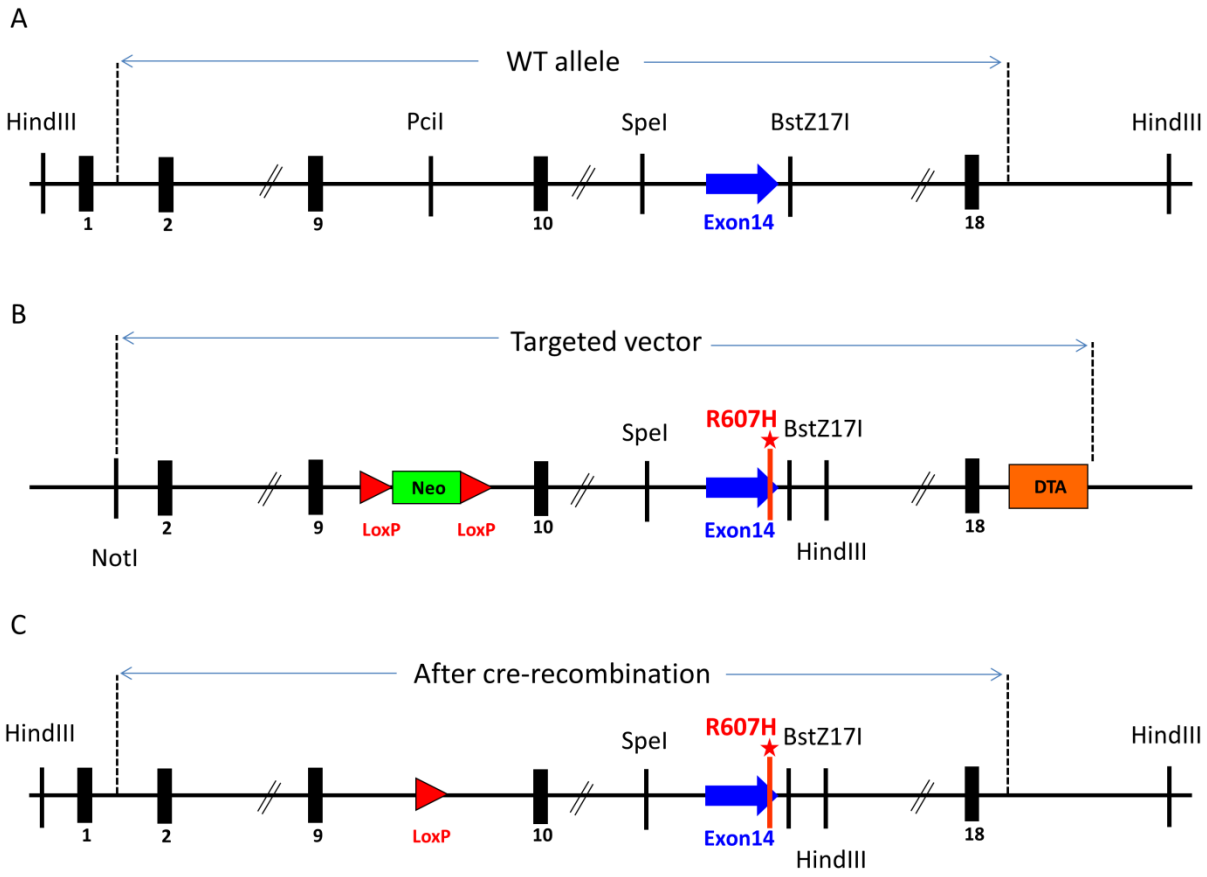

Figure 3.1 Schematic representation of the construction of the R607H KI targeting vector. The distance among the exons and the introns have no real co-relation with original gene map. (A) Wild type allele showed the mouse genomic fragment including exon 14 which carried the desired mutation site. (B) Mouse genomic fragment was cloned into pKO vector and an extra HindIII site was introduced to control the successful recombination. A change from CGA(R) →CAT (H) results in R607H mutation. (C) Successful cre-recombination resulted in the excision of neo-cassette.

Two independent ʎ-phage clones comprising the genomic regions of interest to target the different parts of the Ae1 gene were isolated and were initially cloned into the pBluescript II KS^{+} vector. Sequencing of the Ae1 genomic fragments revealed the targeting vectors for both KI mice. R607H fragment included exon 2 to exon 18 and the L919X KI construct comprised

of exon 14 to exon 20 with a 3' flanking arm of 10 kb. These genomic fragments were subsequently cloned into the PKO Scrambler V901 vector carrying the DTA cassette.

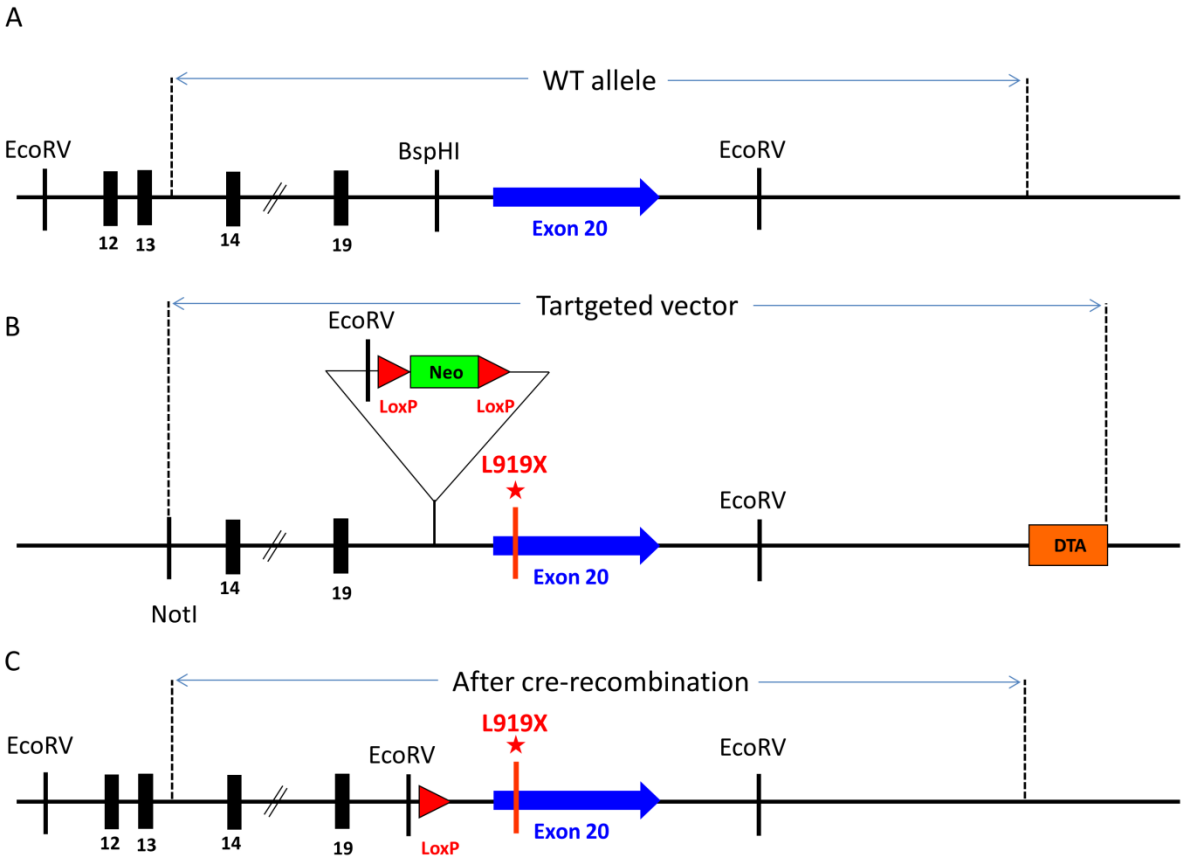

Figure 3.2 Schematic representation of the construction of the L919X KI targeting vector. The distance among the exons and the introns have no real co-relation with original gene map. (A) Wild type allele indicated by the isolated mouse genomic fragment used for the generation of targeting construct including exon 20 carried the desired mutation site. (B) Mouse genomic fragment was cloned into the pKO vector with the neo selection cassette. An extra EcoRV site was introduced to control the successful recombination. A site directed mutagenesis led to a change of CTG (L) →TAG(X) resulted in L919X. (C) Successful cre-recombination excised the neo-cassette in knock in allele.

In case of the R607H KI mouse model a 1.5 kb fragment was subcloned with SpeI and Bstz17I to generate a point mutation by site specific mutagenesis. This point mutation led to a single amino acid change from arginine (R) to histidine (H). The neo-cassette flanked by loxP sites (floxed neo) was inserted as a positive selection marker at the PciI restriction site of the EcoRV-XhoI subclone. An extra HindIII site was introduced close to the point mutation in the neighbouring intron for selection of the positively recombined clones by southern blot analysis with an external 3' probe (figure 3.1).

Ae1 mouse genomic fragment carrying the exon 20 was used to create the targeting construct for L919X KI mouse model. The nonsense mutation L919X was introduced in a sub clone by site directed mutagenesis. The change from leucine (L) to stop codon (X) that led to the truncation of last 11 amino acids of the Ae1 protein. An EcoRV-AscI linker was added closed to the target exon, at the BspHI restriction site to place the floxed neo cassette. The insertion on an extra EcoRV restriction site enabled the successful verification of recombined clones via southern blot with a 5' external probe (figure 3.2).

3.1.2. Detection of homologous recombination

The targeting vectors for both mouse lines were linearized with NotI and transfected into the ES cells by electroporation. ES cells were treated with (neomycin) selection medium and 300-400 neomycin resistant ES cell clones were isolated. These clones were expanded and passaged into four replica plates. Two replica plates were frozen and the remaining two were used for the extraction of genomic DNA. The cell culture was performed by the members of the core unit for transgenic animals' facility of the University hospital Jena.

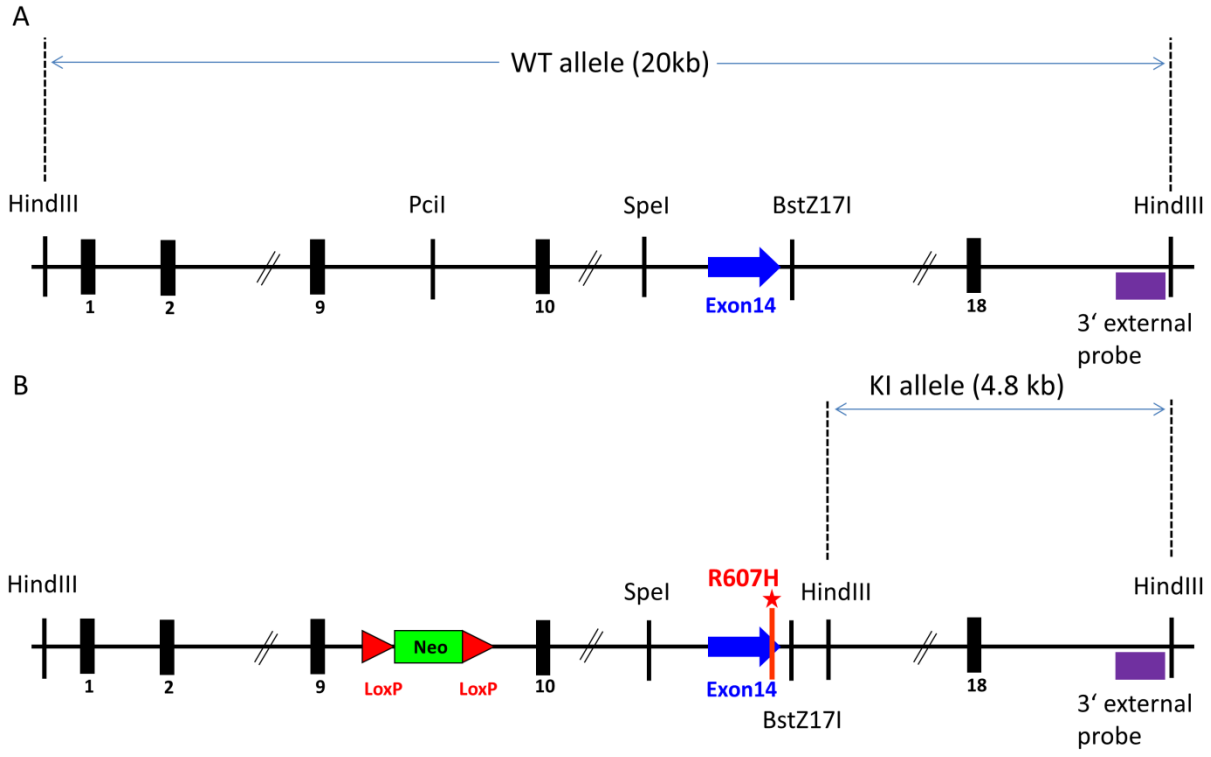

Figure 3.3 Southern blot strategy used for the detection of homologous recombination in R607H ES cell clones. (A) A 20 kb of genomic fragment can be detected in southern screening as a WT allele. (B) In case of successful recombination a 4.8 kb genomic fragment can be seen in KI allele due to presence of an extra HindIII site via an external 3' probe. Four hundred ES clones were analysed by southern blot and one of the four positive ES clones was injected to generate R607H KI mouse line.

Successful recombination events in the ES cell clones was analysed by southern blot. Either HindIII or EcoRV were used as restriction enzymes for the digestion of the genomic DNA of the R607H and L919X clones, respectively.

The HindIII digestion of the genomic DNA of R607H clones resulted in wild type fragments of 20kb and a recombinant fragment of 4.8 kb due to the insertion of an extra HindIII restriction site in the targeting vector. These DNA fragments were identified with a downstream 3' external probe (Figure 3.3 for schematic representation).

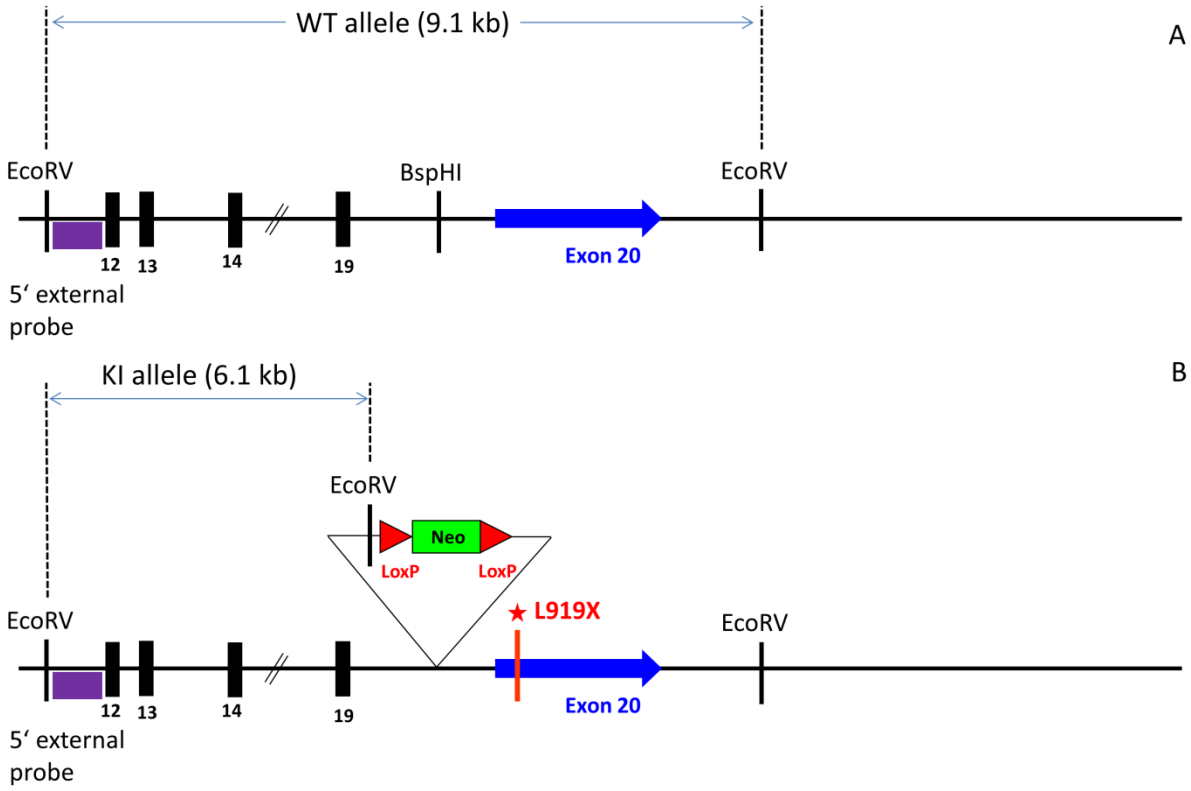

Figure 3.4 Southern blot strategy used for the detection of homologous recombination in L919X ES cell clones. (A) A wild type allele can be distinguished as a 9.1 kb of genomic fragment by an external 5' southern probe. (B) Accomplishment of the recombination was indicated by a 6.1 kb genomic fragment via a 5' southern probe in KI allele. Three hundred ES clones were analysed by southern blot and one of the nine positive ES clones was injected to generate R607H KI mouse line.

In case of L919X ES clones the EcoRV digestion of the genomic DNA showed the successfully recombined clones with a wild type band of 9.1 kb and a recombinant band of 6.1 kb. These DNA fragments were identified with an upstream 5' external probe (Figure 3.4 shows the details).

The southern blot results revealed the successful recombination events in both of the KI mouse lines. The ^{32}P labelled probes were used to detect the wild type and recombinant allele band. Two successfully recombined clones from each KI line were chosen, expanded and then injected into 3.5 days old blastocysts harvested from C57BL/6J mouse line.

Injected blastocysts were then transferred into the uterus of C57BL/6J foster mice. Foster mice gave birth to male chimeric mice, which were bred with C57BL/6J female mice. The successful germ line transfer was analysed by the coat colour and genotyping PCR. The presence of the mutations was verified by sequencing in both KI mouse lines. Both the R607H and the L919X KI mouse lines were mated with cre-recombinase expressing mice to delete the floxed neo cassette. After removal of the neo-cassette the cre-recombinase transgene was removed by breeding. For experiments only neo negative mice were used.

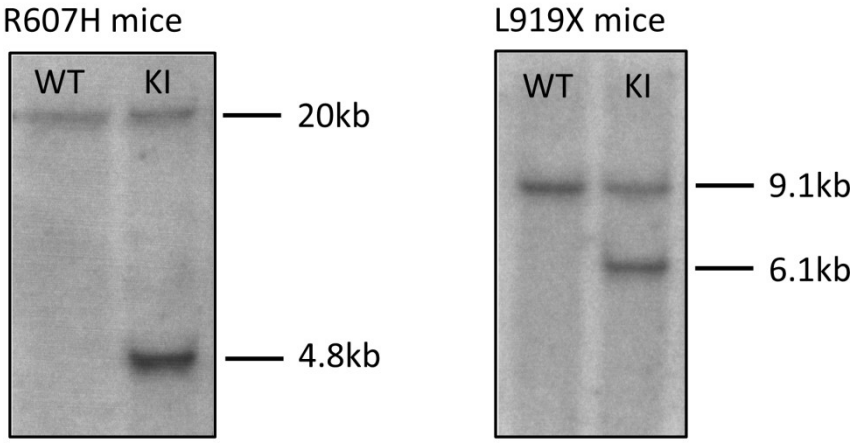

Figure 3.5 Southern blot analyses of both KI mouse lines. Homologous recombination in R607H KI mice was observed by KI band at 4.8kb and wild type band (control) at 20kb. In the same way L919X mice have shown a successful recombination by a 6.1 kb KI band and the 9.1 kb WT band.

3.1.3. Confirmation of germ line transfer in both KI mice

As a result of site directed mutagenesis two independent mouse lines (R607H & L919X) were obtained. Several methods were used for the confirmation and analysis of germ line transfer from chimeric mice. Genotyping PCR was one of the methods used most frequently to keep track of the genotype of new born mice after each breeding step.

At first the successful removal of the neo-cassette was confirmed by a genotyping PCR. Three primers were used to detect the presence or absence of the neo-cassette. When the mice were obtained without neo-cassette, only one primer set (Forward & Reverse) was used to trace the mice genotype for each knock in line independently (Figure 2.1 & 2.2 shows the detailed genotyping PCR scheme).

The germ line transfer was further verified by southern blot analysis. The genomic DNA purified from mice tail biopsies was used in this analysis. The 3' and 5' radiolabelled external probes were taken to trace the germ line transfer in R607H and L919X KI mice, respectively.

The results obtained from genotyping PCR and southern blot analysis could reveal the successful recombination and germ line transfer.

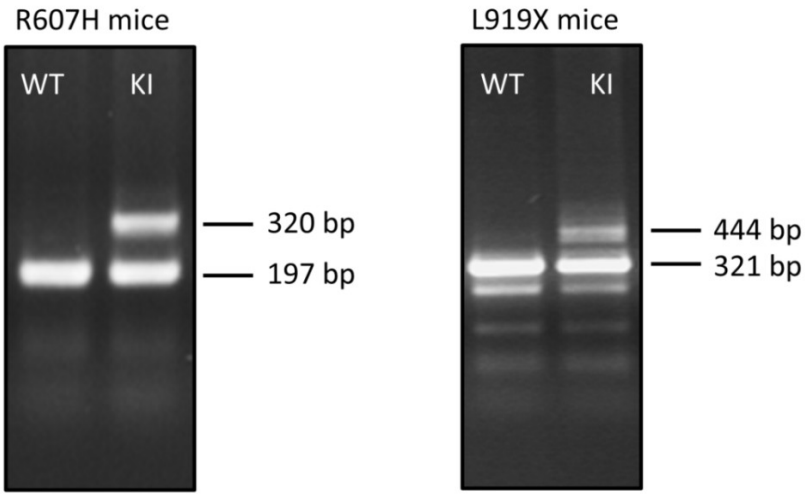

Figure 3.6 Genotyping PCR of R607H and L919X KI mice. Mice genomic DNA from tail biopsies were used for the genotyping PCR. In R607H mice WT band of 197 bp and KI band at 320 bp can be seen. In L919X mice the WT band of 321 bp and the KI band at 444 bp were observed.

The existence of the desired mutations at specific sites in both KI mouse lines was controlled with the sequencing of the mouse genomic DNA.

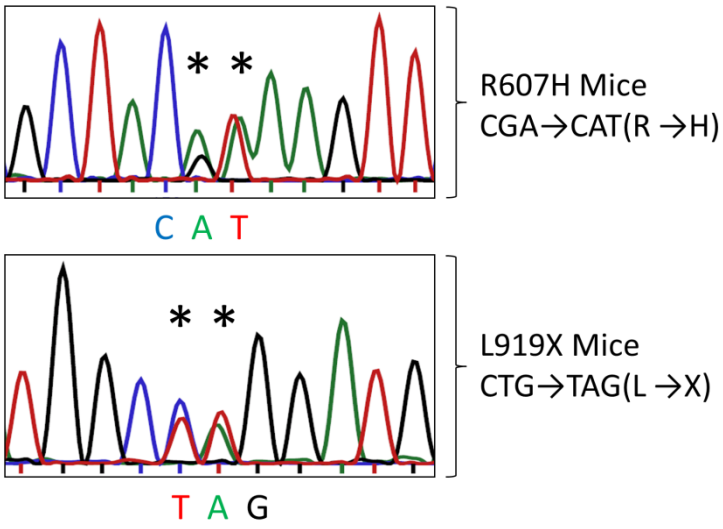

Figure 3.7 Electropherogram of for both KI mice. Point mutations in KI mice are indicated by *. In R607H mice a change from CGA (R) to CAT (H) and in L919X mice CTG (L) to TAG (stop codon) can be seen.

3.2 Phenotypic characterization of Ae1 KI mice

The phenotypic analysis of both KI mice was an important part of the study. It was expected that both mutants serve as a model for autosomal dominant (AD) type of distal renal tubular acidosis (dRTA). Phenotypic analysis showed both KI mice were born at the expected Mendelian ratio (100 pups for each KI mouse line), indicating no embryonic lethality. Both of

the KI mice were normal at birth, were viable, fertile and could not be distinguished from their genetically unmodified siblings. A statistical analysis of the body weight and the body size of KI verses WT animals showed no significant differences (data not shown).

3.3. Blood and urine analysis of (R607H & L919X) mice

Blood gas parameters and urine pH of wild type and littermates R607H KI, L919X KI was examined under steady state conditions.

Table 3.1 Blood gas values and urine electrolyte composition in R607H KI mice. Urine electrolytes were normalized to urine creatinine. The data shown are mean values ±SEM.

R607H mice	WT (n=6)	KI (n=6)	p-value
Blood			
pH	7,31 ± 0,01	7,28 ± 0,02	0,24
pCO_2 (mmHg)	48,28 ± 0,77	51,66 ± 1,58	0,06
HCO_3^- (mM)	24,14 ± 0,75	23,65 ± 0,97	0,69
	WT (n=6)	KI (n=6)	p-value
Urine			
pH	6,83 ± 0,07	7,67 ± 0,07	0,00001
Creatinine(mM)	3,58 ± 0,25	4,25 ± 0,15	0,04
[Na^+/Creatinine](mM)	34,35 ± 2,51	41,67 ± 1,78	0,03
[K^+/Creatinine] (mM)	102,2 ± 11,3	120,1 ± 11,9	0,29
[Cl^-/Creatinine] (mM)	46,68 ± 5,15	48,51 ± 3,35	0,77
[NH_4^+/Creatinine] (mM)	4,6 ± 0,39	1,96 ± 0,28	0,0003

Table 3.2 Blood gas values and urine electrolyte composition in L919X KI mice. Urine electrolytes were normalized to urine creatinine. The data shown are mean values ±SEM.

L919X mice	WT (n=8)	KI (n=8)	p-value
Blood			
pH	7,33 ± 0,01	7,317 ± 0,01	0,34
pCO_2 (mmHg)	49,87 ± 1,27	51,13 ± 1,73	0,57
HCO_3^- (mM)	26,01 ± 0,65	25,53 ± 0,99	0,69
	WT (n=6)	KI (n=6)	p-value
Urine			
pH	6,77 ± 0,04	7,322 ± 0,07	0,0001
Creatinine(mM)	4,16 ± 0,15	3,97 ± 0,16	0,41
[Na^+/Creatinine](mM)	33,81 ± 0,9	36,9 ± 1,19	0,06
[K^+/Creatinine] (mM)	91,71 ± 3,89	103,5 ± 2,9	0,03
[Cl^-/Creatinine] (mM)	45,67 ± 3,09	51,31 ± 2,74	0,2
[NH_4^+/Creatinine] (mM)	4,32 ± 0,59	3,02 ± 0,55	0,13

3.3.1. Urine analysis of KI mice

WT and KI mice 8-12 weeks of age of both genders were housed in metabolic cages to collect urine. Urine was collected under oil for 24h at the same time on consecutive days. The concentrations of substances in the urine were normalized to urine creatinine (Table 3.1 & 3.2). All parameters of the urine of both KI mice were compared with their respective wild type littermates. On day 7 of the experiment mice were challenged with an acid load in the form of 0.28M NH4Cl for 24h, which is a standard test to study an acid secretion defect of the kidney. Differences in urine pH were observed in both KI mouse lines indicating a renal acid secretion defect (Figure 3.8). Significance levels were analysed by a 2-Way ANOVA and post hoc test.

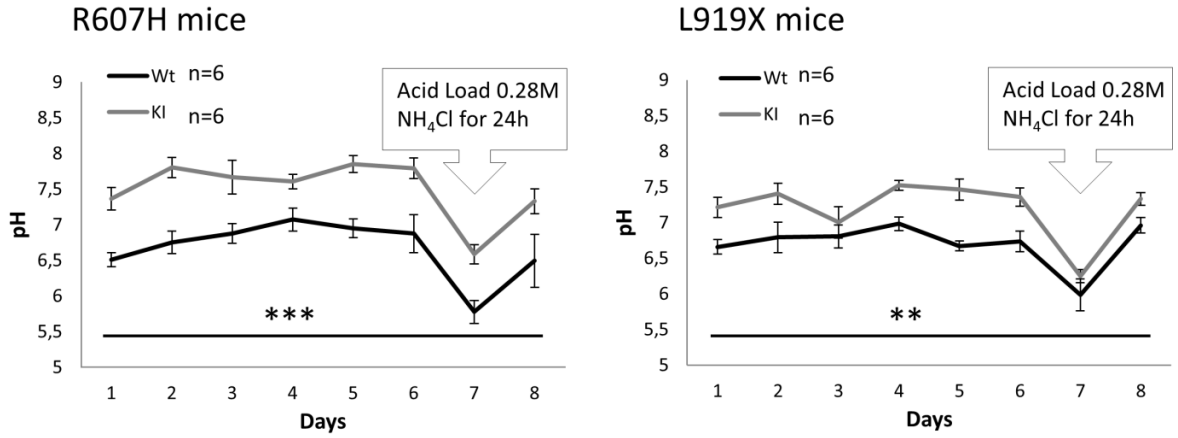

Figure 3.8 Urine pH analysis of R607H and L919X KI mice. Urine was collected after every 24h interval, on day 7 mice were challenged with the acid load of 0.28 M NH_4Cl a decrease in the pH is observed. Both KI mice have shown a significant difference. 2-Way ANOVA and post hoc test was performed to test the significance of repeated measurements.

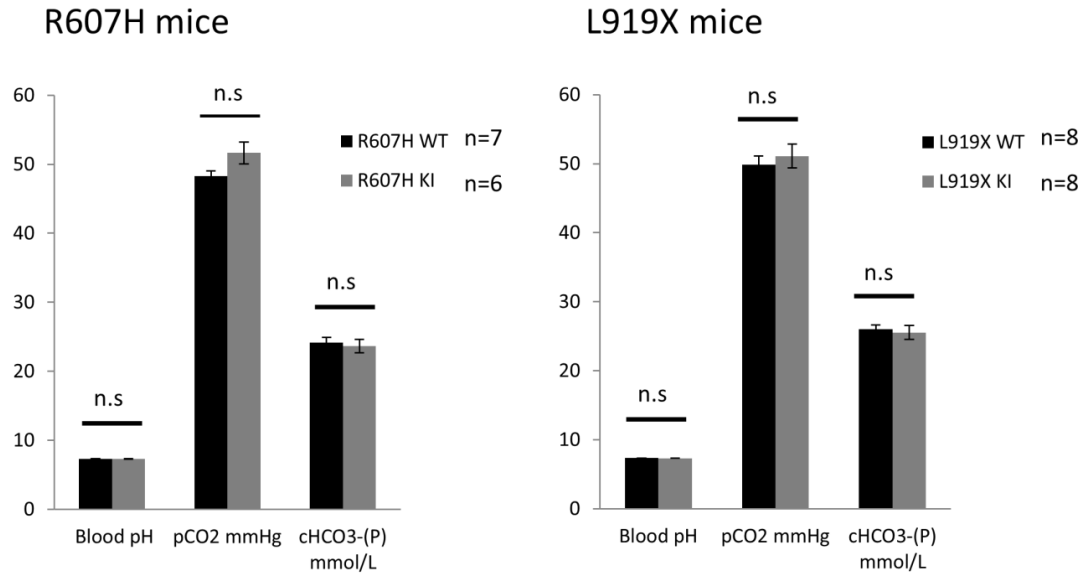

Figure 3.9 Blood gas analysis of R607H and L919X KI mice with respective littermates. Both KI mice did not show any significant difference in blood pH values as well as the pCO_2 and the HCO_3^- concentrations.

3.3.2. Blood gas analysis of KI mice

Blood samples of both KI mouse lines with their respective littermates of both genders were analysed. Blood pH and HCO_3^- concentration in WT and KI were indistinguishable therefore; no significant difference in blood pH, pCO_2 and HCO_3^- values was observed (Figure 3.9).

3.4. Ae1 expression studies in KI mice by immunohistochemistry

The kidney specific shorter isoform of the Ae1 is strongly expressed in highly specialized and polarized, acid secreting cells (α-IC) of the distal tubule in kidney. Ae1 is a membrane protein and its localization is confirmed to the basolateral membranes of the α-IC cells. Here, Ae1 localization and expression was analysed by immunofluorescence staining of 8-10 weeks old R607H and L919X KI mice.

3.4.1. Immunohistochemical analysis of R607H mice

To evaluate the expression of Ae1 in mouse kidney, immunohistochemistry was performed by using 7μm thick frozen sections. The antibodies directed against Ae1 and pendrin demonstrated basolateral staining of the Ae1 in α-IC cells of the cortical and medullary collecting ducts (CCD, MCD). The distribution of the pendrin staining was observed predominantly in apical sides of β- IC cells along the CCD. Immunohistochemistry revealed abundant fluorescence labelling of Ae1 and pendrin in WT mice compared to a reduced level of the Ae1 expression in the cortex of the R607H KI mice kidney.

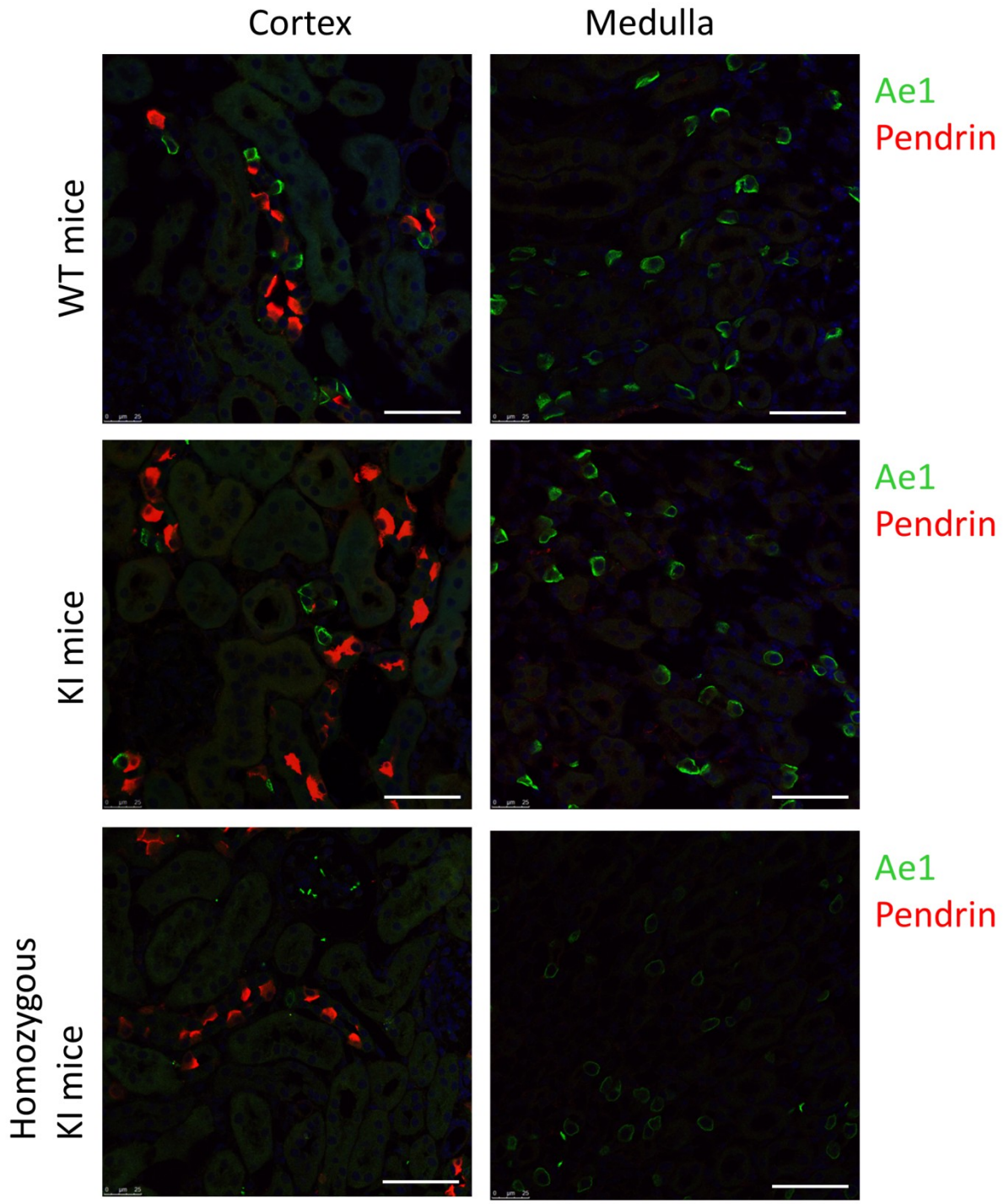

Figure 3.10 Expression of Ae1 in α-intercalated cells and Pendrin in β-intercalated cells of R607H mice. Immunofluorescence staining of Ae1 (Alexa Fluor 488-mediated green staining) and Pendrin (Alexa Fluor 555-mediated red staining) was performed on 0.7µm thick kidney cryosections. Immunolocalization of Ae1 to the basolateral side of the α-intercalated cells and the Pendrin to the apical sides of the β-intercalated cells were observed. DAPI was used to stain cell nuclei. (Scale bar 50µm)

There was no difference recognized in Ae1 expression in the medulla in R607H KI mice compared to WT littermates (figure 3.10). Homozygous KI (both alleles with R607H mutation) mice have almost lost the Ae1 staining in the cortex and a residual protein expression can be seen in the medulla.

The number and subtypes of IC cells was quantified in the CCD and MCD by immunofluorescence staining of Ae1, vH^+-ATPase and Pendrin. IC cells were defined as those stained positive for the B1 subunit of the vH^+-ATPase. The α-IC cells were defined as those that did not express pendrin, whereas β-IC cells had pendrin staining.

These results revealed a significant decrease in number of Ae1 stained cells in the cortex as well as in the medulla of R607H KI versus WT mice (Figure 3.14 A). The number of Pendrin positive cells in the cortex remains unchanged in R607H KI mice compared to WT littermates. The immunofluorescence quantification also showed that the expression of pendrin was limited to the cortical collecting ducts and connecting tubules and the staining was absent from the medullary collecting duct.

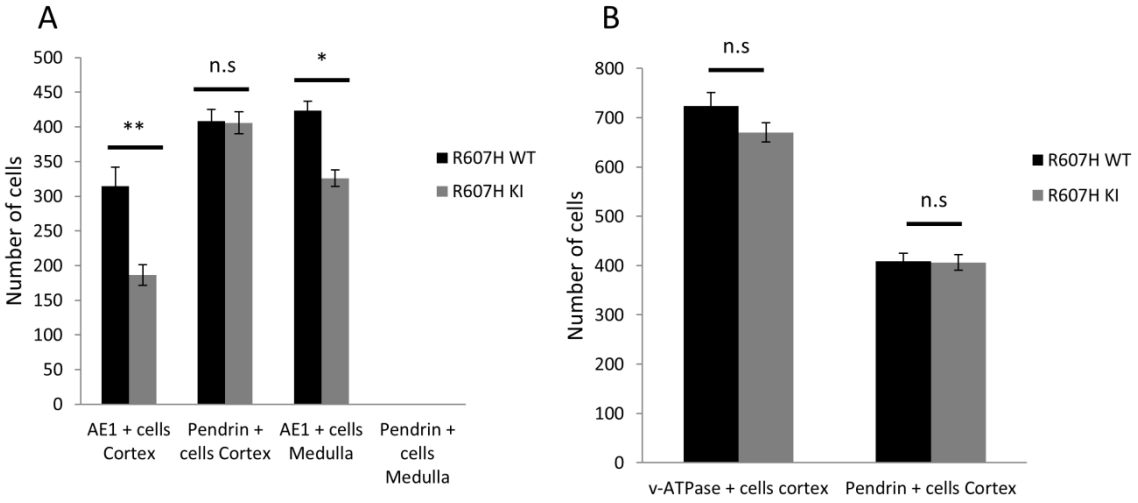

Figure 3.11 Analysis of the number of α and β-intercalated cells in R607H mice. (A) The number of α and β-intercalated cells quantified in cortex and medulla. Ae1 and Pendrin were used as the markers for α and β-IC cells respectively. The number of α-IC cells in cortex and medulla of KI mice was significantly reduced as compared to the WT mice. (B) The total number of IC cells in the cortex compared with only β-IC cells in the cortex. There was no significant difference found in any of the group.

The quantification of V-ATPase stained cells in the cortex was performed to analyse the difference in number of α-IC cells in the cortex. The cells stained with the vH^+-ATPase anti body indicated no difference in the number of α-IC cells in the cortex (Figure 3.14 B). The quantification results could signify a reduction of Ae1 stained cells in R607H KI mice instead of change in the number of α-IC cells in the cortex.

3.4.2. Immunohistochemical analysis of L919X mice

The expression of Ae1 in L919X KI mice was analysed compared to the WT littermates by immunofluorescence staining of frozen kidney sections. In two independent experiments, the first set of studies was performed with antibodies directed against Ae1 and vH^+-ATPase (figure 3.12). The second set of studies accomplished with the antibodies targeted to Ae1 and pendrin in L919X KI and WT kidney sections (figure 3.13).

The immunofluorescence labelling demonstrated the basolateral staining of Ae1 in α-IC cells of the CCD and MCD of kidney. The distribution of the vH^+-ATPase staining was observed predominantly in apical and sub-apical sides of both α- & β- IC cells along the CCD and MCD. Immunohistochemistry revealed abundant fluorescence labelling of Ae1 and vH^+-ATPase in WT mice. A reduced level of the Ae1 expression was observed in the cortex of the KI mice kidney. There was no difference recognized in the expression of Ae1 in the medulla in KI mice compared to WT littermates.

A further Immunohistochemical analysis of L919X KI mice kidney by double immunofluorescence staining of Pendrin and Ae1 was performed. The WT littermates were compared with the heterozygous KI and homozygous KI mice. The kidney cortex exhibited a decrease in the expression of Ae1 in heterozygous and homozygous KI mice. In homozygous KI mice the Ae1 expression is completely lost in the cortex but the Ae1 staining in the medulla indicated the presence of some residual Ae1 protein. There was no change observed in the subcellular localization of the heterozygous and homozygous L919X KI mice.

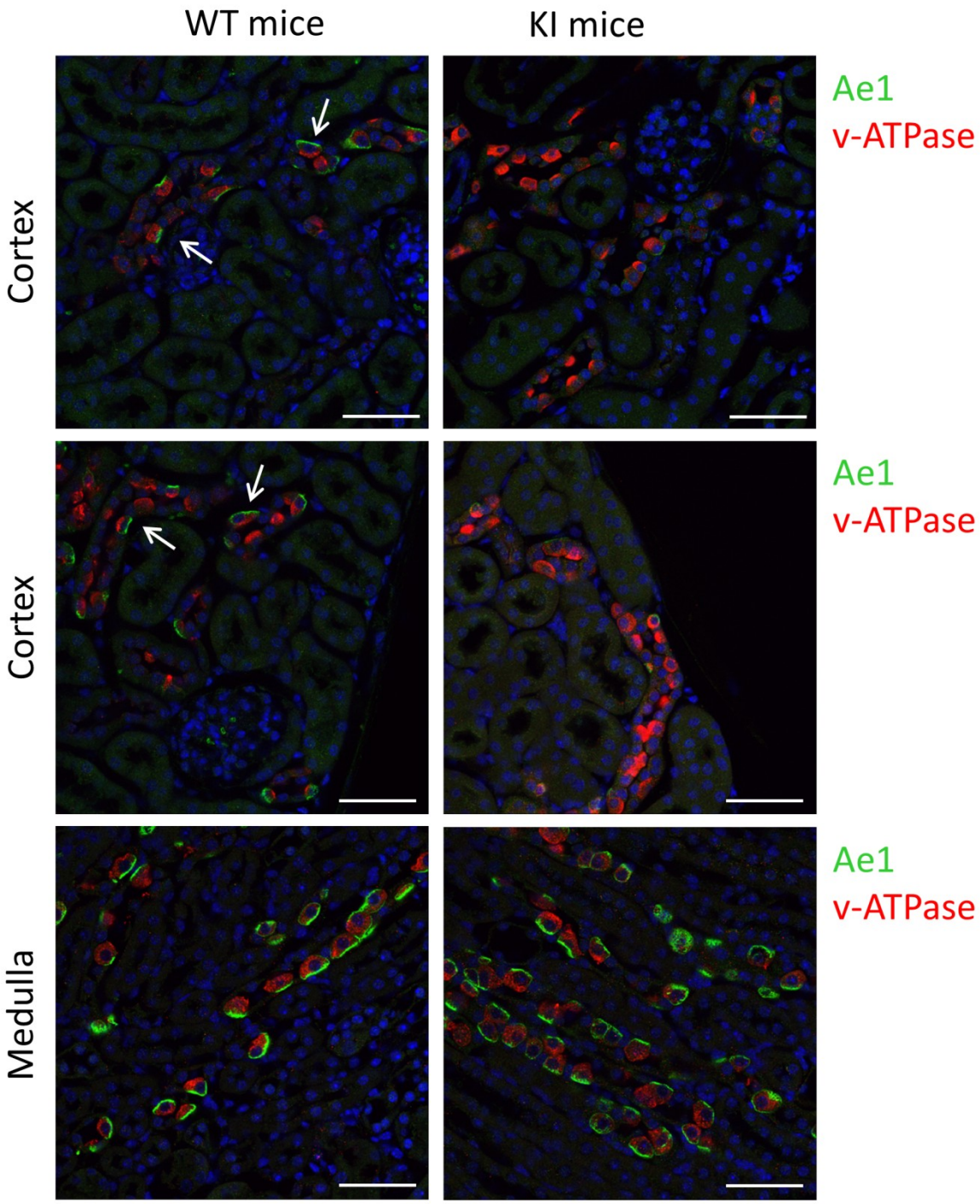

Figure 3.12 Localization of Ae1 in α-IC of L919X mice. Immunostaining of Ae1 (Alexa Fluor 488 green) and V-ATPase (Alexa Fluor 555 red) was performed on 0.7µm thick kidney cryosections. Ae1 is localized at the basolateral side of α-intercalated cells and the vH^+-ATPase is located at the apical side of the same cell type. DAPI was used to stain cell nuclei. (Scale bar 50µm)

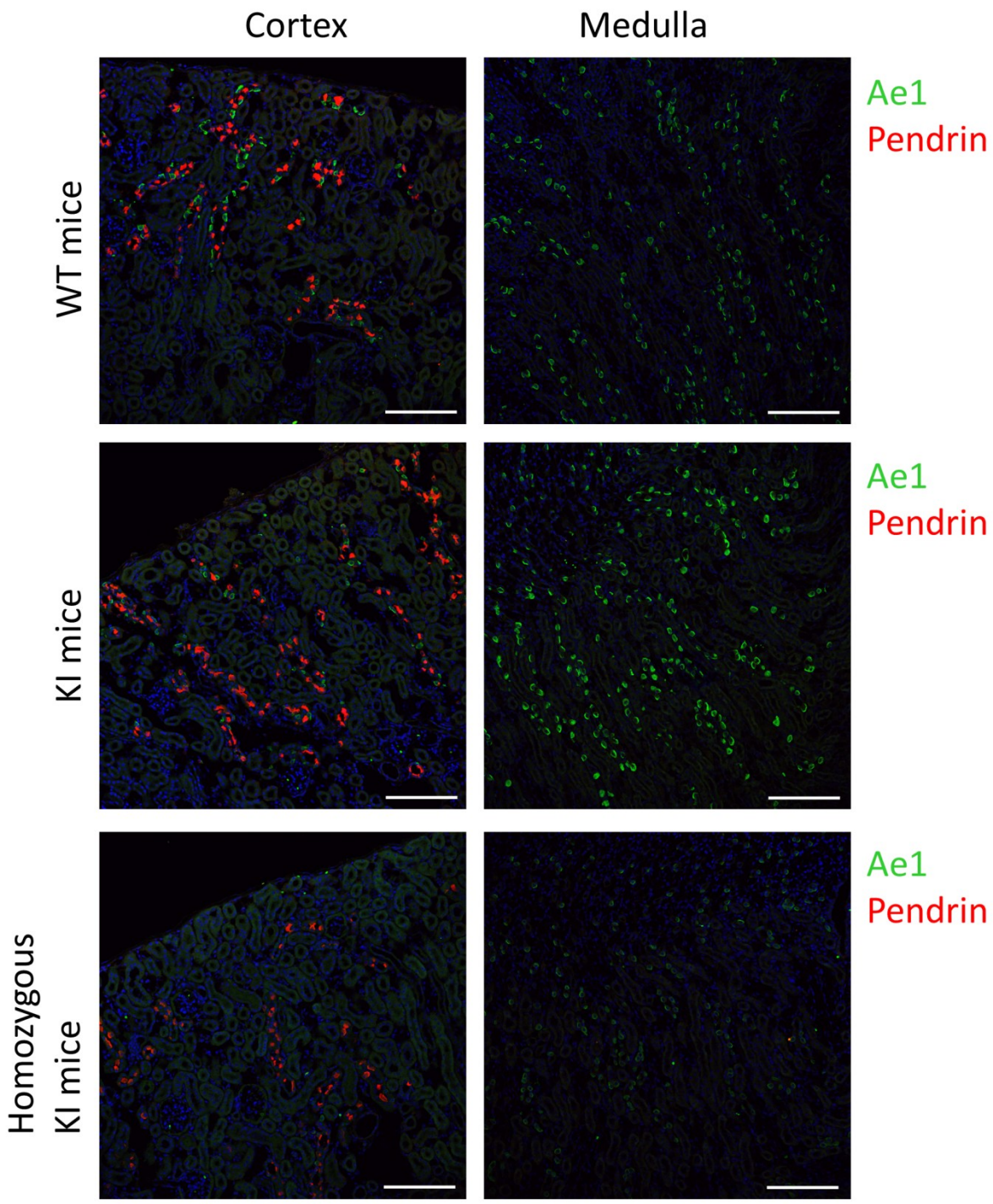

Figure 3.13 Expression of Ae1 in α-intercalated cells and Pendrin in β-intercalated cells of L919X mice. Immunostaining of Ae1 (Alexa Fluor 488 green) and Pendrin (Alexa Fluor 555 red) were performed on 0.7µm thick kidney cryosections. Immunolocalization of Ae1 at the basolateral side of α-intercalated cells and the Pendrin to the apical sides of the β-intercalated cells were observed. DAPI was used to stain cell nuclei. (Scale bar 150µm)

Foe each KI and WT littermates six sections were used for the quantification. The kidney sections were either co-stained with Ae1 and Pendrin or vH^{+}-ATPase and Pendrin. The number of Ae1 stained cells in the cortex was significantly decreased in L919X KI mice

compared to the WT littermates. Interestingly, no significant difference was observed in Ae1 positive cells in MCD in L919X KI mice compared to WT animals.

The number of pendrin positive cells in the cortex remains unchanged in KI mice versus WT littermates. The immunofluorescence quantification also revealed that the expression of pendrin was limited to the cortical distal segments of the nephron and the staining was absent from the MCD. There was no difference observed in the number of vH^{+}-ATPase stained cells in the CCD of L919X KI mice in comparison with WT littermates (Figure 3.14).

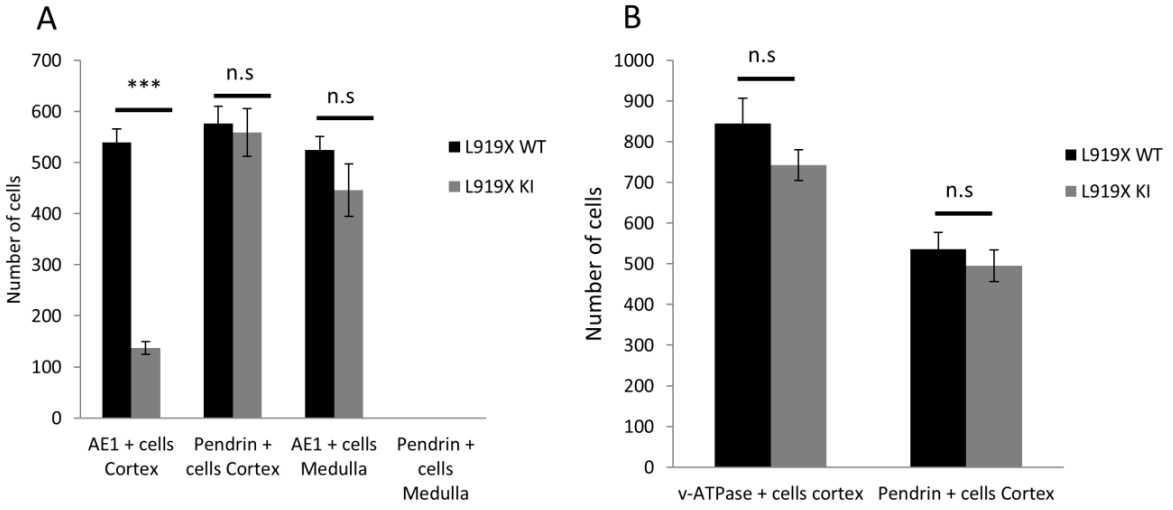

Figure 3.14 Analysis of the number of α and β-IC cells in L919X mice. (A) The number of α and β-IC quantified in cortex and medulla. Ae1 and pendrin were used as the markers for α and β-IC cells respectively. The number of α-IC cells in the cortex of KI mice was significantly reduced as compared to the WT mice. (B) The total number of IC cells in the cortex compared with only β-IC cells in the cortex. There was no significant difference found in any of the group.

3.5. Analysis of protein expression by immunoblot

In order to verify the decrease in the Ae1 protein level by a more quantitative approach Western blot analysis was performed in L919X KI mice in comparison with WT mice. Two independent animals per genotype were used. The kidneys were separated into cortex and medulla and the membrane proteins were prepared. Proteins were separated on SDS-PAGE and subsequent blotting led to the detection of Ae1 by specific antibody.

Results shown in figure 3.15 revealed that there was a decrease in the expression level of Ae1 protein in the cortex as well as in the medulla of L919X KI mice. The western blot results were consistence with the immunohistochemical analysis. β-actin was used as loading control.

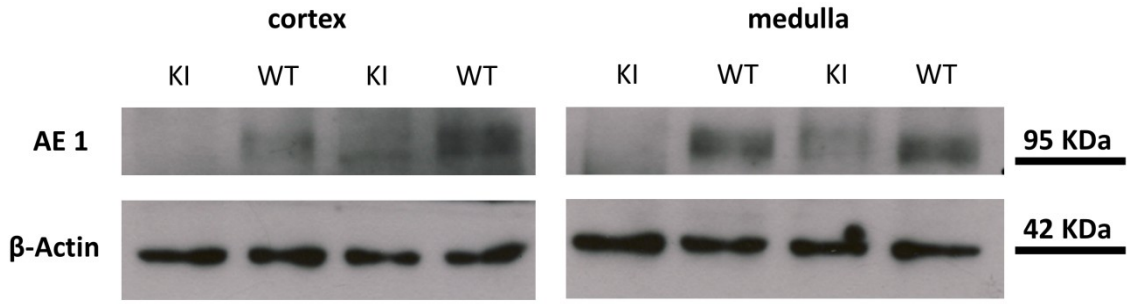

Figure 3.15 Immunoblot analysis of Ae1 protein in L919X mice kidney. The Ae1 specific protein band can be seen at approx.100 kDa. β-actin was used as loading control.

3.6. Real time Q-PCR analysis of transcript level in both KI mice

Transcript levels for both KI mice (R607H & L919X) were analysed by Real time quantitative PCR to detect any change in the transcript abundance. The kidneys were separated into cortex and medulla to isolate the mRNA from both KI mice. 50ng of cDNA was used for each PCR reaction. Analysis of the ct values indicated a 2 fold decrease in the mRNA level of R607H KI mice cortex versus WT mice but no difference was observed for the medulla. There was no significant difference found in the case of L919X KI verses WT mice. A decrease of Ae1 transcript was observed in R607H KI mice compared to WT mice but only 2 animals per genotype were taken. β-actin was used to normalise the values.

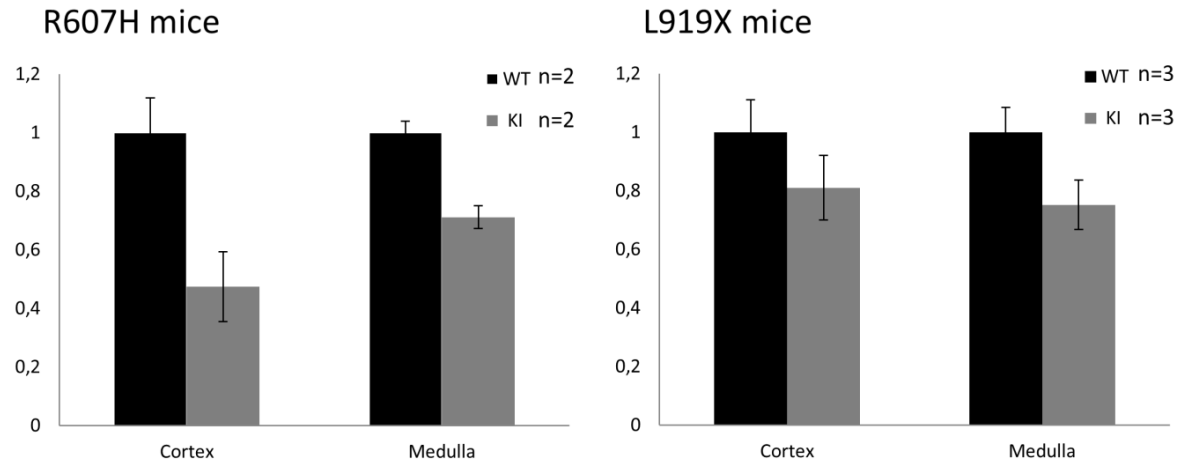

Figure 3.16 RT-PCR analyses of mRNA levels in both KI mice. (A) R607H mice have shown a 2-fold decrease in mRNA level in cortex but no difference can be observed in medulla. (B) L919X mice have shown no significant difference in transcript levels. β-actin was used to normalise the values.

4. Discussion

The anion exchanger 1 is a member of the SLC4 family (Romero, Fulton et al. 2004) which mediates Cl^-/HCO_3^- exchange in red blood cells as well as in the α-intercalated cells (α-IC) of collecting ducts in kidney (Rothstein and Ramjeesingh 1982; Drenckhahn, Schluter et al. 1985). Mutations in AE1 are the main cause of hereditary distal renal tubular acidosis (dRTA) in the kidney and structural disorders of red blood cells in humans (Casey and Reithmeier 1998; Bruce and Tanner 1999; Tanner 2002). These mutations are primarily deletions or amino acid substitutions of the amino acids, that do not affect the anion exchange function of the protein (Yenchitsomanus, Kittanakom et al. 2005).

R589H and R901X are two frequent human mutations of AE1 in autosomal dominant dRTA (Bruce, Cope et al. 1997; Jarolim, Shayakul et al. 1998; Toye, Bruce et al. 2002).
To study the detailed pathophysiology of these mutations in an *in vivo* system, we have generated two knock-in mouse models to mimic the human dRTA phenotype. Cell culture studies have suggested that these mutations cause mistrafficking of the protein. Absence of any immortal cell line originated from intercalated cells was an obstacle to correlate the human phenotype to cell culture systems (Shayakul and Alper 2004; Toye 2005; Cordat 2006). An important aim of the study was to provide an *in vivo* system to address the shortcomings of the cell culture system.

4.1. Generation of knock-in mice

Gene targeting via homologous recombination was used to generate both KI mouse models. To generate the mouse mutants, the human (AE1) and mouse (Ae1) protein sequences were aligned to identify the corresponding amino acids in the mouse. Both KI mice generated and analysed during this study carry the respective mutations. Successful generation of the KI mice was confirmed by southern blot and sequencing of the respective mutated sites.

4.2. R607H and L919X mice exhibit distal renal tubular acidosis

Both KI mice were characterized for the distal renal tubular acidosis by metabolic cage experiments, (Stehberger, Shmukler et al. 2007) to identify any change in the urine pH as seen in the patients carrying the same mutations (Yenchitsomanus, Kittanakom et al. 2005). Analysis of the urine which was collected over a 24 hour period revealed that there was a significant increase in the urine pH in KI mice as compared to WT littermates. This indicates the insufficiency of the KI mouse kidneys to acidify the urine that leads to dRTA in these mice.

A classical acid load test with NH_4Cl (Wrong and Davies 1959; Chambrey, Goossens et al. 2005; Stehberger, Shmukler et al. 2007) was performed over a period of 24 hours. Urine pH in R607H WT mice dropped to pH 5.5 whereas KI mice failed to acidify their urine pH below 6.5. This is consistent with a defect in normal urine acidification. Human patients heterozygous for R589H (Karet, Gainza et al. 1998) failed to acidify the urine pH below 5.7 after a standard acid load test. The significant difference between the urine pH in KI versus WT mice was observed over a period of one week. Surprisingly the impaired urine acidification did not result in systematic acidosis as seen in the blood gas analysis of the KI mice. So, it is likely that there is still residual acid secretion mechanism to compensate the effect of the acid secretion defect in these mice. There are several proteins (AE2, AE3, AE4 and NBCn1) expressed in the renal distal tubule and their role in renal acid base balance is still unknown (Wagner, Devuyst et al. 2009) therefore, both of these KI mice displaying dRTA can serve as an interesting model to uncover the role of other proteins in distal tubule acid secretion.

The second KI model carried the L919X mutation which correspond to the human R901X mutation was also established (Toye, Bruce et al. 2002). L919X KI mice were also analysed for any change in the urine pH and again a significant difference was found in mutated mice under steady state conditions. Human patients with this truncating mutation (R901X) were also unable to acidify urine after an acid load test (Toye, Bruce et al. 2002). L901X KI mice treated with NH_4Cl failed to acidify the urine, a feature of classical dRTA.

Both KI mice did not show any abnormality in the erythrocyte shape or structure, indicating that these mutations do not interfere with red blood cell function and only affect the distal tubules in the kidney. In human patients carrying either AE1 R589H missense mutation or the R901X truncating mutation, no clinical red blood cells abnormalities have been observed (Jarolim, Shayakul et al. 1998; Rodriguez-Soriano 2000; Toye, Bruce et al. 2002).

The analysis of blood pH and HCO_3^- concentration in both KI mice did not show differences compared to the WT littermates. This can be observed commonly in an autosomal dominant form of dRTA. It is often observed that the blood HCO_3^- concentration stays normal, and the defect in renal acid excretion can only be demonstrated by an acid load (Laing, Toye et al. 2005). The human patients carrying the corresponding heterozygous dominant mutation in the AE1 gene, diagnosed with hereditary autosomal dominant (AD) dRTA (Karet, Gainza et al. 1998; Toye, Bruce et al. 2002) have shown no difference in blood pH and HCO_3^- concentrations compared to the healthy patients.

Mutations in the B1 and a4 subunits of the vacuolar H^+-ATPase are also responsible for dRTA in humans (Karet, Finberg et al. 1999; Smith, Skaug et al. 2000; Stover, Borthwick et al. 2002). Both of these subunits are expressed in all types of intercalated cells (Finberg, Wagner et al. 2003; Stehberger 2003; Miller, Zhang et al. 2005). Interestingly, a mouse model deficient for the B1 subunit of the vH^+-ATPase does not show obvious signs of metabolic acidosis (Finberg, Wagner et al. 2005) as well, although patients with a B1 defect are severely affected. This may be explained by differences in acid secretion in mouse and man.

In contrast, a mouse model lacking Ae1 ($slc4a1^{-/-}$) both in red blood cells and the kidney α-intercalated cells had a high postnatal lethality, possibly as a result of anaemia and metabolic acidosis (Akel, Wagner et al. 2007; Stehberger, Shmukler et al. 2007). Mice surviving into adulthood showed retarded growth, severe hyperchloremic metabolic acidosis, and an inappropriately alkaline urine pH with reduced net acid excretion (Stehberger, Shmukler et al. 2007). Similarly, Ae1-deficient mice show renal calcium phosphate calcifications, predominantly in the medulla similar to dRTA patients, and have higher urinary phosphate and calcium excretion with reduced citrate levels. Ae1 deficient mice thus show a wide spectrum of phenotypic alterations reflecting the symptoms of inborn dRTA (Wagner 2007).

It is also known that patients with autosomal dominant dRTA differ from those with autosomal recessive dRTA in clinical presentation and disease severity. Autosomal recessive dRTA is frequently associated with a family history of consanguinity, is manifested early in life and is usually associated with a more severe phenotype than autosomal dominant dRTA and also linked with hereditary deafness (Batlle, Ghanekar et al. 2001).

Secondary effects of dRTA in patients such as growth retardation, osteomalacia, hypercalciuria, hypocitraturia and nephrocalcinosis are common (Alper 2010). These effects

have been described either in recessive or dominant conditions (Fry and Karet 2007). Patients with recessive mutations are more sensitive to the secondary effects of dRTA such as growth retardation and nephrocalcinosis compared to the patients with the dominant mutations.

Up to the age of 4 months no secondary effects related to the dRTA phenotype was observed in R607H and L919X mice. It would be interesting to observe secondary effects of dRTA in both KI mice at older age. It is common to identify the dRTA phenotype in patients with dominant AE1 mutations in adult age (Jarolim, Shayakul et al. 1998; Karet, Gainza et al. 1998; Toye, Bruce et al. 2002).

A significant decrease in NH_4^+ secretion into the urine is observed in R607H KI mice, this is also sometimes observed in patients with dRTA as they have low ammonia secretion rates due to the failure to trap ammonia in the tubular lumen of the collecting duct because of the inability to lower the luminal pH (Dubose 2008).

4.3. Immunohistochemical analysis revealed a decreased Ae1 expression in kidney α-intercalated cells

Immunohistochemistry was performed to analyse the localization and expression of Ae1 in the kidney of R607H and L919X KI mice.

Kidneys of R607H KI mice were first analysed for the localization and expression of Ae1 to observe any change in expression and/or localization of Ae1. Ae1 is normally localized to the basolateral sides of α-intercalated (α-IC) cells in collecting ducts and the H^+-ATPase is present on the apical side of the same cells. The H^+-ATPase also expressed at the apical and/or basolateral side of β-intercalated (β-IC) cells (Kopito, Andersson et al. 1987; Alper, Natale et al. 1989; Sahr, Taylor et al. 1994; Kim, Kim et al. 1999).

Our experiments demonstrate a decrease in the expression of Ae1 in α-IC cells of kidney tubules in KI mice as compared to the WT littermates, but this effect was more pronounced in cortical collecting ducts (CCD) as compared to medullary collecting ducts (MCD). Kidney biopsy samples from one human patient carrying the heterozygous R589H mutation have also shown a deficiency or total loss of AE1 expression (Shayakul 2004; Shayakul and Alper 2004) confirming our observations. These observations suggest a reduction of Ae1 expression in kidney tubules possibly due to an impairment of the mutant protein trafficking to the cell surface. The possible explanation for the reduced cell surface expression of mutated forms of Ae1 due to the intracellular retention and degradation of the protein while no significant changes in the transcript levels have been monitored in both KI mice models.

Extensive *in vitro* cells culture studies tried to address the cellular consequences of the AD dRTA mutation in AE1. Coexpression studies of kAE1 (Kidney AE1) R589H in non-polarized human embryonic kidney 293 cells (HEK 293) as well as in Madin Darby canine kidney cells (MDCK) both in non-polarized and polarized cells indicate a reduction in the cell surface expression of AE1. It is thought that the heterodimer formation leads to a dominant negative effect (Quilty, Li et al. 2002; Toye, Banting et al. 2004; Cordat, Kittanakom et al. 2006). Other missense mutations at amino acid position 589 the R589H, R589C and R589S also prevented the trafficking of mutated protein to the cell surface, indicating that this conserved arginine residue is important for proper trafficking (Quilty, Li et al. 2002; Wrong, Bruce et al. 2002). The frequent involvement of AE1 R589 in different dominant mutations suggests that codon 589 is a "mutational hotspot" of AE1 and may imply that, this residue is particularly important in the normal acidification process (Rodriguez-Soriano 2000; Pereira, Miranda et al. 2009). Arginine at 589 position of human AE1 protein is present at the intracellular border of the sixth transmembrane domain next to the Lysine at 590. These basic amino acid residues are conserved in all known vertebrate AE1 orthologs and may form part of the site of intracellular anion binding (Karet, Gainza et al. 1998).

We next examined whether the absence of Ae1 staining can be explained by a reduction of α-IC cells. A semi quantification was performed for Ae1 and pendrin stained α- and β-IC cells in the cortex and the medulla (Gao, Eladari et al. 2010). The counting of IC cells in kidney cortex and medulla allowed us to exclude a change in the number of IC cells. A significant reduced number of Ae1 positively stained cells in cortex of KI mice versus WT littermates was observed. There was no change found in the expression pattern of pendrin in β-IC cells. Pendrin stained cells were totally absent in the medulla where β-IC cells are generally not detected (Schuster 1990). The significant decrease in the Ae1 expression was also observed in the medulla of KI mice compared to WT. The analysis of total number of α- and β- IC cells in cortex was quantified by H^+-ATPase staining and no difference was observed.

These findings revealed that the R607H mutation leads to a decrease in the cell surface expression of Ae1 in comparison to WT mice. Here we showed that the R607H mutation results in less cell surface expression possibly due to intracellular retention of the protein in endoplasmic reticulum and subsequent degradation.

L919X KI mouse was a model for patients with the autosomal dominant truncating mutation R901X. It was analysed for the expression and localization of Ae1 protein in Kidney α-IC cells. Mice kidneys were stained with Ae1, pendrin and H^+-ATPase antibodies and the immunohistochemical analysis revealed the reduction of Ae1 expression in KI mice as compared to WT littermates.

Early expression studies in non-polarized MDCK cell lines stably transfected with the human R901X truncating mutation indicated an intracellular retention of the transfected protein (Toye, Bruce et al. 2002). *In vitro* HEK-293 cells transfection with the R901X truncating mutation and cell-surface biotinylation experiments suggested an intracellular retention of the mutant protein (Quilty, Cordat et al. 2002). A dominant negative effect resulted in the trafficking defect of wild type proteins due to the R901X mutants when co-expressed with WT cDNA (Quilty, Cordat et al. 2002).

A series of C-terminal truncations were studied to resolve the role of the C-terminal domain for Ae1 expression, which led to the conclusion that these mutations impair the protein trafficking to the cell membrane (Cordat, Li et al. 2003). Another important study in polarized kidney-derived MDCK cells suggested loss of polarized trafficking of Ae1 as the primary cause of dysfunction of α-IC cells dRTA associated with Ae1 truncating mutation (Devonald, Smith et al. 2003).

This abnormal distribution of R901X mutant was mimicked in epitope tagged kAE1-Y904A, suggested an important role for the "YXXF" sorting motif (904YDEV907) in the selectively basolateral accumulation of kAE1 and pointed out the role of C-terminal tail carrying the basolateral targeting signal (Devonald, Smith et al. 2003). The C-terminal mutation (R901X) contains a tyrosine motif and a type II PDZ interaction domain and this tyrosine residue (Tyr904), but not the PDZ domain, is critical for basolateral localization of AE1 protein in α-IC cells (Toye 2005).

These studies revealed the role of the C-terminal tail of Ae1 in protein trafficking to the basolateral membrane in polarized cells and the authors used polarized MDCK and rat IMCD cell lines in the absence of a better model for α-intercalated cells. Polarization of kidney cells is obviously associated with changes in the endogenous trafficking pathways that result in the generation of discrete apical and basolateral membrane domains (Toye, Bruce et al. 2002).

The R901X truncated protein still retains the carbonic anhydrase II (CA II) binding motif and shows no defect in CA II binding (Quilty, Cordat et al. 2002). The immunofluorescence staining of the L919X KI mice exhibits a reduction of Ae1 expression in the α-IC cells of the CCD in kidney tubules. Our observation did not show any mistargeting of the mutant protein to the apical side of the α-IC cells instead of the basolateral side.
The semi quantitative analysis of the Ae1 expression in L919X KI Kidney versus WT was performed by counting IC cells independently in the cortex and medulla. The counting of the Ae1 and pendrin stained IC cells helped us to confirm a decrease in the expression of Ae1 in the α-IC cells rather than a difference in the number of α- & β- IC cells.

These studies revealed a significant reduction in the expression levels of Ae1 in the CCD in KI mice versus WT littermates but the expression pattern of pendrin in β-IC cells remained same. The expression of Ae1 in MCD also remained same in KI compared to WT mice. The H^+-ATPase staining revealed no alteration in the number of IC cells in the cortex. This analysis helped to exclude the possibility of reduction in α-IC cell number. Therefore, it is proposed that both mutant mice have an intracellular retention of the protein and this is perhaps the cause of dRTA phenotype.

Angiotensin II and aldosterone stimulates the H^+-ATPase activity in α-intercalated cells and the upregulation of the renin–angiotensin–aldosterone system during metabolic acidosis has been well documented. It is thought angiotensin and aldosterone participates in the compensatory increase in renal acid excretion (Rothenberger, Velic et al. 2007; Winter, Kampik et al. 2011). Consequently, it would be interesting to investigate the levels of Angiotensin II and aldosterone in these mutant mice.

Breeding of the heterozygous KI mice results the homozygous KI mice for both independent mouse lines. These mice were viable and showed no morphological differences compared to the heterozygous littermates. Immunoflorescence staining of Ae1 was analysed in both homozygous KI mice. R607H homozygous KI mice showed almost loss of Ae1 protein in CCD however residual protein expression can be observed in MCD. The same effect was observed in L919X homozygous KI mouse line.

The reduction of Ae1 staining was subsequently studied by western blot analysis. These results showed a reduction of Ae1 expression in L919X KI mice as compared to the WT

littermates. These observations were consistent with the Immunohistochemical analysis of KI mice kidney. This dramatic decrease in the Ae1 protein concentration can be due to the dominant negative effect resulted in the intracellular degradation of the protein. The dRTA phenotype observed in these mice is possibly due to reduced expression of the functional protein at cell surface.

Reverse Transcriptase quantitative PCR (RTq-PCR) analysis of both KI mice was performed with the RNA isolated from the dissected cortex and medulla of KI and WT mice kidney (Bonnici and Wagner 2004). Three and two mice were used respectively for L919X and R607H in each genotype group. Analysis of the results was done according to the Delta Delta Ct Method (Livak and Schmittgen 2001; Schmittgen and Livak 2008).

By analysing the RTq-PCR results no significant change at the transcript levels in L919X KI mice with respect to the WT littermates has been observed. Immunohistochemical analysis and the immunoblotting results demonstrate a decrease in protein expression possibly due to the protein degradation. Therefore, it was expected that there is no observable change present in the transcript level of KI mice versus WT littermates.

5. Concluding remarks

The anion exchanger 1 (AE1) gene encodes two isoforms expressed in erythrocytes (eAE1) and in acid secreting intercalated (α-IC) cells of the kidney (kAE1). AE1 contributes to urinary acidification by providing the important exit route for HCO_3^- across the basolateral membrane (Batlle, Ghanekar et al. 2001). Mutations in AE1 are the major cause of hereditary autosomal dominant distal renal tubular acidosis in human.

Both KI mouse models generated during this study exhibit a failure to acidify the urine due to a defect in H^+-secretion. A reduced expression of Ae1 in KI mice kidneys was observed compared to the WT littermate. This may suggest an intracellular retention of mutant protein due to dominant negative effect. Further investigation is required to elucidate whether intracellular retention of the protein underlies dRTA. The effect of the long term exposure to acid and its effect on kidney function also have to be addressed in the future.

Homozygous KI mice did not show any gross morphological or physiological defect up to the age of 8 week. It can only be explained by some unknown H^+ secretory pathway and a compensatory HCO_3^- reclamation in the blood. Any change in the expression levels or other important proteins such as pendrin or H^+-ATPase in the distal collecting tubules of the kidney also needs to be analysed. Candidates for this regulation are AE2, AE3, AE4 and NBCn1. Further studies have to address whether one or more of these candidates are involved in compensatory pathways. These mice will also allow the investigation of the underlying mechanisms of secondary manifestations of the disease such as nephrocalcinosis that was limiting in cell culture system.

6. Literature:

Akel, A., C. A. Wagner, et al. (2007). "Enhanced suicidal death of erythrocytes from gene-targeted mice lacking the Cl-/HCO(3)(-) exchanger AE1." Am J Physiol Cell Physiol **292**(5): C1759-1767.

Allen, S. J., A. O'Donnell, et al. (1999). "Prevention of cerebral malaria in children in Papua New Guinea by southeast Asian ovalocytosis band 3." Am J Trop Med Hyg **60**(6): 1056-1060.

Alper, S. L. (2002). "Genetic diseases of acid-base transporters." Annu Rev Physiol **64**: 899-923.

Alper, S. L. (2006). "Molecular physiology of SLC4 anion exchangers." Exp Physiol **91**(1): 153-161.

Alper, S. L. (2009). "Molecular physiology and genetics of Na+-independent SLC4 anion exchangers." J Exp Biol **212**(Pt 11): 1672-1683.

Alper, S. L. (2010). "Familial renal tubular acidosis." J Nephrol **23 Suppl 16**: S57-76.

Alper, S. L., R. B. Darman, et al. (2002). "The AE gene family of Cl/HCO3- exchangers." J Nephrol **15 Suppl 5**: S41-53.

Alper, S. L., R. R. Kopito, et al. (1988). "Cloning and characterization of a murine band 3-related cDNA from kidney and from a lymphoid cell line." J Biol Chem **263**(32): 17092-17099.

Alper, S. L., J. Natale, et al. (1989). "Subtypes of intercalated cells in rat kidney collecting duct defined by antibodies against erythroid band 3 and renal vacuolar H+-ATPase." Proc Natl Acad Sci U S A **86**(14): 5429-5433.

Arnett, T. R. (2008). "Extracellular pH regulates bone cell function." J Nutr **138**(2): 415S-418S.

Bailey, J. L. (2005). "Metabolic acidosis: an unrecognized cause of morbidity in the patient with chronic kidney disease." Kidney Int Suppl(96): S15-23.

Batlle, D., H. Ghanekar, et al. (2001). "Hereditary distal renal tubular acidosis: new understandings." Annu Rev Med **52**: 471-484.

Batlle, D. and N. A. Kurtzman (1982). "Distal renal tubular acidosis: pathogenesis and classification." Am J Kidney Dis **1**(6): 328-344.

Bonar, P. T. and J. R. Casey (2008). "Plasma membrane Cl/HCO exchangers: structure, mechanism and physiology." Channels (Austin) **2**(5): 337-345.

Bonnardeaux, A. and D. G. Bichet (2008). Inherited Disorders of the Renal Tubule. Brenner & Rector's the kidney. B. M. Brenner and F. C. Rector. Philadelphia, PA, Saunders Elsevier.

Bonnici, B. and C. A. Wagner (2004). "Postnatal expression of transport proteins involved in acid-base transport in mouse kidney." Pflugers Arch **448**(1): 16-28.

Boron, W. F., E. L. Boulpaep, et al. (2009). Medical physiology a cellular and molecular approach. Philadelphia, PA, Saunders/Elsevier,**:** xii, 1337 p.

Brosius, F. C., 3rd, S. L. Alper, et al. (1989). "The major kidney band 3 gene transcript predicts an amino-terminal truncated band 3 polypeptide." J Biol Chem **264**(14): 7784-7787.

Bruce, L. J., D. L. Cope, et al. (1997). "Familial distal renal tubular acidosis is associated with mutations in the red cell anion exchanger (Band 3, AE1) gene." J Clin Invest **100**(7): 1693-1707.

Bruce, L. J. and M. J. Tanner (1999). "Erythroid band 3 variants and disease." Baillieres Best Pract Res Clin Haematol **12**(4): 637-654.

Bruce, L. J., O. Wrong, et al. (2000). "Band 3 mutations, renal tubular acidosis and South-East Asian ovalocytosis in Malaysia and Papua New Guinea: loss of up to 95% band 3 transport in red cells." Biochem J **350 Pt 1**: 41-51.

Campanella, M. E., H. Chu, et al. (2008). "Characterization of glycolytic enzyme interactions with murine erythrocyte membranes in wild-type and membrane protein knockout mice." Blood **112**(9): 3900-3906.

Caruana, R. J. and V. M. Buckalew, Jr. (1988). "The syndrome of distal (type 1) renal tubular acidosis. Clinical and laboratory findings in 58 cases." Medicine (Baltimore) **67**(2): 84-99.

Casey, J. R., S. Grinstein, et al. (2010). "Sensors and regulators of intracellular pH." Nat Rev Mol Cell Biol **11**(1): 50-61.

Casey, J. R. and R. A. Reithmeier (1998). "Anion exchangers in the red cell and beyond." Biochem Cell Biol **76**(5): 709-713.

Chambrey, R., D. Goossens, et al. (2005). "Genetic ablation of Rhbg in the mouse does not impair renal ammonium excretion." Am J Physiol Renal Physiol **289**(6): F1281-1290.

Chang, S. H. and P. S. Low (2003). "Identification of a critical ankyrin-binding loop on the cytoplasmic domain of erythrocyte membrane band 3 by crystal structure analysis and site-directed mutagenesis." J Biol Chem **278**(9): 6879-6884.

Chu, H., A. Breite, et al. (2008). "Characterization of the deoxyhemoglobin binding site on human erythrocyte band 3: implications for O2 regulation of erythrocyte properties." Blood **111**(2): 932-938.

Chu, H. and P. S. Low (2006). "Mapping of glycolytic enzyme-binding sites on human erythrocyte band 3." Biochem J **400**(1): 143-151.

Cohen, R. M., G. M. Feldman, et al. (1997). "The balance of acid, base and charge in health and disease." Kidney Int **52**(2): 287-293.

Cordat, E. (2006). "Unraveling trafficking of the kidney anion exchanger 1 in polarized MDCK epithelial cells." Biochem Cell Biol **84**(6): 949-959.

Cordat, E. and J. R. Casey (2009). "Bicarbonate transport in cell physiology and disease." Biochem J **417**(2): 423-439.

Cordat, E., S. Kittanakom, et al. (2006). "Dominant and recessive distal renal tubular acidosis mutations of kidney anion exchanger 1 induce distinct trafficking defects in MDCK cells." Traffic **7**(2): 117-128.

Cordat, E., J. Li, et al. (2003). "Carboxyl-terminal truncations of human anion exchanger impair its trafficking to the plasma membrane." Traffic **4**(9): 642-651.

Dahl, N. K., L. Jiang, et al. (2003). "Deficient HCO3- transport in an AE1 mutant with normal Cl- transport can be rescued by carbonic anhydrase II presented on an adjacent AE1 protomer." J Biol Chem **278**(45): 44949-44958.

Devonald, M. A., A. N. Smith, et al. (2003). "Non-polarized targeting of AE1 causes autosomal dominant distal renal tubular acidosis." Nat Genet **33**(2): 125-127.

Devonald, M. A. J. (2004). "Renal Epithelial Traffic Jams and One-Way Streets." Journal of the American Society of Nephrology **15**(6): 1370-1381.

Drenckhahn, D., K. Schluter, et al. (1985). "Colocalization of band 3 with ankyrin and spectrin at the basal membrane of intercalated cells in the rat kidney." Science **230**(4731): 1287-1289.

Dubose, T. D., Jr. (2008). Disorders of Acid-Base Balance. Brenner & Rector's the kidney. B. M. Brenner and F. C. Rector. Philadelphia, PA, Saunders Elsevier.

Everett, L. A., B. Glaser, et al. (1997). "Pendred syndrome is caused by mutations in a putative sulphate transporter gene (PDS)." Nat Genet **17**(4): 411-422.

Finberg, K. E., C. A. Wagner, et al. (2005). "The B1-subunit of the H(+) ATPase is required for maximal urinary acidification." Proc Natl Acad Sci U S A **102**(38): 13616-13621.

Finberg, K. E., C. A. Wagner, et al. (2003). "Molecular cloning and characterization of Atp6v1b1, the murine vacuolar H+ -ATPase B1-subunit." Gene **318**: 25-34.

Frische, S., T. H. Kwon, et al. (2003). "Regulated expression of pendrin in rat kidney in response to chronic NH4Cl or NaHCO3 loading." Am J Physiol Renal Physiol **284**(3): F584-593.

Fry, A. C. and F. E. Karet (2007). "Inherited renal acidoses." Physiology (Bethesda) **22**: 202-211.

Gao, X., D. Eladari, et al. (2010). "Deletion of hensin/DMBT1 blocks conversion of beta- to alpha-intercalated cells and induces distal renal tubular acidosis." Proc Natl Acad Sci U S A **107**(50): 21872-21877.

Giebisch, G. and E. Windhager (2009). Transport of acids and bases. Medical physiology : a cellular and molecular approach. W. F. Boron and E. L. Boulpaep. Philadelphia, PA, Saunders/Elsevier**:** xii, 1337 p.

Hamm, L. L. and N. L. Nakhoul (2008). Renal Acidification. Brenner & Rector's the kidney. B. M. Brenner and F. C. Rector. Philadelphia, PA, Saunders Elsevier.

Hamm, L. L. and E. E. Simon (1987). "Roles and mechanisms of urinary buffer excretion." Am J Physiol **253**(4 Pt 2): F595-605.

Hassoun, H. and J. Palek (1996). "Hereditary spherocytosis: a review of the clinical and molecular aspects of the disease." Blood Rev **10**(3): 129-147.

Hassoun, H., Y. Wang, et al. (1998). "Targeted inactivation of murine band 3 (AE1) gene produces a hypercoagulable state causing widespread thrombosis in vivo." Blood **92**(5): 1785-1792.

Huber, S., E. Asan, et al. (1999). "Expression of rat kidney anion exchanger 1 in type A intercalated cells in metabolic acidosis and alkalosis." Am J Physiol **277**(6 Pt 2): F841-849.

Jarolim, P., H. L. Rubin, et al. (1995). "Mutations of conserved arginines in the membrane domain of erythroid band 3 lead to a decrease in membrane-associated band 3 and to the phenotype of hereditary spherocytosis." Blood **85**(3): 634-640.

Jarolim, P., C. Shayakul, et al. (1998). "Autosomal dominant distal renal tubular acidosis is associated in three families with heterozygosity for the R589H mutation in the AE1 (band 3) Cl-/HCO3- exchanger." J Biol Chem **273**(11): 6380-6388.

Jehle, S., A. Zanetti, et al. (2006). "Partial neutralization of the acidogenic Western diet with potassium citrate increases bone mass in postmenopausal women with osteopenia." J Am Soc Nephrol **17**(11): 3213-3222.

Karet, F. E. (2002). "Inherited Distal Renal Tubular Acidosis." Journal of the American Society of Nephrology **13**(8): 2178-2184.

Karet, F. E. (2002). "Inherited distal renal tubular acidosis." J Am Soc Nephrol **13**(8): 2178-2184.

Karet, F. E. (2008). Distal Renal Tubular Acidosis. Genetic diseases of the kidney. R. P. Lifton, S. Somlo, G. H. Giebisch and D. W. Seldin, Elsevier/Academic Press.

Karet, F. E., K. E. Finberg, et al. (1999). "Mutations in the gene encoding B1 subunit of H+-ATPase cause renal tubular acidosis with sensorineural deafness." Nat Genet **21**(1): 84-90.

Karet, F. E., F. J. Gainza, et al. (1998). "Mutations in the chloride-bicarbonate exchanger gene AE1 cause autosomal dominant but not autosomal recessive distal renal tubular acidosis." Proc Natl Acad Sci U S A **95**(11): 6337-6342.

Keskanokwong, T., H. J. Shandro, et al. (2007). "Interaction of integrin-linked kinase with the kidney chloride/bicarbonate exchanger, kAE1." J Biol Chem **282**(32): 23205-23218.

Kim, J., Y. H. Kim, et al. (1999). "Intercalated cell subtypes in connecting tubule and cortical collecting duct of rat and mouse." J Am Soc Nephrol **10**(1): 1-12.

Kim, Y. H., T. H. Kwon, et al. (2002). "Immunocytochemical localization of pendrin in intercalated cell subtypes in rat and mouse kidney." Am J Physiol Renal Physiol **283**(4): F744-754.

Kittanakom, S., E. Cordat, et al. (2004). "Trafficking defects of a novel autosomal recessive distal renal tubular acidosis mutant (S773P) of the human kidney anion exchanger (kAE1)." J Biol Chem **279**(39): 40960-40971.

Koolman, J. and K.-H. Röhm (2005). Color atlas of biochemistry. Stuttgart ; New York, Thieme.

Kopito, R. R., M. Andersson, et al. (1987). "Structure and organization of the murine band 3 gene." J Biol Chem **262**(17): 8035-8040.

Kopito, R. R., M. A. Andersson, et al. (1987). "Multiple tissue-specific sites of transcriptional initiation of the mouse anion antiport gene in erythroid and renal cells." Proc Natl Acad Sci U S A **84**(20): 7149-7153.

Kopito, R. R. and H. F. Lodish (1985). "Primary structure and transmembrane orientation of the murine anion exchange protein." Nature **316**(6025): 234-238.

Kudrycki, K. E. and G. E. Shull (1993). "Rat kidney band 3 Cl-/HCO3- exchanger mRNA is transcribed from an alternative promoter." Am J Physiol **264**(3 Pt 2): F540-547.

Kurschat, C. E. and S. L. Alper (2008). Hereditary Renal Tubular Acidosis. Molecular and Genetic Basis of Renal Disease D. B. Mount and M. R. Pollak, Saunders/Elsevier.

Kurtzman, N. A. (2000). "Renal tubular acidosis syndromes." South Med J **93**(11): 1042-1052.

Laing, C. M., A. M. Toye, et al. (2005). "Renal tubular acidosis: developments in our understanding of the molecular basis." Int J Biochem Cell Biol **37**(6): 1151-1161.

Landowski, C. P., Y. Suzuki, et al. (2008). The Mammalian Transporter Families. Seldin and Giebisch's The kidney : physiology and pathophysiology. R. J. Alpern, S. C. Herbert, D. W. Seldin and G. H. Giebisch. Amsterdam ; New York, Elsevier/Academic Press.

Lightwood, R. (1935). "Calcium Infarction of the Kidneys in Infants." Arch Dis Child (10): 205–206.

Livak, K. J. and T. D. Schmittgen (2001). "Analysis of relative gene expression data using real-time quantitative PCR and the 2(-Delta Delta C(T)) Method." Methods **25**(4): 402-408.

Lodish, H. F. (2003). Molecular Cell Biology, W H Freeman & Co.

Madsen, K. M., S. Nielsen, et al. (2008). Anatomy of the Kidney. Brenner & Rector's the kidney. B. M. Brenner and F. C. Rector. Philadelphia, PA, Saunders Elsevier.

Miller, R. L., P. Zhang, et al. (2005). "V-ATPase B1-subunit promoter drives expression of EGFP in intercalated cells of kidney, clear cells of epididymis and airway cells of lung in transgenic mice." Am J Physiol Cell Physiol **288**(5): C1134-1144.

Muller, D. J., N. Wu, et al. (2008). "Vertebrate membrane proteins: structure, function, and insights from biophysical approaches." Pharmacol Rev **60**(1): 43-78.

Pereira, P. C., D. M. Miranda, et al. (2009). "Molecular pathophysiology of renal tubular acidosis." Curr Genomics **10**(1): 51-59.

Peters, L. L., R. A. Shivdasani, et al. (1996). "Anion exchanger 1 (band 3) is required to prevent erythrocyte membrane surface loss but not to form the membrane skeleton." Cell **86**(6): 917-927.

Petrovic, S., Z. Wang, et al. (2003). "Regulation of the apical Cl-/HCO-3 exchanger pendrin in rat cortical collecting duct in metabolic acidosis." Am J Physiol Renal Physiol **284**(1): F103-112.

Pushkin, A. and I. Kurtz (2006). "SLC4 base (HCO3 -, CO3 2-) transporters: classification, function, structure, genetic diseases, and knockout models." Am J Physiol Renal Physiol **290**(3): F580-599.

Quilty, J. A., E. Cordat, et al. (2002). "Impaired trafficking of human kidney anion exchanger (kAE1) caused by hetero-oligomer formation with a truncated mutant associated with distal renal tubular acidosis." Biochem J **368**(Pt 3): 895-903.

Quilty, J. A., J. Li, et al. (2002). "Impaired trafficking of distal renal tubular acidosis mutants of the human kidney anion exchanger kAE1." Am J Physiol Renal Physiol **282**(5): F810-820.

Reithmeier, R. A. (2001). "A membrane metabolon linking carbonic anhydrase with chloride/bicarbonate anion exchangers." Blood Cells Mol Dis **27**(1): 85-89.

Reuss, L. (2008). Mechanisms of Ion Transport Across Cell Membranes and Epithelia. Seldin and Giebisch's The kidney : physiology and pathophysiology. R. J. Alpern, S. C. Herbert, D. W. Seldin and G. H. Giebisch. Amsterdam ; New York, Elsevier/Academic Press.

Richards, S. M., M. E. Jaconi, et al. (1999). "A spliced variant of AE1 gene encodes a truncated form of Band 3 in heart: the predominant anion exchanger in ventricular myocytes." J Cell Sci **112 (Pt 10)**: 1519-1528.

Rodriguez-Soriano, J. (2000). "New insights into the pathogenesis of renal tubular acidosis--from functional to molecular studies." Pediatr Nephrol **14**(12): 1121-1136.

Rodriguez Soriano, J. (2002). "Renal Tubular Acidosis: The Clinical Entity." Journal of the American Society of Nephrology **13**(8): 2160-2170.

Romero, M. F. (2005). "Molecular pathophysiology of SLC4 bicarbonate transporters." Curr Opin Nephrol Hypertens **14**(5): 495-501.

Romero, M. F., C. M. Fulton, et al. (2004). "The SLC4 family of HCO 3 - transporters." Pflugers Arch **447**(5): 495-509.

Rothenberger, F., A. Velic, et al. (2007). "Angiotensin II stimulates vacuolar H+ -ATPase activity in renal acid-secretory intercalated cells from the outer medullary collecting duct." J Am Soc Nephrol **18**(7): 2085-2093.

Rothstein, A. and M. Ramjeesingh (1982). "The red cell band 3 protein: its role in anion transport." Philos Trans R Soc Lond B Biol Sci **299**(1097): 497-507.

Royaux, I. E., S. M. Wall, et al. (2001). "Pendrin, encoded by the Pendred syndrome gene, resides in the apical region of renal intercalated cells and mediates bicarbonate secretion." Proc Natl Acad Sci U S A **98**(7): 4221-4226.

Sahr, K. E., W. M. Taylor, et al. (1994). "The structure and organization of the human erythroid anion exchanger (AE1) gene." Genomics **24**(3): 491-501.

Salhany, J. M., K. S. Cordes, et al. (2005). "Identification and characterization of a second 4,4'-dibenzamido-2,2'-stilbenedisulphonate (DBDS)-binding site on band 3 and its relationship with the anion/proton co-transport function." Biochem J **388**(Pt 1): 343-353.

Salomao, M., X. Zhang, et al. (2008). "Protein 4.1R-dependent multiprotein complex: new insights into the structural organization of the red blood cell membrane." Proc Natl Acad Sci U S A **105**(23): 8026-8031.

Schmittgen, T. D. and K. J. Livak (2008). "Analyzing real-time PCR data by the comparative C(T) method." Nat Protoc **3**(6): 1101-1108.

Schuster, V. L. (1990). "Organization of collecting duct intercalated cells." Kidney Int **38**(4): 668-672.

Scott, D. A., R. Wang, et al. (1999). "The Pendred syndrome gene encodes a chloride-iodide transport protein." Nat Genet **21**(4): 440-443.

Shayakul, C. (2004). "Characterization of a highly polymorphic marker adjacent to the SLC4A1 gene and of kidney immunostaining in a family with distal renal tubular acidosis." Nephrology Dialysis Transplantation **19**(2): 371-379.

Shayakul, C. and S. L. Alper (2000). "Inherited renal tubular acidosis." Curr Opin Nephrol Hypertens **9**(5): 541-546.

Shayakul, C. and S. L. Alper (2004). "Defects in processing and trafficking of the AE1 Cl-/HCO3- exchanger associated with inherited distal renal tubular acidosis." Clin Exp Nephrol **8**(1): 1-11.

Smith, A. N., J. Skaug, et al. (2000). "Mutations in ATP6N1B, encoding a new kidney vacuolar proton pump 116-kD subunit, cause recessive distal renal tubular acidosis with preserved hearing." Nat Genet **26**(1): 71-75.

Stefanovic, M., N. O. Markham, et al. (2007). "An 11-amino acid beta-hairpin loop in the cytoplasmic domain of band 3 is responsible for ankyrin binding in mouse erythrocytes." Proc Natl Acad Sci U S A **104**(35): 13972-13977.

Stehberger, P. A. (2003). "Localization and Regulation of the ATP6V0A4 (a4) Vacuolar H+-ATPase Subunit Defective in an Inherited Form of Distal Renal Tubular Acidosis." Journal of the American Society of Nephrology **14**(12): 3027-3038.

Stehberger, P. A., N. Schulz, et al. (2003). "Localization and regulation of the ATP6V0A4 (a4) vacuolar H+-ATPase subunit defective in an inherited form of distal renal tubular acidosis." J Am Soc Nephrol **14**(12): 3027-3038.

Stehberger, P. A., B. E. Shmukler, et al. (2007). "Distal renal tubular acidosis in mice lacking the AE1 (band3) Cl-/HCO3- exchanger (slc4a1)." J Am Soc Nephrol **18**(5): 1408-1418.

Sterling, D., R. A. Reithmeier, et al. (2001). "A transport metabolon. Functional interaction of carbonic anhydrase II and chloride/bicarbonate exchangers." J Biol Chem **276**(51): 47886-47894.

Stewart, A. K., C. E. Kurschat, et al. (2008). The SLC4 Anion Exchanger Gene Family. Seldin and Giebisch's The kidney : physiology and pathophysiology. R. J. Alpern, S. C. Herbert, D. W. Seldin and G. H. Giebisch. Amsterdam ; New York, Elsevier/Academic Press.

Stover, E. H., K. J. Borthwick, et al. (2002). "Novel ATP6V1B1 and ATP6V0A4 mutations in autosomal recessive distal renal tubular acidosis with new evidence for hearing loss." J Med Genet **39**(11): 796-803.

Tanner, M. J. (1997). "The structure and function of band 3 (AE1): recent developments (review)." Mol Membr Biol **14**(4): 155-165.

Tanner, M. J. (2002). "Band 3 anion exchanger and its involvement in erythrocyte and kidney disorders." Curr Opin Hematol **9**(2): 133-139.

Tanphaichitr, V. S., A. Sumboonnanonda, et al. (1998). "Novel AE1 mutations in recessive distal renal tubular acidosis. Loss-of-function is rescued by glycophorin A." J Clin Invest **102**(12): 2173-2179.

Thomas, S. R. (2009). "Kidney modeling and systems physiology." Wiley Interdiscip Rev Syst Biol Med **1**(2): 172-190.

Toye, A. M. (2005). "Defective kidney anion-exchanger 1 (AE1, Band 3) trafficking in dominant distal renal tubular acidosis (dRTA)." Biochem Soc Symp(72): 47-63.

Toye, A. M., G. Banting, et al. (2004). "Regions of human kidney anion exchanger 1 (kAE1) required for basolateral targeting of kAE1 in polarised kidney cells: mis-targeting explains dominant renal tubular acidosis (dRTA)." J Cell Sci **117**(Pt 8): 1399-1410.

Toye, A. M., L. J. Bruce, et al. (2002). "Band 3 Walton, a C-terminal deletion associated with distal renal tubular acidosis, is expressed in the red cell membrane but retained internally in kidney cells." Blood **99**(1): 342-347.

Toye, A. M., S. Ghosh, et al. (2005). "Protein-4.2 association with band 3 (AE1, SLCA4) in Xenopus oocytes: effects of three natural protein-4.2 mutations associated with hemolytic anemia." Blood **105**(10): 4088-4095.

Tresguerres, M., J. Buck, et al. (2010). "Physiological carbon dioxide, bicarbonate, and pH sensing." Pflugers Arch **460**(6): 953-964.

Unwin, R. J., D. G. Shirley, et al. (2002). "Urinary acidification and distal renal tubular acidosis." J Nephrol **15 Suppl 5**: S142-150.

van Adelsberg, J. S., J. C. Edwards, et al. (1993). "The apical Cl/HCO3 exchanger of beta intercalated cells." J Biol Chem **268**(15): 11283-11289.

van Hille, B., H. Richener, et al. (1994). "Heterogeneity of vacuolar H(+)-ATPase: differential expression of two human subunit B isoforms." Biochem J **303 (Pt 1)**: 191-198.

Vince, J. W. and R. A. Reithmeier (1998). "Carbonic anhydrase II binds to the carboxyl terminus of human band 3, the erythrocyte C1-/HCO3- exchanger." J Biol Chem **273**(43): 28430-28437.

Wagner, C. A. (2007). "Metabolic acidosis: new insights from mouse models." Curr Opin Nephrol Hypertens **16**(5): 471-476.

Wagner, C. A., O. Devuyst, et al. (2009). "Regulated acid-base transport in the collecting duct." Pflugers Arch **458**(1): 137-156.

Wagner, C. A., K. E. Finberg, et al. (2004). "Renal vacuolar H+-ATPase." Physiol Rev **84**(4): 1263-1314.

Wagner, C. A., K. E. Finberg, et al. (2002). "Regulation of the expression of the Cl-/anion exchanger pendrin in mouse kidney by acid-base status." Kidney Int **62**(6): 2109-2117.

Wagner, C. A. and J. P. Geibel (2002). "Acid-base transport in the collecting duct." J Nephrol **15 Suppl 5**: S112-127.

Wagner, C. A., J. Kovacikova, et al. (2006). "Renal acid-base transport: old and new players." Nephron Physiol **103**(1): p1-6.

Watts, B. A., 3rd and D. W. Good (2004). "An apical K(+)-dependent HCO(3)- transport pathway opposes transepithelial HCO(3)- absorption in rat medullary thick ascending limb." Am J Physiol Renal Physiol **287**(1): F57-63.

Williamson, R. C. and A. M. Toye (2008). "Glycophorin A: Band 3 aid." Blood Cells Mol Dis **41**(1): 35-43.

Winter, C., N. B. Kampik, et al. (2011). "Aldosterone stimulates vacuolar H+-ATPase activity in renal acid-secretory intercalated cells mainly via a protein kinase C dependent pathway." Am J Physiol Cell Physiol.

Wrong, O., L. J. Bruce, et al. (2002). "Band 3 mutations, distal renal tubular acidosis, and Southeast Asian ovalocytosis." Kidney Int **62**(1): 10-19.

Wrong, O. and H. E. Davies (1959). "The excretion of acid in renal disease." Q J Med **28**(110): 259-313.

Yenchitsomanus, P. T. (2003). "Human anion exchanger1 mutations and distal renal tubular acidosis." Southeast Asian J Trop Med Public Health **34**(3): 651-658.

Yenchitsomanus, P. T., S. Kittanakom, et al. (2005). "Molecular mechanisms of autosomal dominant and recessive distal renal tubular acidosis caused by SLC4A1 (AE1) mutations." J Mol Genet Med **1**(2): 49-62.

Young, M. T., R. Beckmann, et al. (2000). "Red-cell glycophorin A-band 3 interactions associated with the movement of band 3 to the cell surface." Biochem J **350 Pt 1**: 53-60.

Zhu, Q. and J. R. Casey (2004). "The substrate anion selectivity filter in the human erythrocyte Cl-/HCO3- exchange protein, AE1." J Biol Chem **279**(22): 23565-23573.

Zhu, Q., D. W. Lee, et al. (2003). "Novel topology in C-terminal region of the human plasma membrane anion exchanger, AE1." J Biol Chem **278**(5): 3112-3120.

Appendix

Curriculum Vitae

Personal details:

Name:	Rizwan Mumtaz
Adresse:	Rudolf-Breitscheid-straße - 44, 07747-Jena
Date of birth:	01.12.1979
Place of birth:	Lahore (Pakistan)
Nationality:	Pakistani
Email:	rizwanmumtaz1979@gmail.com
Telephone:	0176 24289112

Education:

February 2008-October 2011	**PhD thesis** Institute of Human Genetics University Hospital Jena
October 2004 – March 2007	**Master of Science in Molecular Biotechnology** University of Bonn **Master thesis**: Identification of putative YB-1 regulated genes by Chromatin Immunoprecipitation. Centre for advanced European studies and research, (Caesar) Bonn.
January 2001 – March 2003	**Master of Science in Botany** University of Punjab Lahore
October 1998 – August 2000	**Bachelor of Science (Botany, chemistry and zoology)** University of Punjab Lahore

1998:	**Higher secondary school certificate**
	Board of intermediate and secondary education Lahore
1995:	**Secondary school certificate**
	Board of intermediate and secondary education Lahore

Work experience

September 2007 – January 2008	Worked as Scientific assistant in Department of Molecular Biology University of Aarhus Denmark
July 2003 – October 2004	Worked as Research assistant in centre of excellence in Molecular Biology University of Punjab Lahore

Publications:

Mahmood S, Beetz C, Tahir MM, Imran M, **Mumtaz** R, Bassmann I, Jahic A, Malik M, Nürnberg G, Hassan SA, Rana S, Nürnberg P, Hübner CA. First HPSE2 missense mutation in urofacial syndrome. *Clinical Genetics* 2012 Jan; 81(1):88-92.

Varga RE, **Mumtaz** R, Jahic A, Rudenskaya GE, Sánchez-Ferrero E, Auer-Grumbach M, Hübner CA, Beetz C. MLPA-based evidence for sequence gain: pitfalls in confirmation and necessity for exclusion of false positives. *Analytical Biochemistry* 2012 Feb 15; 421(2):799-801.

Beetz C., Pamminger T., Khundadze M., Kurth I., **Mumtaz R**., Hübner A.K., Hennings J.C., Irintchev A., Deufel T., Hübner C.A. (2010) Cellular mechanisms resulting in hereditary spastic paraplegia type SPG31. *Journal of Medizinische Genetik* Vol: 22, Number 1 / February, 2010. (Abstract)

Acknowledgements

In the name of "ALLAH", the most beneficent, the most merciful, who granted me all these graces to fulfil this work and supported me for everything in my life.

First and foremost I offer my sincerest gratitude and appreciation to my supervisor Prof. Dr. Christian Hübner for providing me the opportunity to accomplish my doctoral thesis in his lab and throughout supporting me with his patience and knowledge whilst allowing me the room to work in my own way. I am especially very thankful to his encouragement and effort and without him this thesis would not have been completed or written.

I would like to thank Prof. Dr. Aria Baniahmad, Prof. Dr. Carsten Wagner and Prof. Dr. Dominique Eladari for kind acceptance to act as an examiner for this thesis. I am especially thankful to Dr. Antje Hübner, Dr. Lutz Liebmann and Christopher Hennings for their continuous help during the whole PhD work, for their comments on thesis and for being very nice colleagues. I am very much grateful to PD. Dr. Ingo Kurth for giving nice comments on my thesis and for the German translation of the summary.

In my daily work I have been blessed with a friendly and cheerful group of fellow colleagues in functional genetics lab, I would like to thank all of them especially to Frau Katrin Schorr without her help the generation of mice would not be possible as well as my former colleagues in the departments of Clinical Chemistry, especially to Dr. Christian Beetz for his valuable advices during the whole time.

I am extremely grateful to my parents, who did all their best to help me in my education, for their great support, encouragement and lot of prayers for me that gave me the strength to study abroad and finish this doctoral thesis.

Finally, I like to say thanks to my wife, for her continuous support and understanding and my beloved son who makes me fresh every evening when I come back home.

Ehrenwörtliche Erklärung

Hiermit erkläre ich, dass mir die Promotionsordnung der Friedrich-Schiller-Universität bekannt ist, ich die Dissertation selbst angefertigt habe und alle von mir benutzten Hilfsmittel, persönlichen Mitteilungen und Quellen in meiner Arbeit angegeben sind. Bei der Auswahl und Auswertung des Materials sowie bei der Herstellung des Manuskripts unterstützten mich: Prof. Dr. Christian Hüber, PD Dr. Ingo Kurth, Dr. Lutz Liebmann und Dr. A. Hübner. Die Hilfe eines Promotionsberaters wurde nicht in Anspruch genommen. Dritte erhielten weder unmittelbar noch mittelbar geldwerte Leistungen von mir für Arbeiten, die im Zusammenhang mit dem Inhalt der vorgelegten Dissertation stehen. Ich versichere, daß die vorliegende Dissertation noch nicht als Prüfungsarbeit für eine staatliche oder andere wissenschaftliche Prüfung eingereicht wurde und dass die gleiche, oder eine in wesentlichen Teilen ähnliche oder eine andere Abhandlung nicht bei einer anderen Hochschule als Dissertation eingereicht wurde.

Jena, 24.10.2011 Rizwan Mumtaz